MICROCOPY RESOLUTION TEST CHART
NATIONAL BUREAU OF STANDARDS-1963-A

NAVAL POSTGRADUATE SCHOOL
Monterey, California

THESIS

AN EVALUATION OF DISCRETIZED CONDITIONAL
PROBABILITY AND LINEAR REGRESSION THRES-
HOLD TECHNIQUES IN MODEL OUTPUT STATISTICS
FORECASTING OF VISIBILITY OVER THE NORTH
ATLANTIC OCEAN

by

Mark Diunizio

September 1984

Thesis Advisor: Robert J. Renard

85   03   12   048

REPORT DOCUMENTATION PAGE		READ INSTRUCTIONS BEFORE COMPLETING FORM
1. REPORT NUMBER	2. GOVT ACCESSION NO.	3. RECIPIENT'S CATALOG NUMBER
4. TITLE (and Subtitle) An Evaluation of Discretized Conditional Probability and Linear Regression Threshold Techniques in Model Output Statistics Forecasting of Visibility over the North Atlantic Ocean		5. TYPE OF REPORT & PERIOD COVERED Master's Thesis September 1984
		6. PERFORMING ORG. REPORT NUMBER
7. AUTHOR(s) Mark Diunizio		8. CONTRACT OR GRANT NUMBER(s)
9. PERFORMING ORGANIZATION NAME AND ADDRESS Naval Postgraduate School Monterey, California 93943		10. PROGRAM ELEMENT, PROJECT, TASK AREA & WORK UNIT NUMBERS
11. CONTROLLING OFFICE NAME AND ADDRESS Naval Postgraduate School Monterey, California 93943		12. REPORT DATE September 1984
		13. NUMBER OF PAGES 233
14. MONITORING AGENCY NAME & ADDRESS(If different from Controlling Office)		15. SECURITY CLASS. (of this report) Unclassified
		15a. DECLASSIFICATION/ DOWNGRADING SCHEDULE

16. DISTRIBUTION STATEMENT (of this Report)

Approved for public release; distribution unlimited

17. DISTRIBUTION STATEMENT (of the abstract entered in Block 20, If different from Report)

18. SUPPLEMENTARY NOTES

19. KEY WORDS (Continue on reverse side If necessary and Identify by block number)

Model Output Statistics, Visibility, North Atlantic Ocean Visibility, Marine Horizontal Visibility, Discretization, Conditional Probability, Physically Homogeneous Ocean Areas, Minimum Probable Error Threshold Models, Weather Forecasting,

20. ABSTRACT (Continue on reverse side If necessary and Identify by block number)

This report describes the application and evaluation of four primary statistical models in the forecasting of horizontal marine visibility over selected physically homogeneous areas of the North Atlantic Ocean. The main focus of this study is to propose an optimal model output statistics (MOS) approach to operationally forecast visibility at the 00-hour model initialization time and the 24-hour and 48-hour model forecast

DD $_{1 \text{ JAN } 73}^{\text{FORM}}$ 1473 EDITION OF 1 NOV 65 IS OBSOLETE
S N 0102-LF-014-6601

#19 - KEY WORDS - (CONTINUED)

Maximum-Likelihood-of-Detection Threshold Models,
Linear Regression, Natural Regression,
Maximum Probability

#20 - ABSTRACT - (CONTINUED)

projections. The technique utilized involves the
manipulation of observed visibility and Navy Operational
Global Atmospheric Prediction System (NOGAPS) model output
parameters. The models employ the statistical methodolo-
gies of maximum conditional probability, natural regression
and minimum probable error linear regression threshold
techniques. Additionally, an evaluation of the 1983
predictive arrays/equations using 1984 NOGAPS data fields
and a maximum-likelihood-of-detection threshold model were
accomplished. Results show that two statistical approaches,
namely a maximum conditional probability strategy uti-
lizing linear regression equation predictors and the
minimum probable error threshold models, produce the best
results achieved in this study.

An Evaluation of Discretized Conditional Probability
and Linear Regression Threshold Techniques in Model
Output Statistics Forecasting of Visibility over the
North Atlantic Ocean

by

Mark Diunizio
Lieutenant, United States Navy
B. S., United States Naval Academy, 1977

Submitted in partial fulfillment of the
requirements for the degree of

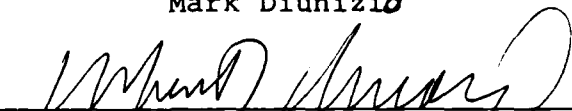MASTER OF SCIENCE IN METEOROLOGY AND OCEANOGRAPHY

from the

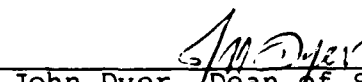NAVAL POSTGRADUATE SCHOOL
September 1984

Author: _____
                          Mark Diunizio

Approved by: _____
                   Robert J. Renard, Thesis Advisor

_____
        Paul R. Lowe, Second Reader

_____
        Robert J. Renard, Chairman, Department
                   of Meteorology

_____
John Dyer, Dean of Science and Engineering

3

ABSTRACT

This report describes the application and evaluation of four primary statistical models in the forecasting of horizontal marine visibility over selected physically homogeneous areas of the North Atlantic Ocean. The main focus of this study is to propose an optimal model output statistics (MOS) approach to operationally forecast visibility at the 00-hour model initialization time and the 24-hour and 48-hour model forecast projections. The technique utilized involves the manipulation of observed visibility and Navy Operational Global Atmospheric Prediction System (NOGAPS) model output parameters. The models employ the statistical methodologies of maximum conditional probability, natural regression and minimum probable error linear regression threshold techniques. Additionally, an evaluation of the 1983 predictive arrays/equations using 1984 NOGAPS data fields and a maximum-likelihood-of-detection threshold model were accomplished. Results show that two statistical approaches, namely a maximum conditional probability strategy utilizing linear regression equation predictors and the minimum probable error threshold models, produce the best results achieved in this study.

TABLE OF CONTENTS

LIST OF TABLES

LIST OF FIGURES

9

11

I.   INTRODUCTION AND BACKGROUND

One of the most significant advances in objective weather prediction, since the introduction of numerical weather prediction in the 1950's and satellite remote sensing capabilities in the 1960's, has been the development of Model Output Statistics (MOS) weather forecasting method by Glahn and Lowry (1972). In general, this technique is the determination of a statistical relationship between an operational weather element (predictand), which may or may not be forecast by numerical methods, and numerical model output variables (predictors), usually via linear regression methods. The resulting predictand/predictor regression equations provide the basis for generating a statistical weather prediction. The National Weather Service (NWS) has included MOS as an integral part of their weather forecasting operations since the early 1970's. Currently, the NWS maintains MOS prediction equations for approximately 15 weather elements (e.g. ceiling, visibility, obstructions to vision, precipitation, etc.) at forecast times ranging from 6 to 48 hours. These forecasts are routinely provided to approximately 295 civilian and 190 military locations throughout the continental United States (CONUS) and Alaska [Glahn, 1983].

Based on the impressive results achieved with the NWS MOS program, the Department of Defense (DOD), through the Air

13

Weather Service (AWS), implemented and operated a quasi-global version of the NWS MOS system at the Air Force Global Weather Center (AFGWC), Offutt AFB, Nebraska [Best and Pryor, 1983]. The first operational forecasts obtained from the AWS MOS system were produced by AFGWC in December 1980 and the system ran operationally for a period of approximately 18 months. Regions for which operational MOS forecasts were produced included Europe, Asis (including Korea and Japan), the South China Sea (including the Philippines and Taiwan), the near and middle east and northern Africa. The AWS MOS program was terminated with the recent decision to replace the current hemispheric primitive equation (PE) model with a spectral global dynamic model [Klein, 1981].

Throughout its tenure as an operational forecast scheme, the AWS MOS system provided the U.S. Air Force with a relatively low cost, flexible and responsive prediction network. Further development of the AWS MOS system has been postponed until sufficient spectral model output is archived.

The U.S. Navy, by virtue of its unique marine forecasting responsibilities, has a keen interest in applying MOS forecasting schemes to global oceanic regions. Through the research and development efforts of the Naval Environmental Prediction Research Facility (NEPRF) in Monterey, California, the Navy has sponsored a limited amount of research into naval applications of MOS. In particular, statistical studies have been done into forecasting Levante winds in Spain [Godfrey and

14

Lowe, 1979], ceiling and visibility prediction in the southern
California (SOCAL) naval operating area [Lewit, 1980], marine
fog and visibility predictability in the North Pacific Ocean
[Renard et al., 1983 and Renard and Thompson, 1984]. Presently,
a program is in operation which provides MOS forecasts for
selected U.S. Navy and Marine Corps CONUS locations. These
services, which are made available from NWS, are based on the
National Meteorological Center (NMC) limited fine mesh model
predictions. This MOS program was initiated on 10 November
1982 and provides forecasts for twelve weather parameters
which include visibility, obstructions to visibility and
cloud amount [Naval Environmental Prediction Research
Facility, 1982].

The results of these limited studies along with the
encouraging performances of both the NWS and AWS MOS programs
and the implementation of the Navy Operational Global Atmos-
pheric Prediction System (NOGAPS) dynamical primitive equation
(PE) model at the Fleet Numerical Oceanography Center (FNOC),
in Monterey, California prompted the decision in September
1982 for the Navy to pursue its own MOS program.

Fig. 1 is an overview of the currently proposed milestones
for the Navy MOS program. The first operational weather
parameter being investigated in this proposed ten-year Navy
effort is horizontal visibility at sea, with the initial goal
of this project being the investigation and development of
statistical predictive schemes for forecasting horizontal
visibility over the North Atlantic Ocean.

The impact of fog and other impediments to visibility on naval operations is well documented throughout maritime history. Records show countless catastrophes and accidents which were directly attributable to poor visibility at sea. For example, on 29 May 1914, the Canadian liner Empress of Ireland collided with the Norwegian vessel Storstad in dense fog on the Saint Lawrence River resulting in 1,024 fatalities and similarly, the legendary "North Sea haze" was a critical element in the World War I tactics employed at Jutland in 1916. Also, one of the most spectacular maritime disasters in the U.S. Navy's history took place on 9 September 1923 when seven Pacific fleet destroyers struck the rocks and ran aground in dense fog off of Point Arguello, California.

Research into predicting marine visibility via traditional linear regression methodologies has taken place at the Naval Postgraduate School (NPS) since the early 1960's. Generally, early visibility forecasting experiments identified potential physical air/ocean mechanisms [Schramn, 1966] and emphasized the inherent likelihood of human error in at-sea visibility observations [Nelson, 1972]. Later experimentation by Aldinger (1979), Yavorsky (1980) and Selsor (1980) concentrated on various modifications to multiple linear regression schemes and the analysis of prediction skill measurements.

This study presents a direct follow-on to the research presented by Karl (1984), in which statistical methodologies presented by Preisendorfer (1983a,b,c) and multiple linear

regression techniques presented by Lowe (1984a) were compared
and contrasted. In Karl's preliminary study, Preisendorfer's
three strategies, two based on maximum conditional proba-
bility and one based on natural regression, as well as
Lowe's linear regression threshold models were tested and
applied to sets of FNOC model output parameters (MOPs) from
both the North Pacific and North Atlantic Ocean areas. The
North Atlantic Ocean study was separated into effective
physically homogeneous areas [Lowe, 1984b]. Karl's study
specifically dealt with an evaluation of the MOS scheme
applied to oceanic regions for the TAU-00 model output
during the period 15 May to 07 July 1983.

This study concerns itself with a continued evaluation
and further refinement of statistical methods proposed by
Preisendorfer as well as the linear regression threshold
models presented by Lowe. With reference to Karl's study,
other North Atlantic Ocean areas and model forecast projections
(e.g. TAU-24 and TAU-48) are addressed.

17

II. OBJECTIVES AND APPROACH

The primary objectives of this study are to continue the previous NPS horizontal marine visibility prediction research initiated by Karl (1984) and to continue the search for an optimal Model Output Statistics (MOS) prediction scheme to operationally forecast coastal and open ocean visibility over the North Atlantic Ocean. The approach employed in meeting the stated objectives is listed below:

A. Apply and evaluate the Preisendorfer maximum probability and natural regression strategies (1983a,b,c) to additional North Atlantic Ocean homogeneous areas [Lowe, 1983b] using May through July 1983, NOGAPS predictand/predictor data.

B. Expand the Model Output Predictor (MOP) data sets to include the NOGAPS model TAU-00, and the TAU-24 and TAU-48 prognostic times defined in Chapter III.

C. Investigate specific two-stage, equal variance and quadratic multiple linear regression threshold models proposed by Lowe (1984a) for the oceanic areas and model output periods addressed in A. and B. above.

D. Compare and contrast the individual results of the Preisendorfer statistical methodologies to those of the Lowe approach.

E. Conduct a limited series of experiments in which a 1984 data set, 15 May to 23 June, is utilized as an

18

independence evaluation of the predictive models constructed with 1983 NOGAPS data.

F. Based on A. to E. above, present an interim recommendation for an optimal statistical approach to forecast North Atlantic Ocean horizontal visibility as a function of prediction time and homogeneous area.

III. DATA

A. VISIBILITY OBSERVATIONS AND SYNOPTIC CODES

Horizontal visibility observations taken from seagoing platforms are reported as values of ten standardized World Meteorological Organization (WMO) synoptic weather codes. These codes range in value from 90, which corresponds to visibility less than 50 meters, to 99, which corresponds to visibility equal to or greater than 50 kilometers. Human observational error and inexactness in measuring visibility at sea necessitates a generalization of visibility classification for prediction purposes, as follows:

Visibility Category	Synoptic Code	Visibility Range
I	90-94	< 2 km
II	95-96	$\geq$ 2 km to < 10 km
III	97-99	$\geq$ 10 km

The above scheme coincides with the classification scheme proposed by Karl (1984) and is based upon the below listed U.S. Navy operational criteria.

1. 10 km (5 n mi)--U.S. Navy aircraft carrier at-sea flight recovery operations change from visual (VFR) to controlled (IFR) approach guidelines [Department of the Navy, 1979].

2. 2 km (1 n mi)--the sounding of reduced visibility signals for all vessels operating in international waters.

The term "reduced visibility" is not specifically defined in the International Regulations for Preventing Collisions at Sea, 1972. The distance of 1 n mi is generally considered to be the governing operational distance.

B. NORTH ATLANTIC OCEAN DATA

1. Area

The North Atlantic Ocean, from 0°-80° N latitude, was divided into homogeneous oceanic areas by Lowe (1984b) using a statistical cluster analysis technique. The specific homogeneous areas evaluated in this study are identified as areas 2, 3W and 4 on Fig. 2. These areas were selected because they individually represent a range of different relative frequencies of poor visibility observations. Area 3W, which was used by Karl (1984) for his preliminary experimentation, represents an area of relatively frequent occurrence of poor visibility, while area 4 represents an area of relatively sparse occurrence of poor visibility and area 2 represents an intermediate case.

2. Time Period

Data from mid-May 1983 to mid-July 1983 were combined to form a more extensive data set, hereafter referred to as FATJUNE 1983. FATJUNE 1983 was selected as the initial data set for statistical experimentation because of the high frequency of occurrence of poor visibility observations for many areas of the North Atlantic Ocean during this period.

21

1200 GMT synoptic ship report data were used exclusively in this study. This time corresponds to general daylight conditions over the North Atlantic Ocean during FATJUNE. In addition to FATJUNE 1983, a limited May 15 to June 23 1984 data set, possessing the same geographical coverage and daylight characteristics of FATJUNE 1983, was utilized in an independent test of the predictive arrays and equations generated in this study.

For the purpose of this study, TAU-00 generally represents six-hour model forecast fields valid at 1200 GMT. Three specific fields, namely temperature, geopotential height and wind, are model initialization fields valid at 1200 GMT. TAU-24 and TAU-48 are defined as 24-hour and 48-hour model forecast fields, valid at 1200 GMT. TAU-00, TAU-24 and TAU-48 model output parameters (predictors) are employed in the 00, 24 and 48 hour forecast schemes, respectfully. Summaries of the visibility frequencies for each visibility category, as a function of homogeneous area and prediction time, for FATJUNE 1983 and the 15 May to 23 June 1984 data set, are contained in Tables I through III and Table VI respectively.

3. Synoptic Weather Reports

All synoptic visibility observations (predictand data) for this study were provided by the Naval Oceanography Command Detachment (NOCD), Asheville, North Carolina which is co-located with the National Climatic Data Center (NCDC).

22

The observations which contained systematic observer error or were obviously erroneous, as determined from the data quality indicators provided with the data, were deleted from the working data sets.

4. Predictor Parameters

Fifty TAU-00, fifty-four TAU-24 and fifty-four TAU-48 model output predictors (MOP's) were provided by the Fleet Numerical Oceanography Center (FNOC), Monterey, California. These parameters are generated by their current operational atmospheric prediction model, the Navy Operational Global Atmospheric Prediction System (NOGAPS). All MOP's were interpolated from model grid coordinates to synoptic ship report position using a linear interpolation scheme. In addition to the initial group of model output parameters, ten derived parameters representing calculated quantities, such as parameter gradients and products, were included as potential predictors. Of the entire group of potential predictor parameters, only forty TAU-00 and forty-seven TAU-24 and TAU-48 MOP's were actually used to develop the various Preisendorfer (1983a,b,c) and linear regression threshold models [Lowe, 1983a]. The remainder of the NOGAPS model output parameters were dropped from consideration because 1) the MOP lacked a physical linkage to the visibility pre-dictand and/or 2) a lack of significant digits (lost during the transfer of FNOC data to the main computer center's mass storage system) rendered the particular MOP useless.

23

A list of all available TAU-00, TAU-24 and TAU-48 MOP's are included in Appendix B.

For each homogeneous area and model forecast projection, a set of three linear regression equations, in addition to the aforementioned MOP's, were included as potential MOP's for a separate evaluation of the Preisendorfer methodology (the PR+BMD model). These three predictor equations were obtained from two standardized linear regression software packages, namely P2R--stepwise regression and P9R--all possible subsets regression, as addressed in the BMDP Statistical Software [University of California, 1983]. The P2R was initially employed in the evaluation of areas 2 and 4, TAU-00 data, while the P9R program was employed in the remainder of the cases studied. The change to the P9R program was initiated as a safeguard against any potential predictor selection bias incorporated in the P2R software. Specific details concerning these statistical software packages are addressed in Appendix A.

C. DEPENDENT/INDEPENDENT DATA SETS

Due to the limited amount of data available to this study for each of the North Atlantic Ocean homogeneous areas, it was necessary to withhold a significant amount of the observations from the developmental model to use as an independent data set. That amount was set as one-third for the experiments reported here. This was accomplished by the

24

use of a counter and transfer statement in the computer
programs which prevented every third observation from enter-
ing the developmental computations. To ensure that the
dependent and independent data were representative of the
same population, a 95% confidence interval for proportions
[Miller and Freund, 1977] was established from the entire
data set, for each visibility category, and the dependent
and independent data sets were constrained to have visibility
frequencies within these established confidence intervals.
Table IV summarizes the dependent and independent data for
the North Atlantic Ocean data set.

IV. PROCEDURES

A. TERMS AND SYMBOLS

The terms and statistical symbols defined below will be used throughout the remainder of this report. The formal mathematical definitions are described in Karl (1984).

1. Maximum probability strategy--choosing forecast visibility category based upon the highest conditional probability of visibility within a predictor interval.

    a. MAXPROB I--designation of the maximum probability strategy in which ties of the highest conditional probabilities in a predictor interval are resolved by the generation of a random number.

    b. MAXPROB II--designation of the maximum probability strategy in which ties of the highest conditional probabilities in a predictor interval are resolved by assigning the lowest visibility category, of those tied, as the forecast category.

2. Natural regression strategy--choosing forecast visibility categories based upon the statistical average of the conditional probabilities of visibility within a predictor interval.

3. A0--the probability of a zero-class visibility category forecast error (e.g., if visiblity category I is forecast and observed).

4. A1--the probability of a one-class visibility category forecast error (e.g., if visibility category I is forecast and category II is observed).

5. CE--class error parameter defined as A0+2A1, used as the primary aid in identifying the first predictor.

6. PP--the potential predictability of visibility by any given predictor.

7. Functional dependence. This is a measure of the stochastic dependence of one predictor upon another. Functional dependence is the probability that one of the predictors will change when the other does. High functional dependence values between one already selected predictor and another potential predictor, indicates that little additional information beyond the selected predictor is possible. Conversely, a low functional dependence value between the same two predictors, indicates that each predictor possesses a high degree of linearly uncorrelated information concerning the predictand. Functional dependence range is 0.0 to 1.0 (1.0 = highest functional dependence). The specific derivation and mathematical description of the concept of "functional dependence" is discussed in greater depth by Preisendorfer (1983c).

8. Root-sum-squared functional dependence. The functional dependence of a predictor on all predictors already included in the developmental model. It is equal to the square-root

27

of the sum of the squares of the individual functional dependence values.

9. TS1--threat score for visibility category I, as computed from a contingency table (see Appendix C).

10. ATS1--adjusted threat score for visibility category I which removes the influence of the data set category frequency (see Appendix C).

11. AA0--adjusted A0. A contingency table statistic which removes the influence of the most frequent visibility category in a set of data (similar to a normalized value) (see Appendix C).

B. COMPUTER PROGRAMS

Four computer programs were developed to test the proposed Preisendorfer (1983a,b,c) methodology. The programs are on file in the Department of Meteorology, Naval Postgraduate School, Monterey, California, 93943.

1. A program to compute A0, A1, CE and PP for all predictors, all strategies (MAXPROB I, MAXPROB II and natural regression) for a particular number of equally populous predictor intervals. Statistics for the three strategies are based upon the same predictor(s) rather than the best predictor(s) for each strategy.

2. A program to compute functional dependence values for all predictors, on a given predictor, for a given number of equally populous predictor intervals and to compute the

associated 96% critical confidence interval value, referred to as functional dependence(96) in this study, by Monte Carlo means.

3. A program to construct contingency tables and to compute skill and threat scores, for both the dependent and independent data sets.

4. A program to generate 100 random data sets, from the marginal probabilities of the predictor(s) in the developmental model, and to compute upper and lower 5% critical confidence interval values for A0 and Al to be used for testing the significance of the results from each of the Preisendorfer models against chance. These confidence interval values are calculated via Monte Carlo means.

C. MODELS

1. Preisendorfer PR Model

This model represents the first of two different applications of the basic Preisendorfer methodology [Preisendorfer, 1983a,b,c]. Karl (1984), in his preliminary research, provides a rigorous interpretation and results associated with this statistical forecasting methodology. Karl's study provides the necessary background for the continued investigation and evaluation of this model and readers interested in specific details are advised to consult this document.

The PR model utilizes the working set of NOGAPS model output parameters (MOP's) and derived parameters

(Appendix B) as potential predictors in constructing a developmental model, based upon the dependent data set, which provides the structure by which the independent data set is tested and evaluated. In general, these potential predictors have their range of values partitioned into discretized equally populous predictor intervals ("cells") and conditional probabilities of the predictand are calculated according to the three modified visibility categories (VISCAT) I, II and III. Three separate strategies of determining the specific VISCAT which is to be identified with each predictor value, are proposed. These strategies, two based upon maximum probability and the third based on a natural regression approach, are addressed as MAXPROB I, MAXPROB II and natural regression in the remaining portions of this study.

Initial evaluation of this model involves varying the equally populous predictor intervals from sizes of four through ten, and selecting an optimal first predictor which provides one of the following requirements in the designated order:

a. the lowest CE value of all the potential predictors

b. the highest PP value of all the potential predictors

Once a first predictor is identified for each of the four through ten equally populous predictor intervals, corresponding VISCAT I, II and III threat and A0 skill scores (Appendix E) are calculated for both the dependent

and independent data sets. The practice of selecting an optimal equally populous predictor interval from the eligible grouping sizes of four through ten, was proposed by Karl (1984) as a practical procedure which would permit the realization of peak skill scores as well as maintain associated computer storage requirements at a manageable level. An unfortunate consequence of this range of potential grouping sizes is that certain statistical calculations associated with equally populous predictor intervals of eight, nine and ten are terminated before completion due to a two megabyte storage ceiling at the NPS W.R. Church Computer Center. When considering potential predictor intervals, the size of the interval is of obvious importance, with lower values being the most desirable. The criterion for determining the optimal equally populous predictor interval is to select the smallest interval value which maximizes the dependent data set adjusted A0 and independent adjusted VISCAT I threat score. For this study, this interval value was fixed for all ensuing aspects of the model evaluation. In practice, the selection of equally populous predictor intervals was based upon the initial adjusted A0 (dependent data) and the adjusted VISCAT I threat score (independent data) for the MAXPROB II strategy. The MAXPROB II scores were routinely found to be the highest for each case evaluated, at this early stage in the evaluation process, and therefore used as the basis for grouping selection. As the equally populous

grouping interval remains constant throughout the Preisen-
dorfer models, the MAXPROB I and natural regression strate-
gies practically play no role in the predictor selection
process.

Once the first predictor and its associated equally
populous predictor interval have been identified, a func-
tional dependence test of the first predictor against those
remaining potential predictors is run. The second, third
and all subsequent predictors are selected only if both of
the following criteria are met:

    a.   subsequent predictors must increase $A0$ over the
        $A0$ value attained at the preceding level, and

    b.   the selected predictor must have the lowest
        functional dependence and root-sum-square
        functional dependence of all the remaining
        potential predictors.

After each predictor selection stage has been com-
pleted, significance tests are run upon the developmental
model to determine if the results are suitably significant
as compared to random chance. This testing is accomplished
via Monte Carlo testing methods using the conditional
probabilities of the selected predictors and assuming equal
probability of occurrence for the three modified visibility
categories. Functional dependence/root-sum-square functional
dependence, $A0$, and $A1$ statistics are calculated for each of
100 randomly generated data sets. For the developmental
model to yield results which are significant at the speci-
fied confidence interval values, each one of the following
criteria must be met:

a. A0 must be equal to or greater than A0(96)

b. A1 must be equal to or less than A1(05)

c. the functional dependence value for a selected
   predictor must be less than functional
   dependence(96)

As with the process of selecting equally populous predictor intervals, the A0, A0(96), A1 and A1(05) statistics (Appendix G), reflect scores for the MAXPROB II strategy. The A0 statistics routinely were found to be the highest for this strategy and thus were used as the basis for ensuring the aforementioned predictor selection criteria were met. However, the MAXPROB I strategy often produced A0 values identical to MAXPROB II. The natural regression strategy regularly lagged the two maximum probability strategies in A0 and A1 scores and consequently played no real role in the prediction selection process. Specific trends in A0/A1 scores can be seen in Appendix G.

From a practical standpoint, the model development continues until computer storage limitations preclude further addition of predictors. This generally occurred at the fifth predictor level.

Once the developmental model is completed, contingency tables of forecast visibility category versus observed visibility category are constructed for both the dependent and independent data sets, and threat and skill scores are computed and compared.

33

2. Preisendorfer PR+BMD Model

This model is still the PR model described above.
Now, sets of three linear regression equations (Appendix D)
are added to the list of potential NOGAPS model output and
derived predictor parameters. The inherent difference of
these predictors is evidenced in both the predictor selec-
tion process as well as in the resulting skill and threat
scores, as will be demonstrated in Chapter V.

3. Equal Variance Threshold Model (EVAR)

This model represents the first of two threshold
models, developed by Lowe (1984a), which were evaluated in
this study. The model uses an algorithm which requires the
assumption that the variances of two normally distributed
populations which are to be separated by a threshold value
are equal, while their means are unequal. A detailed dis-
cussion of the theoretical background of this scheme is
addressed in Appendix A.

A two-stage separation scheme was used to effectively
divide the visibility categories (VISCAT) I, II and III
into a first-stage VISCAT I versus a combined VISCAT II plus
VISCAT III separation, and subsequently VISCAT II versus
VISCAT III separation for each homogeneous area and model
output time. This separation was accomplished by setting
all VISCAT I observations equal to an arbitrary integer value
of zero and the combined VISCAT II plus VISCAT III observations
equal to an arbitrary integer value of one and generating

34

a linear regression equation to suitably describe the
resulting two distributions. This linear regression equation
was then used in the graphical plotting program BMDP5D,
from the BMDP Statistical Software [University of California,
1983], to generate a set of histograms describing the first
stage separation. Included with the graphical histogram
output is a listing of the individual frequency of observa-
tion (P), mean (μ) and standard deviation (σ) of each of the
specified visibility distributions. These statistics are
incorporated into the equal variance threshold algorithm
and a corresponding threshold value is calculated.

Following the first-stage threshold calculation, a
second linear regression equation is generated, based upon
only those VISCAT II plus VISCAT III observations which
exceed the previously calculated threshold value. This
effectively eliminates any VISCAT II plus VISCAT III obser-
vations less than the threshold value (i.e., those observa-
tions contained in the tail of the distribution), from being
included in the second-stage regression. The previous proce-
dure of generating corresponding histograms and statistics
is repeated, based upon all VISCAT II observations being
assigned an arbitrary integer value of zero and all VISCAT
III observations being assigned an integer value of one. A
second-stage equal variance threshold value is then calcu-
lated which separates VISCAT II from VISCAT III.

With the two-stage separation complete, the independent data set is processed through the governing equations and thresholds to obtain a set of observed visibility value results versus calculated "forecast" visibility value results. These results, in contingency table format for each evaluated case, are presented in Chapter V and Appendix G.

4. Quadratic Threshold Model (QUAD)

This model represents the second of two threshold models, developed by Lowe (1984a), which were evaluated in this study. The model uses an algorithm which requires the assumption that both the variances and the means of two normally distributed populations, which are to be separated by a threshold value, are equal. Similar to the EVAR model, a detailed discussion of the theoretical background of this scheme is addressed in Appendix A.

The general two-stage separation procedure employed with this model is identical to that described for the EVAR model in IV.C. above. The only difference between the QUAD and EVAR model is the algorithm, based upon a solution to a quadratic equation in this model, used to calculate the appropriate threshold values.

5. Maximum-Likelihood-of-Detection Model

The maximum-likelihood-of-detection criteria (MLDC) is an additional threshold technique which is included in this study as a possible alternative to the aforementioned EVAR and QUAD minimum probable error threshold models. The

MLDC involves calculating a threshold value based upon the assumptions that the population frequencies and variances of two normally distributed samples which are to be separated are identical. This technique is particularly well suited for cases where the threat frequency (i.e., number of threatening events divided by the total number of threat and non-threat events) approaches very small values (e.g., statistical rare events).

Unlike the EVAR and QUAD models, the two-stage separation employed with this technique utilizes a first-stage VISCAT I+II versus VISCAT III followed by a second-stage VISCAT I versus VISCAT II separation. In calculating the specific threshold values, the lowest frequency visibility category (usually the VISCAT I threat category) is assigned an arbitrary integer value of one. The remaining larger visibility category/ies are assigned the arbitrary integer value of zero. Proceeding in the same manner as described with the EVAR and QUAD models, population means are calculated for each separation stage. The threshold value is simply the mid-point between the two population means. A detailed discussion of the theoretical background of this scheme is addressed in Appendix A.

V. RESULTS

The general procedures outlined in Chapter I were fol-
lowed in evaluating the statistical scoring techniques for
the oceanic homogeneous areas 2, 3W and 4. Certain slight
modifications were required to handle the relatively low
frequency of visibility category I, in area 4 for the TAU-
00, TAU-24 and TAU-48 model output data sets. Fig. 2
displays the individual oceanic homogeneous areas for FATJUNE
1983. Tables I through III identify the frequency of occur-
rence of visibility categories I, II and III at TAU-00,
TAU-24 and TAU-48 for each of the evaluated homogeneous
areas.

In discussing the results of this study, specific comment
is focused upon the optimal model for each case as well as
any significant finding observed by the author. Certain
characteristics of the evaluated cases are repetitious and
are considered adequately described by their associated
figures. Consequently, the entire assemblage of figures in
Appendix G are not individually addressed. These figures
are nevertheless considered noteworthy, as they document the
performance of each tested model in this study, and are
included as a matter of record. The following presentation
of the results of this experimentation are arranged accord-
ing to the specific oceanic homogeneous area and model
output period.

In general, four models are evaluated for each of the predefined homogeneous areas/model forecast projections. The four models are: the Preisendorfer methodology utilizing NOGAPS model output predictors and a limited number of derived predictors (PR), the Preisendorfer methodology utilizing both NOGAPS model output predictors, derived predictors and linear regression equation predictors (PR+BMD), an equal variance linear regression threshold model (EVAR) and a quadratic linear regression threshold model (QUAD).

A. NORTH ATLANTIC OCEAN, AREA 2

Area 2 encompasses a geographic region that extends from the southeastern tip of Newfoundland, across the North Atlantic Ocean to the eastern coast of England, north to the Five Fingers of Iceland and back to the Canadian coast north of Newfoundland. Fig. 2 gives the pictorial representation of the area.

1. Area 2, TAU-00

Fig. 3 shows the relationship of equally populous grouping size to the adjusted A0 (dependent data) and the adjusted VISCAT I threat score (independent data) for the PR model. For this case, a grouping size of eight was selected. Results of the individual MAXPROB I, MAXPROB II and Natural Regression strategies are shown in Figs. 4a though 4c. The MAXPROB II strategy (Fig. 4b) produced the largest overall independent data VISCAT I adjusted threat

39

score, namely 0.23 (unadjusted, 0.30). This peak threat score occurs with the inclusion of the first predictor, E850, and declines marginally with the addition of the remaining four predictors. Of the three strategies, the natural regression strategy (Fig. 4c), yields the poorest overall threat scores with its peak threat score occurring with the addition of the fourth predictor. The predictors selected for this case are E850, ENTR, DVDP, U1000, and STRTH.

The associated functional dependence and A0/A1 statistics and 96%/05% confidence interval values for these predictors are shown in Fig. 5. The trend of functional dependence versus its 96% confidence interval shows that the specific functional dependence values associated with the chosen predictors never falls within the 96% confidence interval. At the first predictor level, for example, the functional dependence of ENTR upon E850 has a value of 0.1146 as compared to a 96% confidence interval value of 0.1039. This infers that the corresponding scores (i.e., threat scores, A0 and A1) are not statistically significant at the preselected 96% confidence interval level.

Fig. 6 shows the relationship of equally populous grouping size to the adjusted A0 (dependent data) and the adjusted VISCAT I threat score (independent data) for the PR+BMD model. For this case an equally populous grouping size of seven was selected. Results of the three individual

Preisendorfer strategies, along with the corresponding con-
tingency tables, can be seen in Figs. 7a through 7c. As
with the PR model, a maximum independent VISCAT I threat
score was obtained with the MAXPROB II strategy using the
first predictor selected, namely the linear regression equa-
tion predictor BMD1 (Appendix D). The overall independent
adjusted VISCAT I threat score achieved with this model is
0.29 (unadjusted, 0.36), which is .06 greater than that for
the PR model. The natural regression strategy (Fig. 7c)
provides the poorest resultant threat scores and these reach
their peak with the inclusion of the fifth predictor. The
predictors selected for this case are BMD1, ENTR, DVDP,
PS and PBLD.

The functional dependence, A1/A0 statistics and 96%/
05% confidence interval values for this model can be seen in
Fig. 8. As with the PR model, the specific functional
dependence values associated with the selected predictors
never fall below the calculated 96% functional dependence
confidence interval.

Figs. 9 and 10 show the contingency tables results
for the EVAR and QUAD threshold models. For each of these
models the independent adjusted VISCAT I threat scores have
identical values of 0.32 (unadjusted, 0.38).

The two-stage linear regression sequence employed
for both of these threshold models yields very similar basic
statistics. For the EVAR model, a threshold value of

0.648497 was calculated for the first-stage VISCAT I versus VISCAT II+III separation. This threshold was based upon a VISCAT I sample size of 190 observations, a mean of 0.659 and standard deviation of 0.205 and a combined VISCAT II+III sample size of 1722 observations, a mean of 0.927 and standard deviation of 0.122. The second-stage VISCAT II versus VISCAT III separation was based on a calculated threshold of 0.580128. Associated with this threshold value were 311 VISCAT II observations with a mean of 0.708 and standard deviation of 0.142 and 1473 VISCAT III observations with a mean of 0.850 and standard deviation of 0.131.

For the QUAD model, a threshold value of 0.642104 was calculated for the VISCAT I versus VISCAT II+III first-stage separation, based upon the sample addressed above. A second-stage quadratic threshold separating the VISCAT II and VISCAT III samples was calculated to be 0.580569. This VISCAT II sample contained 358 observations with a mean of 0.643 and standard deviation of 0.142 while the VISCAT III sample contained 1402 observations with a mean of 0.846 and standard deviation of 0.140.

While no significant difference appears to exist between the results of the two threshold models, the QUAD model yields a slightly higher A0 and slightly lower A1 values for both the dependent and independent data sets.

Table V shows a synopsis of the key statistical results for this case. The best models, as determined by

independent adjusted VISCAT I threat scores, are the two threshold models. Of these two models, the QUAD model achieves the highest adjusted A0, namely 3.16% (unadjusted, 80.73%).

   2.   Area 2, TAU-24

   Fig. 11 shows the relationship of equally populous grouping size to the adjusted A0 (dependent data) and the adjusted VISCAT I threat score (independent data) for the PR model. For this model, adjusted dependent A0 values of -0.03 and adjusted independent threat score of -.01 were obtained for grouping sizes four through nine. At the grouping size of ten, a jump in scores was realized and thus ten is identified as the only possible selection. An associated difficulty in utilizing a grouping size of eight, nine or ten, is that local computer storage resources are limited to two megabytes. This decreases the usual five predictor array to only four predictors as witnessed in this case. The results of the three Preisendorfer strategies are shown in Figs. 12a through 12c. For this model, the MAXPROB I and MAXPROB II strategies yield identical maximum independent adjusted VISCAT I threat scores of 0.21 (unadjusted, 0.27). For each of the maximum probability strategies, an initial threat score of 0.19 (unadjusted, 0.25) was achieved with the first predictor, E850, solely. The slight increase to the overall peak threat score was obtained with the inclusion of the second predictor, ENTR, with subsequent independent

43

VISCAT I threat scores decreasing at the third and fourth
predictor levels. Of the three strategies, natural regression
(Fig. 12c) yielded the poorest overall threat score and per-
cent correct values. These relative peak scores for the
natural regression strategy occur with the inclusion of the
fourth and final predictor. The predictors selected for this
model were: E850, ENTR, DVDP and DIV925.

The associated functional dependence, A0/A1 statis-
tics and 96%/05% confidence intervals for this model are
shown in Fig. 13. For this case, the third and fourth pre-
dictors' root-sum-square functional dependence values exceed
the associated 96% confidence interval values, indicating
significant statistical interdependence of these predictors
at this confidence interval level.

Fig. 14 shows the relationship of equally populous
grouping size to the adjusted A0 (dependent data) and the
adjusted VISCAT I threat score (independent data) for the
PR+BMD model. The dramatic increase in independent threat
score at grouping size of seven identifies it as the optimal
selection. The results of the three Preisendorfer strategies
are shown in Figs. 15a through 15c. For this model, the
MAXPROB I and MAXPROB II strategies yield identical maximum
independent adjusted VISCAT I threat scores of 0.26 (unad-
justed, 0.32). This peak score was achieved with the inclu-
sion of the first predictor. In this case, the first selected
predictor is the second generated linear regression equation

44

predictor, BMD2 (Appendix D). Following the initial threat

score maxima, the scores decreased with the addition of the

subsequent four predictors. While some fluctuation in the

threat score trend was observed with the MAXPROB II strategy,

independent VISCAT I threat scores never surpassed their

initial maximum value. Of the three strategies, natural

regression (Fig. 15c) provides the poorest overall indepen-

dent VISCAT I threat score of 0.21 (unadjusted, 0.28). This

score was achieved with the addition of the fifth and final

predictor. The predictors selected for this model were:

BMD2, VRT925, ENTR, U1000 and RH.

The associated functional dependence, A0/A1 statis-

tics and 96%/05% confidence intervals are shown in Fig. 16.

For this model, a comparison of functional dependence and

functional dependence 96% confidence interval values indi-

cates that the final three predictors have root-sum-square

functional dependence values which are too large to ensure

significant statistical independence at the 96% confidence

interval level.

Figs. 17 and 18 show the contingency tables and

associated statistics for the EVAR and QUAD threshold models.

For each of the models, the independent adjusted VISCAT I

threat scores have identical values, namely 0.29 (unadjusted,

0.24). The two-stage linear regression sequence employed

for both of these models yields fairly similar statistical

results. For the EVAR model, a threshold value of 0.674932

was calculated for the first-stage VISCAT I versus VISCAT II+III separation based upon a VISCAT I sample size of 180, a mean of 0.682 and a standard deviation of 0.227 and a VISCAT II+III sample size of 1580, a mean of 0.938 and a standard deviation of 0.109. The second-stage VISCAT II versus VISCAT III separation was based upon a calculated threshold value of 0.601717. Associated with this threshold were 300 VISCAT II observations with a mean of 0.733 and standard deviation of 0.149 and 1339 VISCAT III observations with a mean of 0.857 and standard deviation of 0.121.

For the QUAD model, a threshold value of 0.675210 was calculated for the first-stage VISCAT I versus VISCAT II+III separation based upon the sample statistics addressed above. The second-stage threshold separating the VISCAT II and VISCAT III samples was calculated to be 0.617455. The VISCAT II sample contained 300 observations with a mean of 0.739 and a standard deviation of 0.125. The VISCAT III sample contained 1339 observations with a mean of 0.885 and standard deviation of 0.118.

While the VISCAT I threat scores for both the dependent and independent data sets are identical for the two models, differences in other statistics are apparent. The EVAR model (Fig. 17), for example, has the higher independent adjusted A0 scores, namely 2.96% (unadjusted, 81.34%), as compared to scores of -63.31% (unadjusted, 68.60%) for the QUAD model (Fig. 18).

In general, for area 2, TAU-24, the threshold models again provide the highest independent VISCAT I threat scores (Table V). Of the two threshold models, the EVAR model has a slight edge in A0 scores.

3. Area 2, TAU-48

Fig. 19 shows the relationship of equally populous grouping size to the adjusted A0 (dependent data) and the adjusted VISCAT I threat score (independent data) for the PR model. For this model, the initial peak values of dependent A0 and independent VISCAT I threat score at the grouping size of four did not sufficiently ascertain four as the optimal grouping selection. For this grouping size, the second selected predictor ENTR had a functional dependence of 0.2952 as compared to the calculated functional dependence 96% confidence interval value of 0.1932. The large disparity between the two functional dependence values indicates a significant statistical correlation between E850 and ENTR at a grouping size of four and thus grouping size four was dropped from consideration. The selected grouping size of nine, which unfortunately carries with it the requirement of a very large computer storage forecast array at the fifth predictor level, had a functional dependence value 0.0930 as compared to a functional dependence 96% confidence interval value of 0.0970 and thus was selected as the optimal grouping size. The associated functional dependence, A0/A1 statistics and 96% confidence intervals are shown in Fig. 20. The first

47

three predictors selected have functional dependence values sufficiently low enough to ensure no significant predictor interdependence.

The results of the three Preisendorfer strategies are shown in Figs. 21a through 21c. The maximum independent VISCAT I threat score achieved for the three strategies was 0.17 (unadjusted, 0.26) and was obtained with the MAXPROB II strategy with the addition of the fifth predictor. It should be noted that the independent adjusted VISCAT I threat scores achieved by both the MAXPROB I and MAXPROB II strategies reached near peak values of 0.16 (unadjusted, 0.24) with the addition of the second predictor, thus greatly minimizing the size of the associated forecast array. Of the three strategies, natural regression (Fig. 21c) yielded the poorest overall adjusted independent VISCAT I threat score, namely 0.09 (unadjusted, 0.18). This score was achieved with the inclusion of the fourth predictor in the forecast array. The predictors selected for this model were E850, ENTR, DVDP, DRAG and DIV925.

Fig. 22 shows the relationship of equally populous grouping size to the adjusted A0 (dependent data) and the adjusted VISCAT I threat score (independent data) for the PR+BMD model. For this model a grouping size of nine was selected. The results of the MAXPROB I, MAXPROB II and natural regression strategies are shown in Figs. 23a through 23c. For this model, MAXPROB I and MAXPROB II provide

48

identical maximum independent adjusted VISCAT I threat scores
of 0.31 (unadjusted, 0.37). These scores were achieved with
the inclusion of the second linear regression equation pre-
dictor BMD2 (Appendix D). For each of these strategies, the
independent VISCAT I threat scores decrease with the addi-
tion of the second and subsequent predictors. While a slight
upward progression is noticed with the MAXPROB II strategy,
the peak score observed at the first predictor level is
never surpassed. Of the three Preisendorfer strategies,
natural regression (Fig. 23c), yields the poorest overall
independent VISCAT I threat score, namely 0.18 (unadjusted,
0.26). This score occurs with the inclusion of the fifth
predictor and culminates in a slow increase in threat score
as each predictor is sequentially added to the forecast array.
The predictors selected for this model were BMD2, VRT925,
ENTR, U500 and DRAG.

Fig. 24 shows the functional dependence, A0/A1 sta-
tistics and 96%/05% confidence interval values for the
selected predictors. For this model, the second and third
predictors' functional dependence values fall below the 96%
confidence interval and thus are not significantly inter-
dependent upon one another. This trend changes with the
fourth and fifth predictors which have functional dependence
values greater than the calculated 96% confidence interval
values.

Figs. 25 and 26 show the contingency table results
for the EVAR and QUAD threshold models. For each of these

49

models, the independent adjusted VISCAT I threat scores have identical values of 0.21 (unadjusted, 0.29).

The two-stage linear regression sequence used to separate the three visibility categories yield very similar results for the two threshold models. For the EVAR model, a threshold value of 0.652554 was calculated for the first-stage VISCAT I versus VISCAT II+III sample separation. This threshold value is based upon a VISCAT I sample size of 182 observations with a mean of 0.686 and a standard deviation of 0.267 and a combined VISCAT II+III sample of 1670 observations with an associated mean of 0.930 and standard deviation of 0.106. The second stage VISCAT II versus VISCAT III regression separation yielded a threshold value of 0.572257 based upon 355 VISCAT II observations, with a mean of 0.711 and standard deviation 0.135, and 1408 VISCAT III observations with a mean of 0.834 and a standard deviation of 0.130.

For the QUAD model, a very similar threshold value of 0.652554 was calculated for the first-stage VISCAT I versus VISCAT II+III separation based upon the sample first-stage statistics addressed above. A second-stage threshold value of 0.564579 was calculated based upon 330 VISCAT II observations with a mean of 0.724 and standard deviation of 0.128, and 1407 VISCAT III observations with a mean of 0.833 and a standard deviation of 0.127.

In general, the results of these two threshold models are nearly identical. The EVAR model shows a very slight advantage in adjusted independent A0 scores, namely 7.07% (unadusted, 80.11%) as compared to 5.05% (unadjusted, 79.68%) for the QUAD model. Similarly, the EVAR model yielded a slightly higher independent adjusted threat score for VISCAT I combined with VISCAT II of 0.02 (unadjusted, 0.23) versus an adjusted score of 0.01 (unadjusted, 0.22) for the QUAD model.

For Area 2, TAU-48 the PR+BMD model provides the highest overall independent VISCAT I threat score (Table V). The difference between the independent adjusted VISCAT I threat scores for the PR+BMD model and the two threshold models is minimal, namely 0.02, while the PR model is 0.14 lower.

B. NORTH ATLANTIC OCEAN, AREA 3W

Area 3W was the North Atlantic homogeneous area selected by Karl (1984) for his initial TAU-00 MOS experimentation. This area borders the United State's eastern seaboard from the vicinity of Cape Charles, Virginia to the southeastern tip of Newfoundland. The area encompasses a large portion of the Georges Banks region and extends to approximately 45° W longitude. The specific detail and proximity of this area can be seen in Fig. 2.

Area 3W constitutes the homogeneous area with the highest relative frequency of VISCAT I observations with approximately

51

19% of the total number of visibility observations being less than 2 kilometers in the TAU-00, TAU-24 and TAU-48 periods. The TAU-24 and TAU-48 prognostic periods will be addressed in this document. The reader is advised to consult Karl (1984) for detailed information concerning area 3W, TAU-00.

1. Area 3W, TAU-24

Fig. 27 shows the relationship of equally populous grouping size to the adjusted A0 (dependent data) and the adjusted VISCAT I threat score (independent data) for the PR model. For this case a grouping size of six was selected. Results of the three Preisendorfer strategies are shown in Figs. 28a through 28c. The MAXPROB II strategy achieves a slightly higher independent adjusted VISCAT I threat score of 0.21 (unadjusted, 0.36) as compared to a score of 0.20 (unadjusted, 0.35) for the MAXPROB I method. For each of these strategies, the maximum threat score is reached with the inclusion of the fifth and final predictor in the fore-cast array. The general trend of these two strategies is nearly identical and show an initial rise in threat score at the first predictor level, a slight decrease with the addition of the second and third predictors and a secondary rise at the fourth and fifth predictor levels. The poorest results for this case were achieved with the natural regres-sion strategy (Fig. 28c), for which an independent adjusted VISCAT I threat score of 0.16 (unadjusted, 0.32) was achieved. This score was similarly reached with the addition of the

fifth and final predictor. The predictors selected for this model were DTDP, SHWRS, ENTR, U1000 and DUDP.

Fig. 29 shows the functional dependence, A0/A1 statistics and 96%/05% confidence intervals for this model. For this case only the second predictor has a functional dependence value which falls below the corresponding 96% confidence interval and thus meets the requisite conditions regarding predictor interdependence. Consequently, the greatest independent threat score achieved, which coincidently meets the functional dependence criteria, occurs with the MAXPROB II strategy at the inclusion of the second predictor. The threat score achieved in this particular instance has a value of 0.13 (unadjusted, 0.30).

Fig. 30 shows the relationship of equally populous grouping size to the adjusted A0 (dependent data) and the adjusted VISCAT I threat score (independent data) for the PR+BMD model. For this case a grouping size of five was selected. Results of the MAXPROB I, MAXPROB II and natural regression strategies are shown in Figs. 31a through 31c. For this model, the two maximum probability strategies provide identical peak independent adjusted VISCAT I threat scores of 0.28 (unadjusted, 0.42) at the first predictor level. For both of these strategies, the addition of subsequent predictors produces a steady drop off in threat score values. The poorest overall results for this case are achieved with the natural regression strategy (Fig. 31c).

53

This method yields an independent adjusted VISCAT I threat score of 0.17 (unadjusted, 0.33) which was obtained with the addition of the fifth and final predictor. The predictors selected for this model were BMD1, D500, DVDP, ENTR and U850.

Fig. 32 shows the associated functional dependence, A1/A0 statistics and 96%/05% confidence interval values for the predictors chosen for this model. The functional dependence versus the 96% confidence interval follows a peculiar trend where the second predictor is significantly dependent upon the first predictor but the third and fourth predictors are conversely sufficiently uncorrelated with the prior predictors to ensure no significant functional dependence. The final predictor returns to being functionally dependent upon the previous predictors. This trend indicates that the relative contribution of the second and subsequent predictors is statistically not significant at the preselected 96% confidence interval level.

Figs. 33 and 34 show the contingency table results for the EVAR and QUAD threshold models. The results of these models are very similar with the EVAR model yielding an independent adjusted VISCAT I threat score of 0.17 (unadjusted, 0.33) as compared to a corresponding threat score of 0.16 (unadjusted, 0.32) for the QUAD model.

For the EVAR model, a first-stage threshold value of 0.561855 was calculated based upon 270 VISCAT I observations

with a mean of 0.590 and standard deviation of 0.203 and
1145 VISCAT II+III observations with a mean of 0.861 and
standard deviation of 0.168. The second-stage VISCAT II
versus VISCAT III separation was based upon a calculated
threshold value of 0.542363. Associated with this threshold
were 299 VISCAT II observations with a mean of 0.647 and
standard deviation of 0.146 and 938 VISCAT III observations
with a mean of 0.794 and standard deviation of 0.153.

For the QUAD model, a similar threshold value of
0.5559971 was calculated based upon the first-stage regres-
sion separation listed above. A second-stage threshold
value of 0.540874, separating VISCAT II from VISCAT III, was
calculated based upon 305 VISCAT II observations with a mean
of 0.639 and standard deviation of 0.157 and 940 VISCAT III
observations with a mean of 0.793 and standard deviation
of 0.154.

In general, the PR+BMD model produced the best overall
results for this case, followed by the PR model and lastly
the two threshold models (Table V). The independent adjusted
A0 score of the PR+BMD model, which corresponds to the maxi-
mum independent adjusted VISCAT I threat score, is similarly
a maximum value for this case, namely 21.68% (unadjusted,
74.96%).

2. <u>Area 3W, TAU-48</u>

Fig. 35 shows the relationship of equally populous
grouping size to the adjusted A0 (dependent data) and the

adjusted VISCAT I threat score (independent data) for the PR

model. For this model, an equally populous grouping size of

six was selected. The results of the three Preisendorfer

strategies are shown in Figs. 36a through 36c. For this

case, the MAXPROB II strategy achieves the highest indepen-

dent adjusted VISCAT I threat score of 0.18 (unadjusted,

0.33) as compared to 0.17 (unadjusted, 0.32) for the MAXPROB

I strategy and 0.12 (unadjusted, 0.22) for natural regression.

The maximum score for each of the three methods was achieved

with the addition of the fifth and final predictor. The

statistical score trends for the two maximum probability

strategies are very similar and reach identical near peak

independent VISCAT I threat scores of 0.15 (unadjusted, 0.30)

at the first predictor level. This is particularly note-

worthy when considering that the computer forecast array

size may be of significant operational concern. The poorest

strategy for this case is natural regression. The predictors

selected for this case are DTDP, SHWRS, ENTR, U850 and

DIV925.

Fig. 37 shows the functional dependence, A0/A1 sta-

tistics and 96%/05% confidence interval values for this

model. In this case, only the second predictor strictly

meets the requisite functional dependence criteria ensuring

no significant dependence of one predictor upon another. The

MAXPROB II independent adjusted A0 score, which corresponds

to the peak independent VISCAT I threat score for this case,

56

is -2.47% (unadjusted, 66.49%) as compared to A0 scores of

4.94% (unadjusted, 68.91%) for MAXPROB I and -16.87% (unad-

justed, 61.78%) for natural regression.

Fig. 38 shows the relationship of equally populous

grouping size to the adjusted A0 (dependent data) and the

adjusted VISCAT I threat score (independent data) for the

PR+BMD model. For this case a grouping size of five was

selected. The results of the three Preisendorfer strategies

are shown in Figs. 39a through 39c. For this case, the

MAXPROB II strategy provides the highest independent ad-

justed VISCAT I threat score of 0.30 (unadjusted, 0.43).

This peak score slightly surpasses the score of 0.29

(unadjusted, 0.42) achieved by the MAXPROB I method. The

trends for these two strategies are nearly identical, showing

only a slight oscillation in independent threat scores as

predictors are added. The peak score achieved by the MAXPROB

II scheme is at the fifth predictor level while the peak

value for MAXPROB I is obtained with the inclusion of the

first predictor. It should be noted that the results at

the first predictor level for the two maximum probability

strategies are identical. A forecast array predicated upon

a one predictor versus five predictor array size requires

four orders of magnitude less computer storage resources and

is therefore a desirable characteristic for an operational

forecast system. Additionally, the independent adjusted

A0 scores, achieved by both schemes, have identical maximum

values of 19.25% (unadjusted, 73.76%) at the first predictor level as compared to a maximum value of 12.76% (unadjusted, 71.47%) for the natural regression strategy at the fifth predictor level. The poorest strategy for this case is natural regression (Fig. 39c). The independent VISCAT I threat scores for this scheme initially yield very low threat score values at the first and second predictor levels with a subsequent rapid rise at the third, fourth and fifth predictor levels. This rapid rise however produces a threat score value of only 0.19 (unadjusted, 0.34) and a corresponding A0 of -1.65% (unadjusted, 66.76%) at the fifth and final predictor level. The predictors selected for this model are BMD2, U1000, ENTR, DVDP and EAIR.

Fig. 40 shows the functional dependence, A0/A1 statistics and 96%/05% confidence interval values for this model. For this case, three of the five selected predictors do not meet the 96% confidence interval criteria for functional independence. This further justifies the use of a single predictor forecast array for possible operational use.

Figs. 41 and 42 show the contingency table results for the EVAR and QUAD threshold models. The results of these two models are very similar with the EVAR model showing a slight advantage in independent adjusted VISCAT I threat score of 0.15 (unadjusted, 0.33) versus 0.14 (unadjusted, 0.31) for the QUAD model. Similarly, the EVAR model achieves a slightly higher independent adjusted A0 of 13.17%

58

(unadjusted, 71.60%) versus 12.76% (unadjusted, 71.47%) for the QUAD model.

For the EVAR model, a first-stage regression threshold value of 0.577452 was calculated based upon a VISCAT I sample size of 290 observations with a mean of 0.620 and standard deviation of 0.211 and a combined VISCAT II+III sample size of 1197 observations with a mean of 0.860 and standard deviation of 0.153. A second-stage threshold value of 0.548587 separating VISCAT II and VISCAT III was calculated based upon a VISCAT II sample size of 328 with a mean of 0.654 and standard deviation of 0.142 and 971 VISCAT III observations with a mean of 0.777 and standard deviation of 0.136.

The first-stage threshold value of 0.572592 for the QUAD model was generated with the above VISCAT I versus VISCAT II+III sample statistics. A second-stage threshold value of 0.548717 was based upon 333 VISCAT II observations with a mean of 0.649 and standard deviation of 0.138.

In general, the model which produces the highest independent VISCAT I threat score for this case is the PR+BMD model while the highest independent A0 score is achieved with the EVAR threshold model (Table V). The relatively large independent threat score dominates the scores however, and therefore the PR+BMD model is determined to be the optimal model in this case.

C.   NORTH ATLANTIC OCEAN, AREA 4

Area 4 was selected for evaluation because of its relatively low frequency (approximately 3% of the total) of VISCAT I observations. It was hoped that this area would statistically represent a region where there was an insufficient number of VISCAT I observations to allow for study of a forecast region where results were anticipated to be poor, yet enough VISCAT I observations to avoid any "rare event" statistical entanglements.

This area encompasses a broad region of the North Atlantic Ocean which is generally to the south of area 2 and east and southeast of area 3W. Area 4's southern border reaches to the northeastern tip of Portugal and extends northward through the English Channel to encompass the southern portion of the North Sea.

1.   Area 4, TAU-00

Fig. 43 shows the relationship of equally populous grouping size to the adjusted A0 (dependent data) and the adjusted VISCAT I threat score (independent data) for the PR model. Several unique characteristics were encountered for this case which had not been previously been observed. The previously observed variation of dependent A0 and independent threat scores, associated with the sequential variation in grouping size from four through ten, was not initially achieved. For this case, non-zero values of dependent A0 and independent VISCAT I threat score were only achieved

after three iterations of the predictor selection procedure. The grouping size of four was deleted from consideration in the third iteration because the associated A0 value, achieved at that predictor level, did not exceed the previous A0 value at the second predictor level. For this case, the independent VISCAT I threat scores maintained indentically low values, while a relative peak in A0 was achieved at a grouping size of eight. For this reason, eight was selected as the optimal grouping size for this model.

Figs. 44a through 44c represent the results of the three Preisendorfer strategies. For each of the schemes, the independent VISCAT I threat scores at the first three predictor levels reveal the near-zero scores encountered in the grouping size selection process. The highest independent adjusted VISCAT I threat score, namely 0.08 (unadjusted, 0.11) is achieved with the MAXPROB II strategy at the fifth and final predictor level. For this model, the MAXPROB I and natural regression strategies yield only slightly inferior, identical independent adjusted threat scores of 0.04 (inadjusted, 0.07) which are achieved at the fifth predictor level. The MAXPROB I strategy yields the highest independent adjusted A0 score of -15.77% (unadjusted, 82.45%) as compared to scores of -28.63% (unadjusted, 80.50%) for natural regression and -34.85% (unadjusted, 79.56%) for the MAXPROB II strategy. The predictors selected for this model are V500, DVDP, STRTTH, E500 and ENTR.

Fig. 45 shows the functional dependence, A0/Al statistics and 96%/05% confidence interval values for this model. In this particular case, only the third predictor displays a functional dependence value less than the 96% confidence interval value. This renders the threat scores achieved by this model, beyond the first predictor level, statistically not significant, if strict adherence to the basic functional dependence criteria is followed.

Fig. 46 shows the relationship of equally populous grouping size to the adjusted A0 (dependent data) and the adjusted VISCAT I threat score (independent data) for the PR+BMD model. For this case a grouping size of nine was selected. The results of the three Preisendorfer strategies are shown in Figs. 47a through 47c. Generally, the results for this model differ very little from the previously discussed PR model. This case reflects the first and only occurrence where the Preisendorfer methodology coupled with linear regression equation predictors (PR+BMD model) did not yield superior results to the PR model. The trends for these three strategies are generally quite similar. The MAXPROB II scheme provides the highest independent adjusted VISCAT I threat score of 0.09 (unadjusted, 0.11), as compared to scores of 0.08 (unadjusted, 0.11) for MAXPROB I and 0.07 (unadjusted, 0.10) for natural regression. For each of these three strategies, the maximum independent VISCAT I threat score was achieved with the inclusion of the fifth

62

and final predictor. The independent A0 scores associated

with the peak threat scores are near their lowest values at

the fifth predictor level with the MAXPROB I scheme yielding

the highest relative independent adjusted A0 of -19.09%

(unadjusted, 81.95%) followed by natural regression with a

score of -26.56% (unadjusted, 80.82%) and lastly MAXPROB II

with a score of -39.42% (unadjusted, 78.87%). The predictors

selected for this model are BMD2, DUDP, ENTR, DEDP and

U1000.

Fig. 48 shows the functional dependence, A0/A1 sta-

tistics and 96%/05% confidence interval values for this

model. Generally, the relative difference between the func-

tional dependence and 96% functional dependence confidence

interval values is much less severe than with the previously

discussed model. While only the third predictor's functional

dependence value meets the 96% confidence interval criteria

for significance, the other predictors are only marginally

insignificant.

The application of the EVAR and QUAD threshold models

to this case presented results which had not been previously

encountered. The first-stage VISCAT I versus VISCAT II+III

separation calculation results in a QUAD threshold value

which is imaginary and an unrealistic EVAR threshold value

of 209.588882. These thresholds were calculated based upon

a VISCAT I sample size of 85 observations with a mean of

-1.012 and standard deviation of 6.280 and a combined VISCAT

63

II+III sample size of 3096 observations with a mean of
-1.864 and standard deviation of 7.092. These results are
linked to the preponderance of VISCAT III observations in
this area coupled with the fact that these employed threshold
models are designed to provide for a minimum error when
separating samples. These results indicate that a forecast
model predicated upon the dependent data set employed in this
case would strictly forecast VISCAT III.

2. <u>Area 4, TAU-24</u>

Fig. 49 shows the relationship of equally populous
grouping size to the adjusted A0 (dependent data) and the
adjusted VISCAT I threat score (independent data) for the
PR model. This case required three iterations of the four
through ten grouping size calculations before any non-zero
dependent A0 or independent VISCAT I threat score values were
achieved. Additionally, for the grouping size of four, no
increase in A0 was observed at the second predictor level
and therefore was deleted from consideration. A grouping
size of five was ultimately selected for this model.

Figs. 50a through 50c represent the results of the
three Preisendorfer strategies. Generally, the independent
VISCAT I threat scores yielded for these schemes are poor
with the highest independent adjusted VISCAT I threat score
of 0.05 (unadjusted, 0.07) being achieved by the MAXPROB II
strategy at the fifth predictor level followed by MAXPROB I
with a score of 0.02 (unadjusted, 0.05) and natural regression

64

with 0.01 (unadjusted, 0.04). The A0 scores corresponding
to these values provide for a slightly different scoring
hierarchy. The highest independent adjusted A0 score,
namely 0.94% (unadjusted, 85.64%), is attained by the
MAXPROB I strategy as compared to scores of -30.05% (unad-
justed, 81.34%) for natural regression and -37.56% (unad-
justed, 80.05%) for MAXPROB II. The predictors selected for
this model are VRT925, DTDP, ENTR, V850 and DVRTDP.

Fig. 51 shows the functional dependence, A0/A1 sta-
tistics and 96%/05% confidence interval values for this
model. For this case, each predictor following VRT925 proved
to be significantly functionally dependent on its predecessors
and therefore only a single predictor forecast array is
justifiable for this model.

Fig. 52 shows the relationship of equally populous
grouping size to the adjusted A0 (dependent data) and the
adjusted VISCAT I threat score (independent data) for the
PR+BMD model. As in the previous case, three iterations of
dependent A0 and independent VISCAT I calculations were
required before any non-zero scores were achieved. Addi-
tionally, in this case, the grouping sizes of four and five
were deleted from consideration as they did not provide an
increase of A0 at the second predictor levels. The grouping
size ultimately selected for this model was nine.

Figs. 53a through 53c show the results of the three
Preisendorfer strategies for this model. The scores for

this model, as in the previously described case, are quite poor and show very little improvement over the PR model. The highest independe_. adjusted VISCAT I threat score, namely 0.06 (unadjusted, 0.09), was achieved by the MAXPROB II strategy followed by scores of 0.05 (unadjusted, 0.07) for the MAXPROB I strategy and 0.03 (unadjusted, 0.06) for natural regression. The corresponding independent adjusted AO scores show a maximum score of -19.25% (unadjusted, 82.71%) for the MAXPROB I strategy followed by scores of -30.05% (unadjusted, 81.14%) for natural regression and -39.91% (unadjusted, 79.71%) for the MAXPROB II strategy.

Fig. 54 shows the functional dependence, AO/Al statistics and 96%/05% confidence interval values for this model. For this case, the relative magnitude of the difference between the actual functional dependence and its 96% confidence interval value is quite small. It is only at the second predictor level, that the calculated values do not exceed the corresponding 96% confidence interval value.

Fig. 55 shows the contingency table results for the EVAR threshold model. The QUAD model provided an imaginary threshold value at the second regression stage and therefore did not allow completion of the entire separation sequence. This represents the only occurrence where a valid equal variance threshold was calculated but a corresponding quadratic threshold proved to be imaginary.

The results of the EVAR model were in keeping with those of the previously described PR and PR+BMD models. An independent adjusted VISCAT I threat score of 0.05 (unadjusted, 0.07), was achieved with a corresponding independent adjusted A0 value of -13.15% (unadjusted, 83.59%).

The first-stage regression separation for this model was based upon a calculated threshold value of 0.908275. Associated with this threshold were 449 VISCAT I observations with a mean of 0.953 and standard deviation of 0.030 and 2489 VISCAT II+III observations with a mean of 0.976 and standard deviation of 0.027. The second-stage VISCAT II versus VISCAT III separation was based upon a calculated threshold value of 0.683569. Associated with this threshold is a VISCAT II sample size of 69 observations with a mean of 0.831 and standard deviation of 0.066 and 887 VISCAT III observations with a mean of 0.912 and standard deviation of 0.078.

For the QUAD model, an initial first-stage threshold value of 0.908275 was successfully calculated with the sample statistics addressed above. The second-stage regression attempt was based upon a VISCAT II sample size of 65 observations with a mean of 0.829 and standard deviation of 0.067 and VISCAT III sample size of 853 observations with a mean of 0.905 and standard deviation of 0.079. These sample statistics produced an imaginary threshold value.

In general Area 4, TAU-24 is characterized by very poor independent VISCAT I threat scores. This indicates

that there is very little skill in forecasting visibility conditions of less than or equal to 2 kilometers in this area. The evaluated models show little variation in scores with the best relative model for this area and forecast projection being the PR+BMD model (Table V).

3. Area 4, TAU-48

Fig. 56 shows the relationship of equally populous grouping size to the adjusted A0 (dependent data) and the adjusted VISCAT I threat score (independent data) for the PR model. As in the TAU-00 and TAU-24 forecast projections for this area, the calculation and evaluation of dependent A0 and independent VISCAT I threat scores had to be run through three iterations before any non-zero statistics were obtained. The grouping sizes of four and five were deleted from consideration because the addition of predictors at those grouping sizes did not provide for any increase in A0 scores. Based on an evaluation of the results as shown on Fig. 56, a grouping size of seven was selected.

Figs. 57a through 57c show the results of the three Preisendorfer strategies for this model. In general, the near-zero statistical scores encountered in the grouping selection process, can be seen through the third predictor level, along with a noticeable increase in scores at the fourth and fifth predictor level. The MAXPROB I strategy yields the highest independent adjusted VISCAT I threat score, namely 0.18 (unadjusted, 0.20), for this model

followed by a natural regression score of 0.16 (unadjusted, 0.19) and lastly by MAXPROB II with a score of 0.13 (unadjusted, 0.16). This is the first and only encountered case where the natural regression strategy effectively achieved a maximum independent VISCAT I threat score which is higher than either of the two maximum probability strategies. The independent A0 scores associated with these peak independent VISCAT I threat scores, adhere to this same scoring sequence, with MAXPROB I achieving a value of -14.94% (unadjusted, 81.86%) followed by natural regression with a score of -27.80% (unadjusted, 79.83%) and MAXPROB II with an independent adjusted A0 of -43.98% (unadjusted, 77.78%).

Fig. 58 shows the functional dependence, A0/A1 statistics and 96%/05% confidence interval values for this model. In this case, only the third predictor's functional dependence value falls below the associated 96% confidence interval value. The predictors selected for this model are VRT925, DVRTDP, ENTR, DUDP and RH.

Fig. 59 shows the relationship of equally populous grouping size to the adjusted A0 (dependent data) and the adjusted VISCAT I threat score (independent data) for the PR+BMD model. As in the previous area 4 cases, three complete iterations of the four through ten grouping size calculations had to be performed before any non-zero dependent A0 or independent VISCAT I values were achieved. The grouping size ultimately selected for this model was nine.

Figs. 60a through 60c represent the results of the
three Preisendorfer strategies. A unique result of this
model is that for the first time, the PR+BMD model did not
achieve independent VISCAT I threat scores which exceed those
achieved by the PR model. The peak independent adjusted
VISCAT I threat score of 0.17 (unadjusted, 0.20) is achieved
by the MAXPROB II strategy at the third predictor level.
The predictors selected for this model are BMD1, DDVDP,
DUDP, ENTR and PRECIP.

Fig. 61 shows the functional dependence, A0/A1 sta-
tistics and 96%/05% confidence interval values for this
model. Only the second predictor sufficiently meets the 96%
confidence interval significance criteria. Based upon a
strict adherence to the preselected 96% confidence interval
significance requirements, these functional dependence
values provide cause for uncertainty in the representative-
ness of the scores achieved after the second predictor level.

Figs. 62 and 63 show the contingency table results
for the EVAR and QUAD threshold models. The results of these
models are very similar and generally quite poor. The QUAD
model achieves the highest relative independent adjusted
VISCAT I threat score of 0.01 (unadjusted, 0.04) as compared
to a score of -0.01 (unadjusted, 0.02) for the EVAR model.
The QUAD model similarly achieves the highest independent
adjusted A0 score of -2.07% (unadjusted, 83.89%) versus a
score of -7.88% (unadjusted, 82.97%) for the EVAR model.

70

For the EVAR model, a first-stage regression threshold value of 0.847203 was calculated based upon a VISCAT I sample size of 109 observations with a mean of 0.918 and standard deviation of 0.052 and 2947 VISCAT II+III observations with a mean of 0.967 and standard deviation of 0.037. The second-stage VISCAT II versus VISCAT III separation was based upon a calculated threshold value of 0.629338. Associated with this threshold is 495 VISCAT II observations with mean of 0.861 and standard deviation of 0.103.

For the QUAD model, a first-stage separation threshold value of 0.847203 was calculated upon the associated sample statistics addressed above. A second-stage threshold value of 0.613739 was calculated based upon 481 VISCAT II observations with a mean of 0.770 and standard deviation of 0.089 and 2522 VISCAT III observations with a mean of 0.862 and standard deviation of 0.100.

The overall results associated with the area 4, TAU-48 case are particularly unique. The independent adjusted TAU-48 VISCAT I threat score represents the highest area 4 independent VISCAT I threat score (by a minimum of 0.09) achieved, as compared to TAU-00 or TAU-24. The maximum independent VISCAT I threat score is achieved by the PR model.

Following the completion of the testing and evaluation of the FATJUNE 1983 data set, a series of preliminary experiments were performed with the May 15 to June 23 1984 data

71

set for the TAU-24 model forecast projection. These experiments consisted of evaluating the TAU-24, 1983 forecast arrays and equations (generated with FATJUNE 1983 data) with training and testing cases of TAU-24, 1984 data. In performing this evaluation, the 1984 data set was divided into "dependent" and "independent" portions. This data separation is a function of the specific mechanics of the computer programs utilized in this study and is not associated with the generation of additional forecast arrays or equations. Two homogeneous areas were evaluated, namely area 2 and area 3W. This essentially provided an independent verification of the utility of the 1983 forecast arrays and equations in predicting observed 1984 visibility in these areas.

In general, the skill and contingency table results for these experiments compare very favorably to those achieved with the FATJUNE 1983 data. A summary of the results of each of the evaluated models is provided in Table VII. For area 2, a peak independent adjusted VISCAT I threat score (1984 data), namely 0.27 (0.33 unadjusted), was achieved with each of the two threshold models. This compares to a peak independent adjusted VISCAT I threat score (1983 data) of 0.29 (0.34 unadjusted) achieved by the same two models. For area 3W, a peak independent adjusted threat score (1984 data) of 0.28 (unadjusted, 0.42) similarly compares to a peak independent adjusted threat score (1983) of 0.13 (unadjusted, 0.36).

The overall results of the 1984 data experiments can be seen in Table VII and are represented by Fig. 64 which illustrates the results of the PR+BMD model, MAXPROB II strategy, for area 2, TAU-24.

A review of the results associated with area 4 for TAU-00, TAU-24 and TAU-48 indicates that none of the models evaluated achieved very encouraging skill and threat scores. Consequently, the maximum-likelihood-of-detection criteria (MLDC) was proposed as an alternative technique to increase threat scores in area 4.

A series of experiments involving an arbitrarily selected population of two hundred normally distributed events, partitioned into eight separate threat/non-threat samples, were performed to demonstrate the theoretical utility of the MLDC at low threat frequencies. Threshold values were calculated, for various threat frequencies, using the EVAR minimum probable error and MLDC techniques and two by two contingency tables were constructed to tabulate the associated threat score, percent correct and false alarm rate results. Fig. 65 shows the resulting plot of threat score versus threat frequency which illustrates the amount of increase in threat score associated with the MLDC model. Associated with these higher threat scores are correspondingly higher "costs," namely higher false alarm rates, illustrated in Fig. 66, and lower percent correct scores, illustrated in Fig. 67.

A set of two experiments was performed, utilizing FATJUNE 1983, TAU-24 data and the two-stage separation scheme outlined in Chapter IV (MLDC model), to evaluate the relative performance of the MLDC and EVAR models on area 4. In general, the results of these two experiments were consistent with the results predicted by the aforementioned theoretical experiments. The most obvious area of agreement is the significantly lower independent adjusted VISCAT I and VISCAT II threat scores (both are considered threatening events in this study), namely 0.01 (unadjusted, 0.04) and -0.14 (unadjusted, 0.00), achieved by the EVAR model, Fig. 68, as compared to the corresponding scores of 0.04 (unadjusted, 0.07) and 0.03 (unadjusted, 0.15) achieved by the MLDC model, Fig. 69.

VI. CONCLUSIONS AND RECOMMENDATIONS

A. CONCLUSIONS

The primary objective of this study was to expand upon
the initial research and experimentation presented by Karl
(1984) and to propose a viable statistical forecasting scheme
suitable for eventual employment in an operational U.S. Navy
marine visibility MOS forecasting system. In general,
while the results of linear regression and the evaluated
Preisendorfer models are roughly comparable, it has been
shown that two specific statistical approaches, namely the
PR+BMD model's MAXPROB II strategy and the linear regression
models, yield the best results (as measured by independent
VISCAT I threat score) achieved in this study. The PR+BMD
model achieved the best results for six of the eight evaluated
cases: area 2, TAU-48; area 3W, TAU-24 and TAU-48; and area
4, TAU-00, TAU-24 and TAU-48. The nearly identical results
of both the equal variance and quadratic linear regression
threshold models provided the best skill and threat scores
for area 2, TAU-00 and TAU-24. A common characteristic of
each of the evaluated cases is that the predictability of
visibility category II is relatively very poor and nearly
always poorer than that for visibility categories I or III.
This pattern affirms the findings of similar Pacific Ocean
visibility studies [Renard and Thompson, 1984] as well as

75

those documented by Karl (1984) and further supports Karl's recommendation to change from a three-category to a two-category visibility forecasting scheme.

An evaluation of the overall results of this study shows that no real connection between individual model/strategy and either the homogeneous oceanic area (2, 3W and 4) or model output time (TAU-00, TAU-24 and TAU-48) can be made. The linear regression threshold models performed best for area 2, the intermediate poor visibility oceanic area, while the Preisendorfer methodology incorporating linear regression equation predictors proved the best in the evaluated homogeneous areas with the greatest and lowest relative concentration of poor visibility observations. The trend of visibility category I skill and threat scores, for each homogeneous area and model output time, seems to contradict the preliminary supposition that peak skill scores would be associated with the area containing the greatest frequency of poor visiblity observations and the TAU-00 model output time. This result is most apparent with area 4, where threat scores increase with increasing model forecast projections until they achieve values at TAU-48, which are nearly identical to those for the other two homogeneous areas. This type of trend in skill and threat scores most likely reflects the overall strength of the statistical relationships for the predictand/predictors involved irrespective of the frequency of specific visibility observations.

In several cases, the maximum independent visiblity category I threat score achieved by the PR+BMD model was reached at the first predictor level. In several additional cases, threat score values which were only marginally lower than peak value, were similarly achieved at the first predictor level. Forecasting arrays involving only one predictor drastically reduce required computer storage and consequently such arrays are a desirable attribute to any operational MOS forecasting system. A MOS-type forecasting system predicatedupon such a small number of predictors would prove extremely beneficial in an independent single station forecasting scenario such as that experienced by an aircraft carrier based U.S. Navy Oceanography Officer.

The concept and practical employment of functional dependence, associated with the Preisendorfer methodology, provides a greater restriction on the statistical significance of the skill and threat score results achieved in this study, as compared to that which was previously experienced by Karl (1984). It was shown that the calculated functional dependence values for each respective predictor or group of predictors often exceeded the associated 96% confidence interval value at the first or second predictor level and rarely met the requirements for significance for an entire array of selected predictors. This restriction further indicates that any operational forecasting scheme should most likely be composed of only a minimal number of select predictors.

The difference between the equal variance and quadratic threshold models was shown to be very minimal. The two-stage visibility category separation approach is designed to handle cases with distinct separability between categories while providing for minimal error in the calculated threshold values. This condition was not met in the area 4, TAU-00 and TAU-24 cases and subsequently lead to unrealistic threshold values.

The preliminary independent evaluation of the 15 May to 23 June 1984 data set provided a crucial test and verification of the utility of the forecast arrays and equations presented in this study.

The introduction and initial evaluation of the maximum-likelihood-of-detection threshold model offers another technique to the pool of visibility prediction schemes. This method appears to be most beneficial in areas of low threat frequency.

B. RECOMMENDATIONS

The following recommendations are offered to future researchers:

1. Remove the MAXPROB I and natural regression strategies of the Preisendorfer methodology from further consideration in the forecasting of marine horizontal visibility.

2. Delete one of the two threshold models evaluated in this study, and investigate additional thresholding

techniques based on the Beta distribution and the maximum-likelihood-of-detection criteria.

3. Revise the current three-category visibility scheme to a two-category scheme where visibility categories I and II are combined. This should be particularly beneficial in those homogeneous areas with extremely low frequencies of visibility category I and II observations.

4. Expand the initial set of potential predictors to include air-sea temperature differences as well as additional derived predictors such as the advections and gradients of temperature, vorticity and moisture in order to more fully simulate the physical processes associated with poor marine visibility. Additionally, include TAU-00 and TAU-24 model output parameter fields as potential predictors in future evaluations of TAU-24 and TAU-48 MOS forecasts.

5. Evaluate 0000GMT data sets to determine the effect of nighttime conditions on both visibility observations and NOGAPS model output parameters.

6. Investigate new procedures to determine the number of equally populous predictor intervals. The following procedure [Preisendorfer, 1984] is proposed:

   a. To establish the number of equally populous predictor intervals for any predictor, consider a bivariate predictand/predictor [Preisendorfer, 1983a]. Start with $m = 1$ and find the potential predictability (PP) for the resultant plot, call it "PP(1)." In general, PP(m) is the

PP for the general case of m. Successively, find PP(m)
for m = 1,2,..., and continue to subidivde the predictor
range as long as PP increases: PP(m) < PP(m+1). Stop at
PP(m) if PP(m+1) $\leq$ PP(m) or if PP(m+1) < PP(m+1|96), where
the later is defined by Preisendorfer (1983a) and denoted
by "PP(96)." This last condition avoids sparse bivariate data
plots, caused by too large an m. It was Karl's 1984 experi-
ence that five to eight equally populous predictor intervals
are sufficient for all predictors. Hence m, for each pre-
dictor, is expected to be in this neighborhood.

   b. Order the set of available predictors in descending
value of potential predictability (PP). Break ties with
A0 (PP and A0 are defined by Preisendorfer (1983a)). A0
is the actual skill, after the prediction has been made.

   c. The first predictor is that with the greatest
PP. Compute associated A0 and A1. Call them $A0^{(0)}$ and $A1^{(0)}$.

   7. Associated with recommendation 6. above, improve
the predictor selection procedure as follows:

   a. Suppose k-1 predictors have been chosen, let
them be $X_1,...,X_{k-1}$. Let Y be a new predictor candidate.
Admit Y as the kth predictor if the three following conditions
are satisfied:

        (1) Functional dependence $(Y|X_i)$ < functional
            dependence$_u$ $(Y|X_i;05)$ for i = 1,...,k-1
            (i.e., the functional dependence of X_i
            and Y is not significantly large for each

80

i = 1,...,k-1. Find functional dependence $(Y|X_i)$ and functional dependence $(Y|X_i;05)$ as described by Preisendorfer (1983c)).

(2) $A0^{(k)} > A0^{(k-1)}$ and $A1^{(k)} > A1^{(k-1)}$

(3) $A0^{(k)} > A0(96)$ and $A1^{(k)} > A1(05)$

All three conditions must hold for admittance of Y to the predictor set.

b. A less stringent predictor selection process would be to form functional dependence $(Y_j|X_i)$, where X_i, i = 1,...,k-1 are the selected predictors, and the Y_j, j = 1,...,q are the as-yet unselected predictors. Here (k-1)+q = p, the original number of potential predictors. Next, form $|\min_j|\max_i$ functional dependence $(Y_j|X_i)||$. This fixes that Y_j for which functional dependence $(Y_j|X_i)$ is the least possible of the maximum functional dependence values over the present X set. This makes the best out of the worst case of functional dependence (i.e., select the Y_j farthest from the set of X_i).

c. Continue to repeat step 7a. above until all potential predictors are used up (the critical values of A0(96) and A1(05) are as defined by Preisendorfer (1983b). Another reason for stopping may be that allotted CPU time is used up before the predictors.

8. Investigate a further and more complete verification of the forecast arrays and equations presented in this study

81

utilizing available 1984 data sets. Specifically, utilize

the 1984 data set as an entire independent test case without

first removing a portion of the data for use as a dependent

forecast array/equation training set. Additionally, gener-

ate an additional set of forecast arrays and equations

based on combined 1983 and 1984 FATJUNE data and evaluate

the statistical stability of the equations as different

years of data are merged into a larger data base.

APPENDIX A

LINEAR REGRESSION AND THRESHOLD MODELS

A. LINEAR REGRESSION

The linear regression techniques used in this study expand upon and slightly modify those first presented by Karl (1984). In this study, two separate least-squares, multiple linear regression software programs; referred to as the BMDP2R--Stepwise Regression and BMDP9R--All Possible Subsets Regression computer programs in the BMDP Statistical Software [University of California, 1983], were used.

The independent variable selection procedure employed in the BMDP2R program is referred to as a forward, step-wise selection process where predictors are selected from a large group of available potential independent variables based upon the highest correlation with the dependent predictand (visibility in this study). This correlation is calculated based upon certain F-to-enter and F-to-remove limits, where F is a ratio which tests the significance of the coefficients of the predictors in the regression equation.

The regression model fitted to the data is

$$y = a + b_1 x_1 + b_2 x_2 + \ldots + b_n x_n + \varepsilon$$

where:

y = the dependent variable (predictand) which
can be either a continuous function or a
discrete value

$x_1, \ldots, x_n$ = the independent variables (predictors)

$b_1, \ldots, b_n$ = the regression coefficients

a = the intercept

p = the number of independent variables

ε = the error with mean zero

The predicted value $\hat{y}$, and the general form of the resulting equation, is

$$\hat{y} = a + b_1 x_1 + b_2 x_2 + \ldots + b_n x_n$$

The step-wise selection of predictors continues until there are no predictors remaining which meet the requisite F-to-enter criteria. The regression equation generated by the BMDP2R program is outputted at each regression step where variables are selected as independent predictors, along with its corresponding R value (the correlation of dependent variable y with the predicted value $\hat{y}$) and R^2 value. The resulting equation sets are reviewed, and that equation containing only those predictors which increased R^2 by at least 0.01 are retained for application.

The procedure employed with the BMDP9R program varies from that of the BMDP2R, in that a "best" possible subset, derived independently of variable or variable sequence, is calculated from the group of potential predictors. Once this

"best" subset is identified, a linear regression equation is fitted to the data, based only upon those selected predictors, in a fashion identical to that for the BMDP2R program. The "best" possible subset is calculated by a Furnville-Wilson algorithm which provides the user with a variety of subordinate subsets in addition to the "best" subset. Three criteria are available to define the "best" possible subset as a function of independent variables (predictors) and a dependent variable (predictand): the sample R^2, the adjusted R^2 and Mallow's Cp. For this study, the Mallow's Cp criteria is defined as:

$$Cp = RSS/S - (N - 2P')$$

where:

RSS = the residual sum of the squares for the new subset being tested

S = the residual mean square based on the linear regression using all independent variables

P' = the number of variables in each subset

N = the total number of cases

For this method, "best" is defined as the smallest Cp value.

Independent variable selection for the BMDP9R program begins with a general screening of the entire set of potential predictors. Variables which are identified as redundant,

85

linear combinations of other variables, with respect to the predictand, in this general screening are deleted from further consideration. The t statistics for the coefficients which minimize the Cp value for each reviewed subset identifies the "best" subset. The number of predictors assigned to each subset can be predefined and for this study each subset equation was required to have six predictors.

The role of regression, once appropriate predictor variables have been selected, is simply that of dimension reduction (representing a multivariate structure by a univariate proxy which constitutes a classificatory or predictive index). This proxy takes the form of a polynomial, linear in its coefficients, of the components of the multivariate structure. The problem now becomes one of determining the form of the state conditional distributions (one for each group of interest; e.g., one, two and three for visibility categories I, II and III, as used in this study). Once an appropriate form has been selected, it remains, then, to determine the parameters of the class conditional distributions (e.g., means and variances) and then apply an appropriate decision criterion or threshold model.

B. THRESHOLDS [Lowe, 1984a]

   1. Notation

         E ≡ an event; this is an indicator variable which
               when E = 1, the threatening event occurs, and
               when E = 0, the non-threatening event occurs.

86

$C \equiv$ the classification of an unknown event which when $C = 1$, the event is classified as a threat, and when $C = 0$, the event is classified as a non-threat.

$P[E = 1] \equiv$ unconditional probability of occurrence of threat.

$P[E = 0] \equiv$ unconditional probability of occurrence of non-threat.

Error of the 1st kind (false alarm) $[C = 1 \cap E = 0]$.

Error of the 2nd kind (miss) $[C = 0 \cap E = 1]$.

$P[C = 1 \cap E = 0] \equiv$ joint probability of an error of the 1st kind.

$P[C = 0 \cap E = 1] \equiv$ joint probability of an error of the 2nd kind.

$P[C = 1 | E = 0] \equiv$ class conditional probability of misclassifying a non-threat.

$P[C = 0 | E = 1] \equiv$ class conditional probability of misclassifying a threat.

$P[C = 1 \cap E = 0] = P[C = 1 | E = 0] \, P[E = 0]$.

$P[C = 0 \cap E = 1] = P[C = 0 | E = 1] \, P[E = 0]$.

$z =$ a value of the predictive index (equivalent to $\hat{y}$, above).

$Z =$ range of the predictive index on the real line.

For a dichotomous problem, Z is into two parts Z_0, Z_1,

$$C = 0 \quad \text{if} \quad z \in Z_0$$

$$C = 1 \quad \text{if} \quad z \in Z_1$$

The decision regions are mutually exclusive and exhaustive (i.e., $Z_0 \cap Z_1 = 0$ and $Z = Z_0 \cup Z_1$).

Thresholds $\equiv$ boundary(s) between decision regions.

$p(z|E=0)$ $\equiv$ class conditional density of z given that E = 0.

$p(z|E=1)$ $\equiv$ class conditional density of z given that E = 1.

$\Lambda(z)$ = $p(z|E=1)/p(z|E=0)$ = the maximum likelihood ratio (i.e., the ratio of class conditional densities).

p_e = $p\{[C=1 \cap E=0] \cup [C=0 \cap E=1]\}$ = the total probability of error.

2. Minimum Probability of Error Criterion

p_e = probability of an incorrect classification.

$$p_e = p[C=1|E=0] \, p[E=0] + p[C=0|E=1] \, p[E=1]$$

where $p[E=1] + p[E=0] = 1$. NOte that the events E = 1 and E = 0 are mutually exclusive and exhaustive. The objective is to select decision regions (thresholds) so as to minimize p_e.

$$p[C=0|E=1] = \int_{z \in Z_0} p(z|E=1) dz = \text{the probability of}$$
$$\text{misclassifying } E = 1.$$

$$p[C=0|E=1] = \int_{z \in Z_0} p(z|E=1) dz + \int_{z \in Z_1} p(z|E=1) dz$$
$$- \int_{z \in Z_1} p(z|E=1) dz$$

$$p[C=0|E=1] = 1 - \int_{z \in Z_1} p(z|E=1) dz \qquad \text{these are substituted into the expression}$$
$$p(C=1|E=0) = \int_{z \in Z_1} p(z|E=0) dz \qquad \text{for } p_e$$

88

then,

$$p_e = p[E = 0] \int\limits_{z \in Z_1} p(z|E = 0) dz + p[E = 1][1 - \int\limits_{z \in Z_1} p(z|E = 1) dz]$$

and algebraic rearrangement yields,

$$p_e = p[E = 1] - \int\limits_{z \in Z_1} \{p[E = 0] \, p(z|E = 0) - p[E = 1] \, p(z|E = 1) \, dz\}$$

In order to minimize p_e, Z_1 (the decision region for $C = 1$) will include all those values of z for which the integrand in the expression for p_e will be negative. The decision regions can be symbolically represented as follows:

$$Z_0 = \{z: p[E = 0] \, p(z|E = 0) - p[E = 1] \, p(z|E = 1) > 0\}$$

$$Z_1 = \{z: p[E = 0] \, p(z|E = 0) - p[E = 1] \, p(z|E = 1) < 0\}$$

An alternative representation is given by,

$$Z_0 = \{z: p[E = 0] \, p(z|E = 0) > p[E = 1] \, p(z|E = 1)\}$$

$$= \{z: p[E = 0]/p[E = 1] > p(z|E = 1)/p(z|E = 0)\}$$

Likewise,

$$Z_1 = \{z: p[E = 0]/p[E = 1] < p(z|E = 1)/p(z|E = 0)\}$$

These statements can be combined to give,

$$p(z|E=1)/p(z|E=0) \quad = \quad \Lambda(z) \quad \mathop{\gtrless}\limits_{c=0}^{c=1} \quad p[E=0]/p[E=1]$$

Thresholds are the value(s) of z for which

$$\Lambda(z) \quad = \quad p[E=0]/p[E=1]$$

This equation can be solved for z either analytically or numerically depending on the forms of the density functions.

3. Threshold Cases

In order to examplify the model, the assumption is made that the class conditional distributions are Gaussian. There are essentially three distinct cases that can arise.

    a.   Case I: Equal variances; different means (Referred to as the equal variance model (EVAR) in the text)

$$p(z|E=1) \quad = \quad k \, \exp\{(-1/2)(z-\mu_1)^2/\sigma^2\}$$

$$p(z|E=0) \quad = \quad k \, \exp\{(-1/2)(z-\mu_0)^2/\sigma^2\}$$

where:

$$k \quad = \quad (2\pi)^{-1/2}\sigma^{-1} \, .$$

$$\Lambda(z) \quad = \quad \frac{\exp\{(-1/2)(z-\mu_1)^2/\sigma^2\}}{\exp\{(-1/2)(z-\mu_0)^2/\sigma^2\}} \quad \mathop{\gtrless}\limits_{c=0}^{c=1} \quad \frac{p_0}{p_1}$$

where Λ is the likelihood ratio and $p_0 = p[E = 0]$ and $p_1 = p[E = 1]$. Thus, the threshold value is

$$z^* = (\mu_0 + \mu_1)/2 + \sigma^2 \ln(p_0/p_1)/(\mu_1 - \mu_0)$$

Classification Index (z)
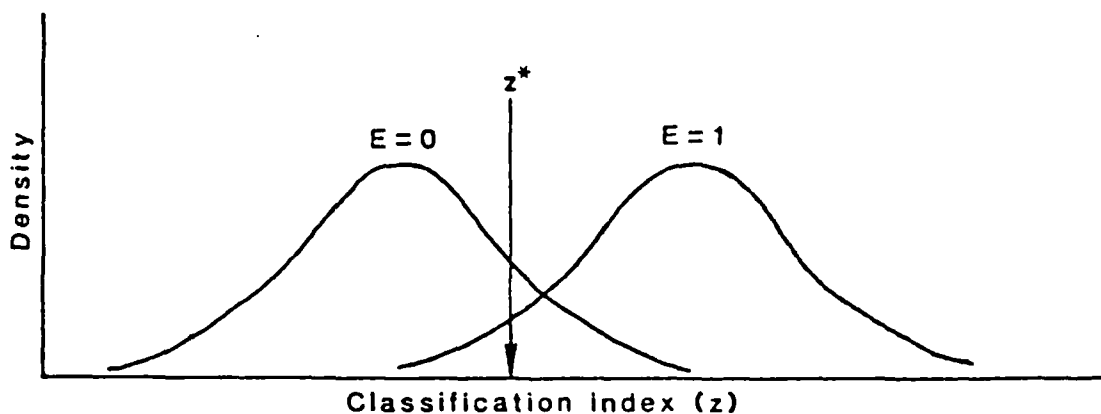
The position of the threshold depends on the relative values of p_1 and p_0. The threshold moves toward the group with the smallest p_i. If $p_1 = p_0$ the threshold will be the value of z where the densities intersect (i.e., where the densities are equal).

b. Case II: Equal means; different variances

$$\Lambda(z) = \frac{\sigma_0 \exp\{(-1/2)(z - \mu_1)^2/\sigma_1^2\}}{\sigma_1 \exp\{(-1/2)(z - \mu_0)^2/\sigma_0^2\}} \quad \begin{matrix} c=1 \\ > \\ < \\ c=0 \end{matrix} \quad \frac{p_0}{p_1}$$

with the threshold

$$z^* = \pm\left[\frac{2\sigma_0^2\sigma_1^2}{(\sigma_1^2 - \sigma_0^2)} \ln\left(\frac{p_0\sigma_1}{p_1\sigma_0}\right)\right]^{1/2}$$

91

Note that in this situation there are two thresholds. The
group having the smaller variance will lie between the two
thresholds.
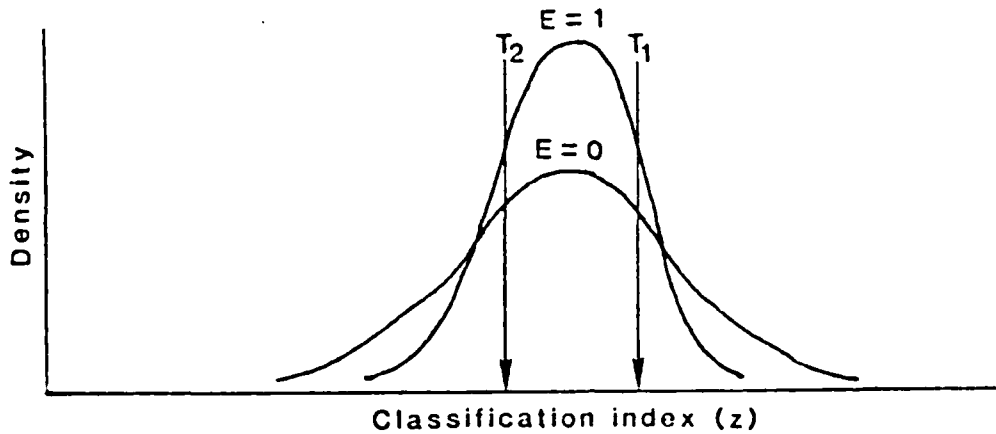
The thresholds shown are typical of a situation where $p_1 < p_0$.
Note that these thresholds lie between the two intersections
of the densities. If the inequality of prior probabilities
were reversed, the thresholds would lie outside of the
region between the two density intersections. Further note
that the decision region for the group having the lesser
variance lies between the thresholds.

        c.   Case III: General Solution (Referred to as the
               Quadratic Model (QUAD) in the text)

$$p(z|E = 1) \quad = \quad k/\sigma_1 \; \exp\{(-1/2)(z - \mu_1)^2/\sigma_1^2\}$$

$$p(z|E = 0) \quad = \quad k/\sigma_0 \; \exp\{(-1/2)(z - \mu_0)^2/\sigma_0^2\}$$

$$\Lambda(z) \quad = \quad \exp\{1/2 \left[(\frac{z - \mu_0}{\sigma_0})^2 - (\frac{z - \mu_1}{\sigma_1})^2 \right] \} \quad \begin{matrix} c=1 \\ > \\ < \\ c=0 \end{matrix} \quad \frac{p_0 \sigma_1}{p_1 \sigma_0}$$

where $k = (2\pi)^{-1/2}$. Algebraic manipulation produces

$$(\sigma_1^2 - \sigma_0^2) z^2 + 2(\sigma_0^2 \mu_1 - \sigma_1^2 \mu_0) z$$

$$+ \left[(\sigma_1^2 \mu_0^2 - \sigma_0^2 \mu_1^2) - 2\sigma_0^2 \sigma_1^2 \ln (p_0 \sigma_1 / p_1 \sigma_0) \right] \quad \begin{matrix} c=1 \\ > \\ < \\ c=0 \end{matrix}$$

which is recognizable as a quadratic equation in z.

$$z^* \quad = \quad -b \pm (b^2 - 4ac)^{1/2} / 2a$$

where:

$$a \quad = \quad \sigma_1^2 - \sigma_0^2$$

$$b \quad = \quad 2(\sigma_0^2 \mu_1 - \sigma_1^2 \mu_0)$$

$$c \quad = \quad (\sigma_1^2 \mu_0^2 - \sigma_0^2 \mu_1^2) - 2\sigma_1^2 \mu_0^2 \ln (p_0 \sigma_1 / p_1 \sigma_0)$$

93
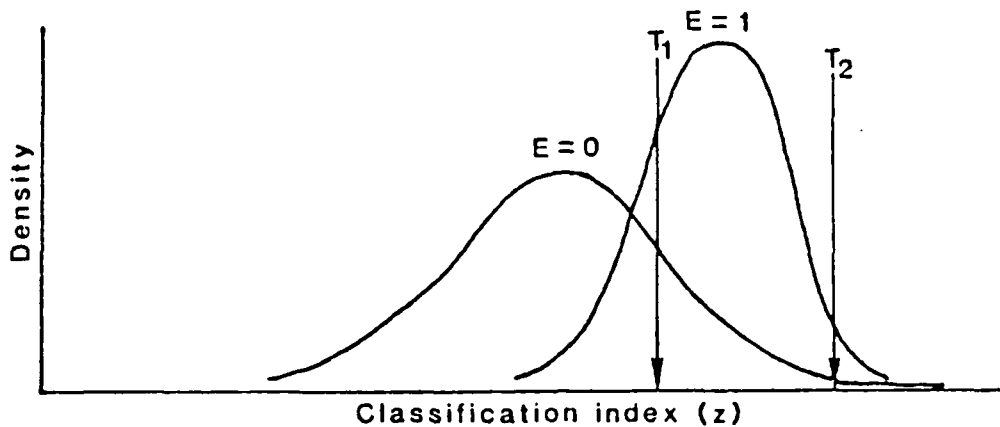
The remarks given for the figures in cases I and II are also
applicable here. More often than not, only one of a pair of
thresholds induced by differing variances will be of real
interest. If the variances of the two groups are radically
different, then both members of the threshold pair become
important.

4. The-Maximum-Likelihood-of-Detection Criteria

For this specific model the following background is
provided:

event space: 2' mutually exclusive populations

π_0, π_1 forecast decision space: 2 possible forecasts
d_0, d_1

d_0 is a correct forecast if π_0 actually occurs

d_1 is a correct forecast if π_1 actually occurs

Problem: select the decision rule d(z) which maps
the observation space Z into some forecast space
in some optimal manner.

94

Z may be an observed variable or it may be an univariate index derived from a number of variables.

For this two decision problem, Z is partitioned into two parts, Z_0 and Z_1.

$d(z) = d_0$ if $z \in Z_0$

$d(z) = d_1$ if $z \in Z_1$

where $Z_0 \cap Z_1 = 0$ and $Z_0 \cup Z_1 = Z$

The maximum-likelihood-of-detection criteria represents the simplest decision model. The basic involves selecting the forecast (decision) corresponding to the observation (signal) which is the most likely symptom of the event subsequently observed. Consider the following example:

problem: diagnose disease A or disease B.

The observed symptoms occur with probability 0.75 for A and 0.1 for B. By the maximum-likelihood-of-detection criteria (MLDC), diagnose disease A because A is the most likely cause of the observed symptoms (if there is no more information). But if we know that A is rare and B is common, the above decision may not be optimal and MLDC may not be appropriate. MLDC requires only that we know the event conditional probability density functions of the observations. That is:
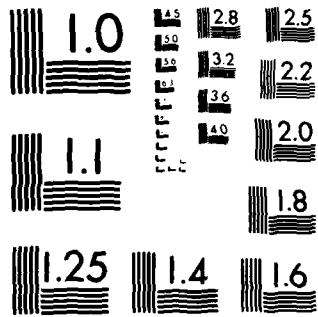
MICROCOPY RESOLUTION TEST CHART
NATIONAL BUREAU OF STANDARDS 1963 A

$p(z|\pi_0)$ and $p(z|\pi_1)$

decision rule: $d(z) = \begin{cases} d_1 \text{ if } p(z|\pi_1) > p(z|\pi_0) \\ \\ d_0 \text{ if } p(z|\pi_1) < p(z|\pi_0) \end{cases}$

In the following development the Gaussian density is used to exemplify the model.

$$p(z|\pi_0) = 1/\sqrt{2\pi\sigma_0} \exp\{-1/2(\frac{z - \bar{z}_0}{\sigma_0})^2\}$$

$$p(z|\pi_1) = 1/\sqrt{2\pi\sigma_1} \exp\{-1/2(\frac{z - \bar{z}_1}{\sigma_1})^2\}$$

definition: likelihood ratio $\Lambda(z) = \dfrac{p(z|\pi_1)}{p(z|\pi_0)}$

for convention sake we assume $\bar{z}_1 > \bar{z}_0$,

$$\sigma_1^2 > \sigma_0^2$$
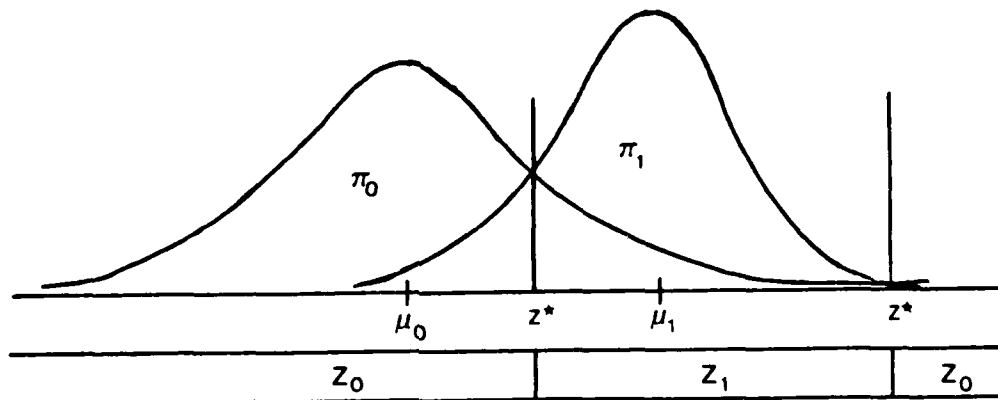
$$\sigma_1^2 > \sigma_0^2$$
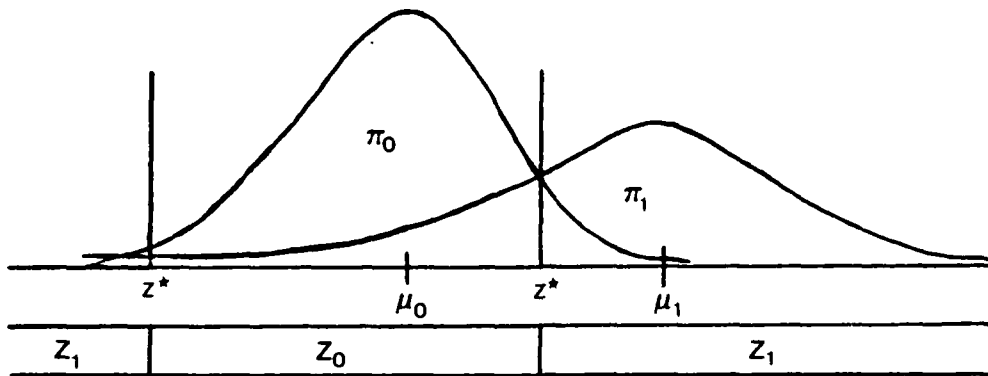
* note the class having the largest variance has a bifurcated decision region.

In the case where the variances are equal, the situation simplifies considerably.

$$2\sigma^2(\bar{z}_1 - \bar{z}_0) + \sigma^2(\bar{z}_0^2 - \bar{z}_1^2) \underset{d_0}{\overset{d_1}{\underset{>}{\lessgtr}}} 0$$

$$2\sigma^2(\bar{z}_1 - \bar{z}_0) - \sigma^2(\bar{z}_1^2 - \bar{z}_0^2) \underset{d_0}{\overset{d_1}{\underset{<}{\gtrless}}} 0$$

$$2z \underset{d_1}{\overset{d_0}{\underset{<}{\gtrless}}} (\bar{z}_1 + \bar{z}_0)$$

$$z \overset{>}{\underset{<}{}} \frac{(\bar{z}_1 + \bar{z}_0)}{2} = z^*$$

$$\sigma_0^2 = \sigma_1^2$$
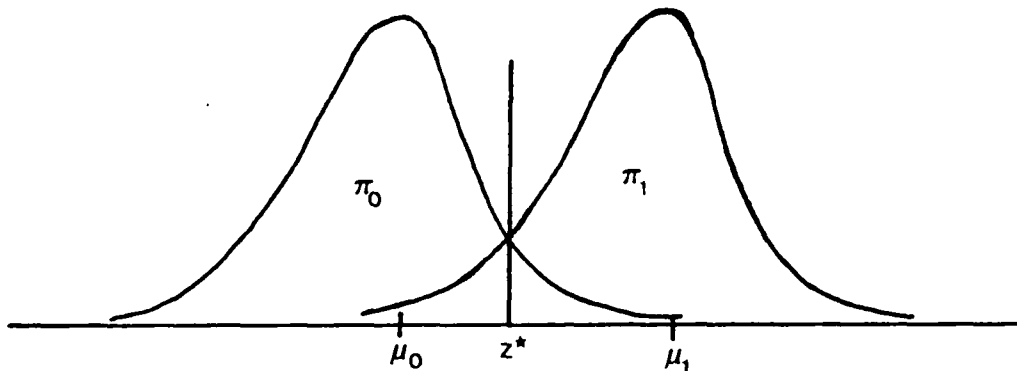
It is obvious that z* is simply the average of the means of the class-conditional distributions and is found at the intersections of the two density curves.

In the foregoing, normal class conditional distributions were assumed. This was done because the Gaussian form admits of a rather clean analytical solution. However, the general concept of the minimum probable error decision criteria may be applied to any form of density function. Indeed, the density function of one group need not even be the same form as that for another group (one might be exponential and the other Gaussian). The difficulty with most non-Gaussian forms is that they seldom admit of closed analytical forms and require numerical means in determination of thresholds.

APPENDIX B

NOGAPS PREDICTOR PARAMETERS AVAILABLE FOR
NORTH ATLANTIC OCEAN EXPERIMENTS

I. Area: Entire North Atlantic Ocean and Mediterranean Sea

Model output time: 1200GMT (TAU-00)
15 May--7 July 1983

A. Model output   Descriptive name of parameter
    parameter

D1000	1000 mb geopotential height
D925	925 mb geopotential height
D850	850 mb geopotential height
D700 *	700 mb geopotential height
D500	500 mb geopotential height
D400 *	400 mb geopotential height
D300 *	300 mb geopotential height
D250 *	250 mb geopotential height
TAIR	Surface air temperature
T1000	1000 mb temperature
T925	925 mb temperature
T700 *	700 mb temperature
T500	500 mb temperature
T400 *	400 mb temperature
T300 *	300 mb temperature
T250 *	250 mb temperature
EAIR	Surface vapor pressure
E1000	1000 mb vapor pressure
E925	925 mb vapor pressure
E850	850 mb vapor pressure
E700 *	700 mb vapor pressure
E500	500 mb vapor pressure
UBLW	Boundary layer zonal wind component

U1000	1000 mb zonal wind component
U925	925 mb zonal wind component
U850	850 mb zonal wind component
U700 *	700 mb zonal wind component
U500	500 mb zonal wind component
U400 *	400 mb zonal wind component
U300 *	300 mb zonal wind component
U250 *	250 mb zonal wind component
VBLW	Boundary layer meridional wind component
V1000	1000 mb meridional wind component
V925	925 mb meridional wind component
V850	850 mb meridional wind component
V700 *	700 mb meridional wind component
V500	500 mb meridional wind component
V400 *	400 mb meridional wind component
V300 *	300 mb meridional wind component
V250 *	250 mb meridional wind component
VOR925 **	925 mb vorticity
VOR500 **	500 mb vorticity
PS	Surface pressure
SMF	Surface moisture flux
PBLD	Planetary boundary-layer depth
STRTFQ	Percent stratus frequency
STRTTH	Stratus thickness
SHF	Surface heat flux
ENTRN	Entrainment at top of marine boundary-layer
DRAG **	Drag coefficient (C_D)

B. Derived parameters

DTDP	Vertical gradient of temperature (1000-925 mbs)
DEDP	Vertical gradient of vapor pressure (1000-850 mbs)
DUDP	Vertical gradient of zonal wind (1000-850 mbs)

DVDP	Vertical gradient of meridional wind (1000-850 mbs)
RH	Surface relative humidity
TV	Virtual temperature
DDVDP	Vertical gradient of geopotential height (1000-850 mbs)
DVRTDP	Vertical gradient of vorticity (500-925 mbs)
ESUM	Sum of vapor pressures (1000-850 mbs)
EPRD	Product of vapor pressures (1000-850 mbs)

II. Area: Entire North Atlantic Ocean and Mediterranean Sea

Model forecast projection: 1200GMT (TAU-24)
15 May--7 July 1983

A. Model output parameter	Descriptive name of parameter

D1000	1000 mb geopotential height
D925	925 mb geopotential height
D850	800 mb geopotential height
D700 *	700 mb geopotential height
D500	500 mb geopotential height
D400 *	400 mb geopotential height
D300 *	300 mb geopotential height
D250 *	250 mb geopotential height
TAIR	Surface air temperature
T1000	1000 mb temperature
T925	925 mb temperature
T700 *	700 mb temperature
T500	500 mb temperature
T400 *	400 mb temperature
T300 *	300 mb temperature
T250 *	250 mb temperature
EAIR	Surface vapor pressure

101

E1000	1000 mb vapor pressure
E925	925 mb vapor pressure
E850	850 mb vapor pressure
E700 *	700 mb vapor pressure
E500	500 mb vapor pressure
UBLW	Boundary layer zonal wind component
U1000	1000 mb zonal wind component
U925	925 mb zonal wind component
U700 *	700 mb zonal wind component
U500	500 mb zonal wind component
U400 *	400 mb zonal wind component
U300 *	300 mb zonal wind component
U250 *	250 mb zonal wind component
VBLW	Boundary layer meridional wind component
V1000	1000 mb meridional wind component
V925	925 mb meridional wind component
V850	850 mb meridional wind component
V700 *	700 mb meridional wind component
V500	500 mb meridional wind component
V400 *	400 mb meridional wind component
V300 *	300 mb meridional wind component
V250 *	250 mb meridional wind component
VOR925	925 mb vorticity
VOR500	500 mb vorticity
PS	Surface pressure
SMF	Surface moisture flux
PBLD	Planetary boundary-layer depth
STRTFQ	Percent stratus frequency
STRTTH	Stratus thickness
SHF	Surface heat flux
ENTRN	Entrainment at top of marine boundary-layer
DRAG	Drag coefficient (C_D)
PRECIP	Total amount (mm.) of model precipitation in the last six hours

SHWRS	Total amount (mm.) of model precipitation associated with cumulus convection in the last six hours
INSTAB	Boundary layer inversion instability
DIV925	925 mb Divergence

B. Derived parameters

DTDP	Vertical gradient of temperature (1000-925 mbs)
DEDP	Vertical gradient of vapor pressure (1000-850 mbs)
DUDP	Vertical gradient of zonal wind (1000-850 mbs)
DVDP	Vertical gradient of meridional wind (1000-850 mbs)
RH	Surface relative humidity
TV	Virtual temperature
DDVDP	Vertical gradient of geopotential height (1000-850 mbs)
DVRTDP	Vertical gradient of vorticity (500-925 mbs)
ESUM	Sum of vapor pressures (1000-850 mbs)
EPRD	Product of vapor pressures (1000-850 mbs)

III. Area: Entire North Atlantic Ocean and Mediterranean Sea

Model forecast projection: 1200GMT (TAU-48)
15 May--9 July 1983

A. Model output parameter | Descriptive name of parameter

D1000	1000 mb geopotential height
D925	925 mb geopotential height
D850	850 mb geopotential height
D700 *	700 mb geopotential height
D500	500 mb geopotential height
D400 *	400 mb geopotential height

103

D300 *	300 mb geopotential height
D250 *	250 mb geopotential height
TAIR	Surface air temperature
T1000	1000 mb temperature
T925	925 mb temperature
T700 *	700 mb temperature
T500	500 mb temperature
T400 *	400 mb temperature
T300 *	300 mb temperature
T250 *	250 mb temperature
EAIR	Surface vapor pressure
E1000	1000 mb vapor pressure
E925	925 mb vapor pressure
E850	850 mb vapor pressure
E700 *	700 mb vapor pressure
E500	500 mb vapor pressure
UBLW	Boundary layer zonal wind component
U1000	1000 mb zonal wind component
U925	925 mb zonal wind component
U850	850 mb zonal wind component
U700 *	700 mb zonal wind component
U500	500 mb zonal wind component
U400 *	400 mb zonal wind component
U300 *	300 mb zonal wind component
U250 *	250 mb zonal wind component
VBLW	Boundary layer meridional wind component
V1000	1000 mb meridional wind component
V925	925 mb meridional wind component
V850	850 mb meridional wind component
V700 *	700 mb meridional wind component
V500	500 mb meridional wind component
V400 *	400 mb meridional wind component
V300 *	300 mb meridional wind component
V250 *	250 mb meridional wind component

VOR 925	925 mb vorticity
VOR500	500 mb vorticity
PS	Surface pressure
SMF	Surface moisture flux
PBLD	Planetary boundary-layer depth
STRTFQ	Percent stratus frequency
STRTTH	Stratus thickness
SHF	Surface heat flux
ENTRN	Entrainment at top of marine boundary-layer
DRAG	Drag coefficient (C_D)
PRECIP	Total amount (mm.) of model precipitation in the last six hours
SHWRS	Total amount (mm.) of model precipitation associated with cumulus convection in the last six hours
INSTAB	Boundary layer inversion instability
DIV925	925 mb Divergence

B. Derived parameters

DTDP	Vertical gradient of temperature (1000-925 mbs)
DEDP	Vertical gradient of vapor pressure (1000-850 mbs)
DUDP	Vertical gradient of zonal wind (1000-850 mbs)
DVDP	Vertical gradient of meridional wind (1000-850 mbs)
RH	Surface relative humidity
TV	Virtual temperature
DDVDP	Vertical gradient of geopotential height (1000-850 mbs)
DVRTDP	Vertical gradient of vorticity (500-925 mbs)
ESUM	Sum of vapor pressures (1000-850 mbs)
EPRD	Product of vapor pressures (1000-850 mbs)

*   Parameters which were not used due to their
        being considered as physically unimportant
        in forecasting marine visibility.

**   Parameters which were not used due to loss of
        significant digits during transfer from tape
        to mass storage.

APPENDIX C

SKILL AND THREAT SCORES, DEFINITIONS [Karl, 1984]

		1	2	3
FORECAST	3	R	S	T
	2	U	V	W
	1	X	Y	Z

OBSERVED

$$\text{Total} = R + S + T + U + V + W + X + Y + Z$$

$$P1 = (R+U+X)/\text{Total} \qquad P3 = (T+W+Z)/\text{Total}$$

$$P2 = (S+V+Y)/\text{Total} \qquad PN = \text{greatest of P1, P2 or P3}$$

Raw Scores

$$A0 = \% \text{ correct} = (X+V+T)/\text{Total}$$

$$A1 = \text{one-class error} = (U+S+Y+W)/\text{Total}$$

$$TS1 = \text{Threat score for visibility category I}$$

$$= X/(R+U+X+Y+Z)$$

$$TS2 = \text{Threat score for visibility category II}$$

$$= V/(S+V+Y+U+W)$$

$$TS12 = \text{Threat score for visibility categories I and II}$$

$$= (X+V)/(\text{Total}-T)$$

TS12 is designed to represent the skill of forecasting
visibility categories I and II as separate categories,
rather than their skill as a combined category, which
would be (U+V+X+Y)/(Total-T).

Adjusted scores

$AA0 = (A0-PN)/(1-PN)$

$ATS1 = (TS1-P1)/(1-P1)$

$ATS2 = (TS2-P2)/(1-P2)$

$ATS12 = (TS12-(P1+P2))/(1-(P1+P2))$

APPENDIX D

BMDP LINEAR REGRESSION EQUATION PREDICTOR SETS,
NORTH ATLANTIC OCEAN EXPERIMENTS (PR+BMD MODEL)

I. Area 2, TAU-00 (BMDP P2R)

BMD1 = 2.842 - 0.21767*E850 + 0.837882E-05*D500
         + 0.03293*SHF + 7.057*DTDP + 0.05872*ESUM **

BMD2 = -10.4469 + 0.11854*EAIR + 0.10124*SMF
         - 0.07409*T925 - 0.16481*E925

BMD3 = 3.47713 - 0.22482*EM + 45.06116*DEDP
         + 0.00521*EPRD

II. Area 2, TAU-24 (BMDP P9R)

BMD1 = -20.9733 - 0.20905*E850 - 0.078694*T925
         + 0.0533674*SHF - 0.0316725*INSTAB
         + 0.0862939*TV + 0.0862983*ESUM

BMD2 = 2.68106 + 0.0356103*TM + 0.53048E-04*V500
         - 0.141302*E925 + 22.0764*DEDP
         + 0.0125618*DDVDP + 0.00563327*EPRD **

BMD3 = -35.2882 + 0.0381891*PS + 0.0273575*T500
         + 0.00449538*PBLD - 0.00625203*STRTFQ
         - 0.0083686*STRTTH + 0.00272894*DTDP

III. Area 2, TAU-48 (BMDP P9R)

BMD1 = -37.7157 - 0.147084*E500 - 0.0897567*T925
         - 0.128407*E925 + 0.022881*SHF + 0.00860574*RH
         + 0.145537*TV

$$\text{BMD2} = 1.85487 + 0.0777253*\text{TM} - 0.0266753*\text{E850}$$
$$- 0.0000390116*\text{U500} - 0.0000366663*\text{V500}$$
$$+ 0.0240246*\text{DDVDP} + 0.105648*\text{ESUM} \quad **$$

$$\text{BMD3} = -13.9637 + 0.0160572*\text{PS} + 0.00308705*\text{PBLD}$$
$$- 0.0031323*\text{STRTFQ} - 0.00846443*\text{DTDP}$$
$$+ 25.6871*\text{DEDP} - 0.00296342*\text{EPRD}$$

IV. Area 3W, TAU-24 (BMDP P2R)

$$\text{BMD1} = 2.673 - 0.09363*\text{E850} - 0.05101*\text{T925}$$
$$- 0.20451*\text{E925} + 0.0305*\text{SHF} + 0.15111*\text{ESUM} \quad **$$

$$\text{BMD2} = 1.15536 + 0.16326*\text{EAIR} + 0.01509*\text{SMF}$$
$$+ 0.13014\text{E-04}*\text{DM} + 8.08795*\text{DEDP}$$
$$+ 0.02091*\text{DDVDP} - 0.00788*\text{EPRD}$$

$$\text{BMD3} = -18.55031 + 0.02089*\text{PS} - 0.30643\text{E-03}*\text{VBLW}$$
$$- 0.01151*\text{STRTFQ} + 0.02772*\text{STRTTH}$$
$$- 0.05736*\text{DUDP}$$

V. Area 3W, TAU-48 (BMDP P9R)

$$\text{BDM1} = 1.92874 - 0.0719817*\text{T925} - 0.201663*\text{E925}$$
$$+ 0.0376905*\text{SHF} + 7.66796*\text{DEDP} + 0.182705*\text{ESUM}$$
$$- 0.00585094*\text{EPRD}$$

$$\text{BMD2} = -33.2574 - 0.1459*\text{E850} - 0.000205441*\text{V925}$$
$$+ 0.325802*\text{SHWRS} + 0.0168064*\text{RH} + 0.124434*\text{TV}$$
$$+ 0.0247277*\text{DDVDP} \quad **$$

$$\text{BMD3} = -10.1316 + 0.0126085*\text{PS} - 0.00032403*\text{VM}$$
$$+ 0.000112099*\text{U500} - 0.00880168*\text{STRTFQ}$$
$$+ 0.0159356*\text{STRTTH} - 0.00174911*\text{DRAG}$$

VI. Area 4, TAU-00 (BMDP P2R)

BMD1 = 2.86828 + 0.4877E-04*U500
         - 0.64632E-04*V500 - 0.30475E-02*STRTFQ

BMD2 = 2.70156 + 0.14946E-04*DM - 0.00904*STRTTH
         + 0.01888*SHF + 4.09377*DTDP   **

BMD3 = 2.84881 + 0.24549E-03*VBLW - 0.10113*E850
         - 0.25666E-3*V850 + 0.03273*ESUM

VII. Area 4, TAU-24 (BMDP P9R)

BMD1 = 3.00017 + 0.0773367*TM - 0.0000464491*V500
         - 0.103205*T925 - 3.76267*VRT925
         - 0.000477853*DTDP + 9.51302*DEDP

BMD2 = 3.05949 - 0.088302*E500 + 0.00372204*PBLD
         - 0.00492842*STRTFQ + 0.0154289*SHF
         - 1.89105*VRT500 + 0.0143745*DVDP   **

BMD3 = -24.6366 + 0.00275966*PS - 0.0549077*E850
         + 0.195977*T500 + 0.0140852*INSTAB
         + 0.0886378*TV + 0.0231264*DDVDP

VIII. Area 4, TAU-48 (BMDP P9R)

BDM1 = -27.0959 - 0.0732462*E850 + 0.01616*T500
         - 0.117787*T925 + 0.287098*SHWRS
         - 4.13253*VRT925 + 0.111855*TV   **

BMD2 = -3.1619 + 0.00678538*PS - 0.0850887*E500
         - 0.0000502297*U500 - 0.0000396501*V500
         - 0.00389051*STRTFQ - 0.00917554*RH

111

$$BMD3 = 2.08319 + 0.0771067 * TM - 0.0282767 * E925$$
$$- 1.5829 * VRT925 - 0.00114379 * DTDP$$
$$+ 13.2073 * DEDP + 0.0289832 * DDVDP$$

** Equation selected as predictors in the PR+BMD model

APPENDIX E

BMDP LINEAR REGRESSION EQUATION PREDICTOR SETS
FOR TWO-STAGE THRESHOLD MODELS

I.   Area 2, TAU-00 Threshold Equations (BMDP P2R)

   a.   VISCAT I vs. VISCAT II+III separation

$$VIS = 0.87475 - 0.11042*E850 + 0.01173*SHF$$
$$+ 2.61984*DTDP + 0.03863*ESUM$$

   b.   VISCAT II vs. VISCAT III separation (EVAR model)

$$VIS = 1.03838 + 0.03668*EAIR - 0.10423*E850$$
$$+ 0.01560*SHF$$

   c.   VISCAT II vs. VISCAT III separation (QUAD model)

$$VIS = 1.03730 + 0.03727*EAIR - 0.10505*E850$$
$$+ 0.01552*SHF$$

II.   Area 2, TAU-24 Threshold Equations (BMDP P9R)

   a.   VISCAT I vs. VISCAT II+III separation

$$VIS = 0.792157 - 0.00404602*SMF + 0.0271941*TM$$
$$- 0.0767329*E850 - 0.0385021*T925$$
$$- 0.0656522*E925 + 0.0683159*ESUM$$

   b.   VISCAT II vs. VISCAT III separation (EVAR model)

$$VIS = -13.9955 - 0.0612856*E850$$
$$+ 0.0478582*SHF - 0.0303761*INSTAB$$
$$- 1.585*VRT925 + 0.0539318*TV$$
$$+ 0.0102962*DDVDP$$

113

c. VISCAT II vs. VISCAT III separation (QUAD model)

$$VIS = -13.1384 - 0.107716*E850$$
$$+ 0.00002923*V500$$
$$+ 0.0122899*SHF + 0.0498382*TV$$
$$+ 0.0105859*DDVDP + 0.0232983*ESUM$$

III. Area 2, TAU-48 Threshold Equations (BMDP P9R)

a. VISCAT I vs. VISCAT II+III separation

$$VIS = -18.0327 - 0.0569882*E850$$
$$- 0.104458*T925 - 0.00116092*PBLD$$
$$+ 0.0957819*PRECIP - 0.0705180*TV$$
$$- 0.0118901*DVDP$$

b. VISCAT II vs. VISCAT III separation (EVAR model)

$$VIS = -14.4404 - 0.0670910*E850 - 0.11931*E500$$
$$+ 0.0157788*SHF - 0.023835*DUDP$$
$$+ 0.0551551*TV + 0.00761201*DDVDP$$

c. VISCAT II vs. VISCAT III separation (QUAD model)

$$VIS = -56.9191 - 0.168467*TM - 0.116816*E500$$
$$+ 0.0201013*SHF + 0.000599864*DTDP$$
$$+ 0.210713*TV - 0.0487371*ESUM$$

IV. Area 3W, TAU-24 Threshold Equations (BMDP P2R)

a. VISCAT I vs. VISCAT II+III separation

$$VIS = 0.88319 - 0.04039*E850 - 0.03385*T925$$
$$- 0.11313*E925 - 0.02692*DVDP$$
$$+ 0.0843*ESUM$$

114

b. VISCAT II vs. VISCAT III separation (EVAR model)

$$VIS = 0.59606 + 0.000012576*DM$$
$$+ 0.0151*INSTAB + 10.23334*DEDP$$
$$- 0.0019117*EPRD$$

c. VISCAT II vs. VISCAT III separation (QUAD model)

$$VIS = 0.73427 - 0.12863*E850 + 0.0015056*PBLD$$
$$+ 0.02073*SHF + 0.04270*ESUM$$

V. Area 3W, TAU-48 Threshold Equations (BMDP P9R)

a. VISCAT I vs. VISCAT II+III separation

$$VIS = 0.424612 - 0.0000997789*VM$$
$$+ 0.0000403063*U500 - 0.0360747*T925$$
$$- 0.132972*E925 + 0.114795*ESUM$$
$$- 0.00286176*EPRD$$

b. VISCAT II vs. VISCAT III separation (EVAR model)

$$VIS = -7.19287 - 0.000788627*PS$$
$$- 0.0685555*E850 - 0.0579988*E500$$
$$+ 0.0222827*SHF + 0.195715*SHWRS$$
$$+ 0.0208835*ESUM$$

c. VISCAT II vs. VISCAT III separation (QUAD model)

$$VIS = -7.28759 - 0.000797890*PS$$
$$- 0.701888*E850 - 0.0547155*E500$$
$$+ 0.0226117*SHF + 0.202564*SHWRS$$
$$+ 0.0212283*ESUM$$

VI. Area 4, TAU-00 Threshold Equations (BMDP P2R)

a. VISCAT I vs. VISCAT II+III separation

$$VIS = 0.98483 - 0.75281E-03*STRTFQ$$
$$+ 0.70578*DTDP$$

115

VII. Area 4, TAU-24 Threshold Equations (BMDP P9R)

   a. VISCAT I vs. VISCAT II+III separation

$$VIS = -3.02386 - 0.200326*T925$$
$$- 0.000654475*STRTFQ - 0.000295813*DRAG$$
$$- 0.466227*VRT925 - 0.00192255*RH$$
$$+ 0.0153547*TV$$

   b. VISCAT II vs. VISCAT III separation (EVAR model)

$$VIS = 1.19369 - 0.0709575*E500$$
$$- 0.000617273*V500 + 0.193681*SHWRS$$
$$- 0.000551506*DRAG - 2.96306*VRT925$$
$$- 0.0180048*DUDP$$

   c. VISCAT II vs. VISCAT III separation (QUAD model)

$$VIS = 1.36198 - 0.0737982*E500$$
$$- 0.000061033*V500 + 0.185475*SHWRS$$
$$- 3.05142*VRT925 - 0.0184565*DUDP$$
$$- 0.00185381*RH$$

VIII. Area 4, TAU-48 Threshold Equations (BMDP P9R)

   a. VISCAT I vs. VISCAT II+III separation

$$VIS = -8.24765 - 0.0085996*T500$$
$$- 0.0333863*T925 - 0.0177121*E925$$
$$- 0.00059629*STRTFQ + 0.000128675*DTDP$$
$$+ 0.0343295*TV$$

   b. VISCAT II vs. VISCAT III separation (EVAR model)

$$VIS = 1.20788 - 0.026601*E850$$
$$- 0.0000310346*U500 - 0.0000480308*V500$$
$$+ 0.203575*SHWRS - 3.2719*VRT925$$
$$+ 4.10651*DEDP$$

116

c. VISCAT II vs. VISCAT III separation (QUAD model)

$$VIS = -12.5384 - 0.0397823*E850$$
$$- 0.0000388604*V500 - 0.043269*T925$$
$$+ 0.201266*SHWRS - 3.46254*VRT925$$
$$+ 0.0500493*TV$$

117

TABLE I. A summary of 1200GMT observations, 15 May--07 July 1983, North Atlantic Ocean homogeneous areas shown in Fig. 1: TAU-00

Area	DEP	IND	Total	DEP VISCAT I	DEP VISCAT II	DEP VISCAT III	IND VISCAT I	IND VISCAT II	IND VISCAT III
1	1817	908	2725	102 (5.6%)	275 (15.1%)	1440 (79.3%)	61 (6.7%)	161 (17.7%)	686 (75.6%)
2	1912	955	2867	190 (9.9%)	214 (11.2%)	1508 (78.9%)	87 (9.1%)	103 (10.8%)	765 (80.1%)
3E	88	43	131	4 (4.5%)	21 (23.9%)	63 (71.6%)	4 (9.3%)	10 (23.3%)	29 (67.4%)
3W	1526	762	2288	296 (19.4%)	190 (12.5%)	1040 (68.3%)	141 (18.5%)	94 (12.3%)	527 (69.2%)
4	3181	1590	4771	85 (2.7%)	400 (12.6%)	2696 (84.8%)	44 (2.8%)	197 (12.4%)	1349 (84.8%)
5	2263	1131	3394	12 (0.5%)	92 (4.1%)	2159 (95.4%)	5 (0.4%)	42 (3.7%)	1084 (95.9%)
6	1985	992	2977	30 (1.5%)	129 (6.0%)	1836 (92.5%)	11 (1.1%)	59 (5.9%)	922 (93.0%)
7	534	267	801	3 (0.6%)	23 (4.3%)	508 (95.1%)	4 (1.5%)	11 (4.1%)	252 (94.4%)
8	856	428	1284	1 (0.1%)	20 (2.3%)	835 (97.5%)	0 (0.0%)	7 (1.6%)	421 (98.4%)

TABLE II. A summary of 1200GMT observations, 15 May--07 July 1983, North Atlantic Ocean homogeneous areas shown in Fig. 1: TAU-24 forecast projection

Area	DEP	IND	Total	DEP VISCAT I	DEP VISCAT II	DEP VISCAT III	IND VISCAT I	IND VISCAT II	IND VISCAT III
1	1702	851	2553	102 (6.0%)	275 (16.2%)	1325 (77.8%)	38 (4.5%)	121 (14.2%)	692 (81.3%)
2	1760	879	2639	180 (10.2%)	206 (11.7%)	1374 (78.1%)	71 (8.1%)	98 (11.1%)	710 (80.8%)
3E	78	38	116	5 (6.4%)	17 (21.8%)	56 (71.8%)	0 (0.0%)	8 (21.9%)	30 (78.9%)
3W	1415	707	2122	270 (19.1%)	173 (12.2%)	972 (68.7%)	137 (19.4%)	89 (12.6%)	481 (68.0%)
4	2938	1469	4407	81 (2.8%)	368 (12.5%)	2489 (84.7%)	38 (2.6%)	175 (11.9%)	1256 (85.5%)
5	2071	1034	3105	10 (0.4%)	95 (4.6%)	1966 (93.9%)	5 (0.5%)	36 (3.5%)	993 (96.0%)
6	1860	930	2790	25 (1.3%)	104 (5.6%)	1439 (93.1%)	13 (1.4%)	65 (6.9%)	852 (91.6%)
7	486	243	729	2 (0.4%)	18 (3.7%)	466 (95.9%)	1 (0.4%)	11 (4.5%)	231 (95.1%)
8	810	404	1214	1 (0.1%)	20 (2.5%)	789 (97.4%)	0 (0.0%)	10 (2.5%)	394 (97.5%)

TABLE III. A summary of 1200GMT observations, 15 May--09 July 1983, North Atlantic Ocean homogeneous areas shown in Fig. 1: TAU-48 forecast projection

Area	DEP	IND	Total	DEP VISCAT I	DEP VISCAT II	DEP VISCAT III	IND VISCAT I	IND VISCAT II	IND VISCAT III
1	1825	912	2737	107 (5.9%)	267 (14.6%)	1451 (79.5%)	52 (5.7%)	154 (16.9%)	706 (77.4%)
2	1852	925	2777	182 (9.8%)	230 (12.4%)	1440 (77.8%)	91 (9.8%)	107 (11.6%)	727 (78.6%)
3E	84	41	125	2 (2.4%)	23 (27.4%)	59 (70.2%)	4 (9.8%)	9 (27.0%)	28 (68.3%)
3W	1487	743	2230	290 (19.5%)	186 (12.5%)	1011 (68.0%)	132 (17.8%)	111 (14.9%)	500 (67.3%)
4	3056	1527	4583	109 (3.6%)	406 (13.3%)	2541 (83.1%)	45 (2.9%)	196 (12.8%)	1286 (84.3%)
5	2170	1084	3254	11 (0.6%)	90 (4.1%)	2069 (95.3%)	6 (0.5%)	42 (3.9%)	1036 (95.6%)
6	1930	963	2893	25 (1.3%)	132 (6.8%)	1773 (91.9%)	14 (1.4%)	58 (6.0%)	891 (92.6%)
7	505	252	757	4 (0.8%)	22 (4.4%)	479 (94.9%)	3 (1.2%)	11 (4.4%)	238 (94.4%)
8	832	416	1248	0 (0.0%)	17 (2.0%)	815 (98.0%)	1 (0.2%)	12 (2.9%)	403 (96.9%)

120

TABLE IV.   Number of observations of three visibility
            categories and 95% confidence intervals for
            the dependent and independent FATJUNE 1983
            data for the North Atlantic Ocean homogeneous
            areas 2 and 4, for TAU-00, TAU-24 and TAU-48
            and area 3W for TAU-24 and TAU-48

TAU 00

Area 2	Total	VISCAT I	VISCAT II	VISCAT III
DEP	1912	190 (.099)	214 (.112)	1508 (.789)
IND	955	87 (.091)	103 (.108)	765 (.801)
95% C.I.		(.086-.107)	(.099-.122)	(.778-.808)

Area 4	Total	VISCAT I	VISCAT II	VISCAT III
DEP	3181	85 (.027)	400 (.126)	2696 (.848)
IND	1590	44 (.028)	197 (.124)	1349 (.848
95% C.I.		(.022-.032)	(.116-.135)	(.838-.858)

TAU 24

Area 2	Total	VISCAT I	VISCAT II	VISCAT III
DEP	1760	180 (.102)	206 (.117)	1374 (.781)
IND	879	71 (.084)	98 (.111)	710 (.808)
95% C.I.		(.081-.106)	(.103-.127)	(.774-.805)

Area 3W	Total	VISCAT I	VISCAT II	VISCAT III
DEP	1415	270 (.191)	173 (.122)	972 (.687)
IND	707	137 (.194)	89 (.126)	481 (.680)
95% C.I.		(.173-.205)	(.109-.137)	(.665-.705)

Area 4	Total	VISCAT I	VISCAT II	VISCAT III
DEP	2938	81 (.028)	368 (.125)	2489 (.847)
IND	1469	38 (.026)	175 (.119)	1256 (.855)
95% C.I.		(.022-.032)	(.114-.133)	(.839-.860)

121

TABLE IV (CONTINUED)

TAU 48

Area 2	Total	VISCAT I	VISCAT II	VISCAT III
DEP	1852	182 (.098)	230 (.124)	1440 (.778)
IND	925	91 (.098)	107 (.116)	727 (.786)
95% C.I.		(.087-.109)	(.109-.133)	(.765-.796)

Area 3W	Total	VISCAT I	VISCAT II	VISCAT III
DEP	1487	290 (.195)	186 (.125)	1011 (.680)
IND	743	132 (.178)	111 (.149)	500 (.673)
95% C.I.		(.173-.205)	(.119-.147)	(.658-.697)

Area 4	Total	VISCAT I	VISCAT II	VISCAT III
DEP	3056	109 (.036)	406 (.133)	2541 (.831)
IND	1527	45 (.029)	196 (.128)	1286 (.842)
95% C.I.		(.028-.039)	(.122-.141)	(.824-.846)

TABLE V. Summary of the contingency table statistics results for all the models used in the North Atlantic homogeneous areas 2, 3W and 4 for the evaluated TAU-00, TAU-24 and TAU-48 model output periods for FATJUNE 1983

Area	TAU	MODEL	DEP AO(%)	DEP AAO(%)	DEP TS1	DEP ATS1	IND AO(%)	IND AAO(%)	IND TS1	IND ATS1
2	00	PR	78.92	0.25	0.29	0.22	80.00	-0.53	0.30	0.23
		PR+BMD	79.34	2.23	0.34	0.27	80.73	3.16	0.36	0.29
		EVAR	80.07	5.69	0.34	0.27	80.63	2.63	0.38	0.32
		QUAD	80.13	5.94	0.34	0.26	80.73	3.16	0.38	0.32
4	00	PR	97.08	80.82	0.77	0.77	79.56	-34.85	0.11	0.08
		PR+BMD	97.86	95.98	0.82	0.82	78.87	-39.42	0.11	0.09
		EVAR	-	-	-	-	-	-	-	-
		QUAD	-	-	-	-	-	-	-	-
2	24	PR	80.00	8.81	0.29	0.21	81.68	-2.37	0.27	0.20
		PR+BMD	78.47	1.81	0.35	0.27	80.32	4.73	0.32	0.26
		EVAR	78.18	0.52	0.33	0.26	81.34	2.96	0.34	0.29
		QUAD	68.64	-43.01	0.33	0.26	68.60	-63.31	0.34	0.29
3W	24	PR	95.55	85.78	0.87	0.83	67.47	-1.77	0.36	0.21
		PR+BMD	75.76	22.57	0.44	0.30	74.96	21.68	0.42	0.28
		EVAR	73.00	13.77	0.38	0.23	71.00	9.29	0.33	0.17
		QUAD	73.22	14.45	0.37	0.22	71.43	10.62	0.32	0.16

TABLE V (CONTINUED)

Area	TAU	MODEL	DEP AO(%)	DEP AAO(%)	DEP TS1	DEP ATS1	IND AO(%)	IND AAO(%)	IND TS1	IND ATS1
4	24	PR	91.49	44.32	0.53	0.52	80.05	-37.56	0.07	0.05
		PR+BMD	98.23	99.44	0.90	0.90	79.71	-39.91	0.09	0.06
		EVAR	82.85	-12.25	0.08	0.05	83.59	-13.15	0.07	0.05
		QUAD	-	-	-	-	-	-	-	-
2	48	PR	96.55	84.95	0.89	0.87	72.86	-26.77	0.26	0.17
		PR+BMD	78.80	2.91	0.32	0.24	80.22	7.58	0.37	0.31
		EVAR	77.59	-0.73	0.29	0.21	80.11	7.07	0.36	0.29
		QUAD	77.43	-1.46	0.29	0.21	79.68	5.05	0.36	0.29
3W	48	PR	93.34	79.20	0.82	0.78	66.49	-2.47	0.33	0.18
		PR+BMD	89.51	67.23	0.74	0.67	71.47	12.76	0.43	0.30
		EVAR	71.49	10.92	0.32	0.15	71.60	13.17	0.31	0.17
		QUAD	71.22	10.08	0.31	0.14	71.47	12.76	0.32	0.17
4	48	PR	96.63	80.00	0.79	0.78	81.86	-14.94	0.20	0.18
		PR+BMD	94.27	66.02	0.64	0.63	79.70	-28.63	0.20	0.17
		EVAR	82.59	-3.30	0.03	-0.01	82.97	-7.88	0.02	-0.01
		QUAD	83.54	2.33	0.05	0.01	83.89	-2.07	0.04	0.01

TABLE VI. A summary of 1200GMT observations, 15 May--23 June 1984, North Atlantic Ocean homogeneous areas shown in Fig. 1: TAU-24 forecast projection

Area	DEP	IND	Total	DEP VISCAT I	DEP VISCAT II	DEP VISCAT III	IND VISCAT I	IND VISCAT II	IND VISCAT III
2	1760	879	2639	180 (10.2%)	206 (11.7%)	1374 (78.1%)	71 (8.1%)	98 (11.1%)	710 (80.8%)
3W	1415	707	2122	270 (19.1%)	173 (12.2%)	972 (68.7%)	137 (19.4%)	89 (12.6%)	481 (68.0%)

TABLE VII. Summary of the contingency table statistics results for all the models used in the North Atlantic homogeneous areas 2 and 3W for the evaluated TAU-24 model forecast projection for 15 May--23 June 1984

Area	TAU	MODEL	DEP AO(%)	DEP AAO(%)	DEP TS1	DEP ATS1	IND AO(%)	IND AAO(%)	IND TS1	IND ATS1
2	24	PR	96.09	88.33	0.88	0.85	62.19	-12.40	0.25	0.06
		PR+BMD	87.04	61.28	0.69	0.62	64.15	-6.59	0.34	0.17
		EVAR	78.07	0.00	0.33	0.25	81.23	2.37	0.33	0.27
		QUAD	78.92	3.89	0.33	0.25	81.46	3.55	0.33	0.27
3W	24	PR	69.68	20.75	0.38	0.16	65.61	7.39	0.31	0.06
		PR+BMD	68.88	18.68	0.37	0.14	69.65	18.29	0.36	0.13
		EVAR	72.86	13.32	0.37	0.22	70.86	8.85	0.33	0.17
		QUAD	72.79	13.09	0.37	0.22	70.58	7.96	0.32	0.15

OPERATIONAL U.S. NAVY
MODEL OUTPUT STATISTICS (MOS)
DEVELOPMENT SCHEDULE

ELEMENT GROUP / OCEAN BASIN	VISIBILITY CEILING CLOUD AMOUNT OBSTR TO VIS	SIG WAVE HT WIND WAVES OCEAN SWELL	SFC WIND SFC TEMP SFC DEWPOINT	PRECIP OCCUR PRECIP AMT TRW OCCUR
NORTH ATLANTIC	1987	1988	1990	1991
MEDITERRANEAN				
NORTH PACIFIC	1988	1989		
INDIAN				
SOUTH ATLANTIC	1989	1990	1991	1992
SOUTH PACIFIC				

Figure 1. Proposed U.S. Navy Model Output Statistics
(MOS) development schedule
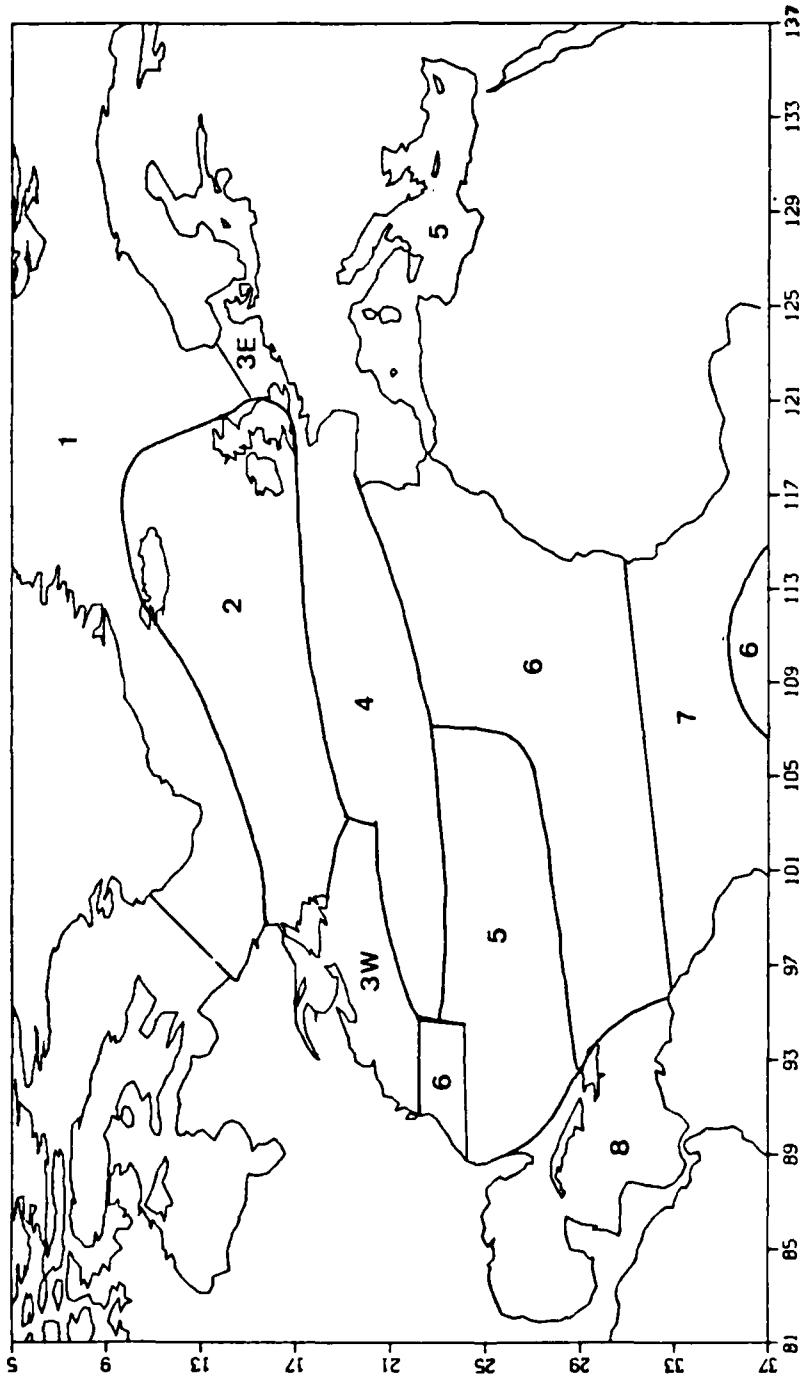
Figure 2. Homogeneous areas for the North Atlantic Ocean, May, June and July, from Lowe (1984b)
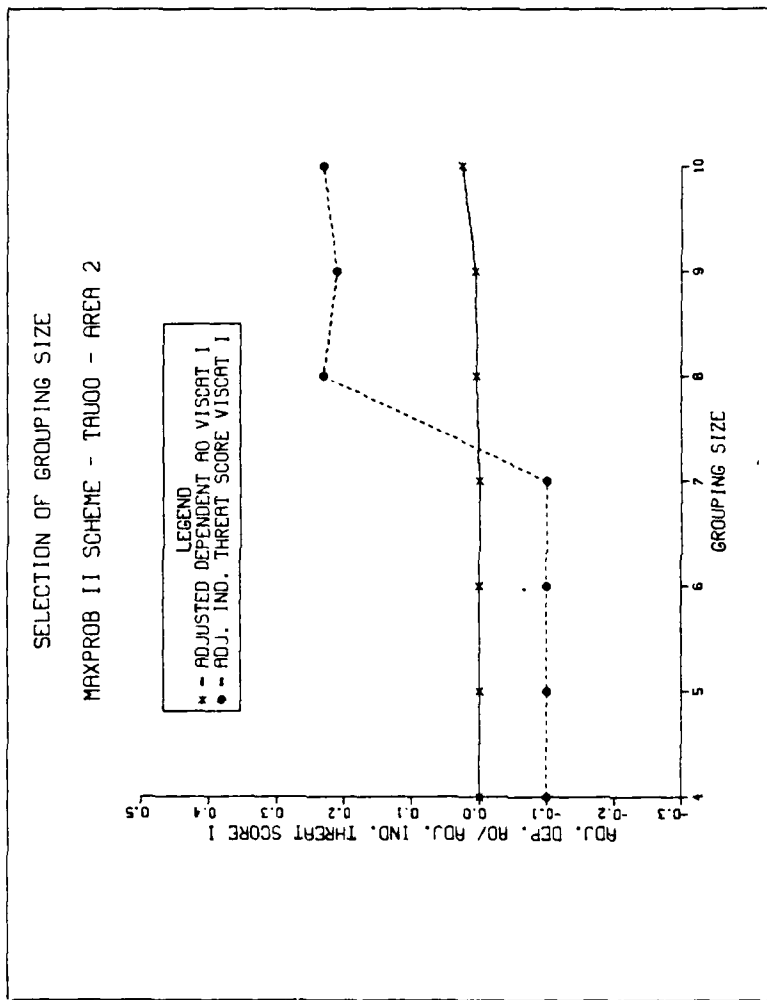
Figure 3. Relationship of equally populous grouping size to the adjusted
AO (dependent data) and the adjusted VISCAT I threat score
(independent data) for area 2, TAU-00 (PR model, MAXPROB II
strategy). For this case a grouping size of eight was selected
strategy).

NUMBER OF PREDICTORS VS. SCORING TECHNIQUES

TAU00 - AREA 2 - MAXPROBI - GROUPING SIZE OF 8
PREDICTORS E850, ENTR, DVDP, U1000, STRTH

INDEPENDENT DATA

			AO = 80.0%	AAO = -0.53%
39	81	716	A1 = 10.79%	
0	0	0	TS1 = 0.30	ATS1 = 0.23
48	22	49	TS2 = 0.0	ATS2 = -0.12
			TS12 = 0.20	ATS12 = 0.0

DEPENDENT DATA

			AO = 78.92%	AAO = 0.25%
94	173	1413	A1 = 11.19%	
0	0	0	TS1 = 0.29	ATS1 = 0.22
96	41	95	TS2 = 0.0	ATS2 = 0.13
			TS12 = 0.19	ATS12 = -0.02

Figure 4a. Skill diagram and contingency table results for area 2, TAU-00
(PR model) for the MAXPROB I strategy. The contingency table
corresponds to those scores associated with the maximum independent
VISCAT I threat score achieved at the first predictor level

130

NUMBER OF PREDICTORS VS. SCORING TECHNIQUES

TAU00 - AREA 2 - MAXPROBII - GROUPING SIZE OF 8

PREDICTORS E850, ENTR, DVDP, U1000, STRTTH

LEGEND
□ - DEP. AO
● - DEP. THR. I
× - INDEP. AO
● - INDEP. THR. I

ADJUSTED AO & THREAT SCORE (VISCAT I)

NUMBER OF PREDICTORS
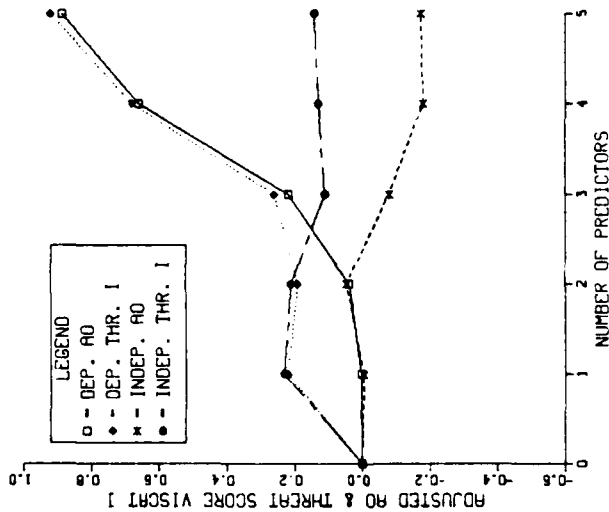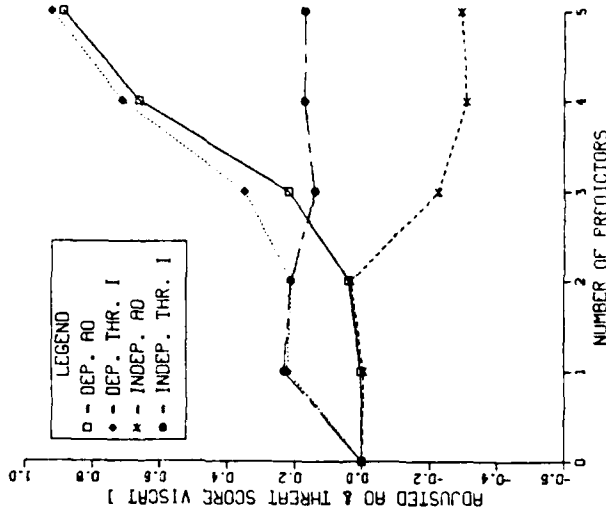
INDEPENDENT DATA

	1	2	3
3	39	81	716
2	0	0	0
1	48	22	49

FORECAST / OBSERVED

AO = 80.0% AAO = -0.53%

A1 = 10.79%

TS1 = 0.30 ATS1 = 0.23

TS2 = 0.0 ATS2 = -0.12

TS12 = 0.20 ATS12 = 0.0

DEPENDENT DATA

	1	2	3
3	94	173	1413
2	0	0	0
1	96	41	95

FORECAST / OBSERVED

AO = 78.92% AAO = 0.25%

A1 = 11.19%

TS1 = .29 ATS1 = .22

TS2 = 0.0 ATS2 = -.13

TS12 = .19 ATS12 = -.02

Figure 4b. Skill diagram and contingency table results for area 2, TAU-00 (PR model) for the MAXPROB II strategy. The contingency table corresponds to those scores associated with the maximum independent VISCAT I threat score achieved at the first predictor level

131
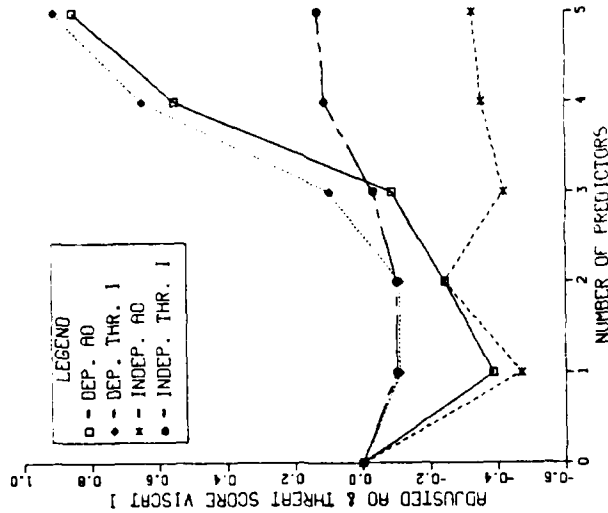
INDEPENDENT DATA

$AO=73.61\%$ $AAO=-32.63\%$
$A1=20.10\%$.
$TS1=0.21$ $ATS1=0.13$
$TS2=0.09$ $ATS2=-0.02$
$TS12=0.15$ $ATS12=-0.07$

FORECAST / OBSERVED

	1	2	3
3	41	75	660
2	22	19	86
1	24	9	19

DEPENDENT DATA

$AO=96.86\%$ $AAO=85.15\%$
$A1=3.14\%$
$TS1=0.92$ $ATS1=0.91$
$TS2=0.75$ $ATS2=0.72$
$TS12=0.86$ $ATS12=0.83$

FORECAST / OBSERVED

	1	2	3
3	0	31	1494
2	15	183	14
1	175	0	0

NUMBER OF PREDICTORS VS. SCORING TECHNIQUES

TAU00 - AREA 2 - NAT REGR - GROUPING SIZE OF 8
PREDICTORS E850, ENTR, OVDP, U1000, STRTH

LEGEND
□ - DEP. AO
♦ - DEP. THR. I
✕ - INDEP. AO
● - INDEP. THR. I

ADJUSTED AO & THREAT SCORE VISCAT I

NUMBER OF PREDICTORS

Figure 4c. Skill diagram and contingency table results for area 2, TAU-00 (PR model) for the natural regression strategy. The contingency table corresponds to those scores associated with the maximum independent VISCAT I threat score achieved at the fifth predictor level

132

Predictor	FD(96)	FD	A0	A0(96)	A1	A1(05)
E850	0.1039		78.9%	37.6%	11.2%	34.6%
ENTR	0.1469	0.1146	79.7%	43.6%	11.2%	35.0%
DVDP	0.1800	0.1554	83.5%	57.6%	10.0%	26.8%
U1000	0.2078	0.2071	92.8%	71.6%	4.9%	17.9%
STRTTH	0.2323	0.2328				

Figure 5. Functional dependence, A0/A1 statistics and 96%/05% confidence interval values for area 2, TAU-00 (PR model, MAXPROB II strategy)

133
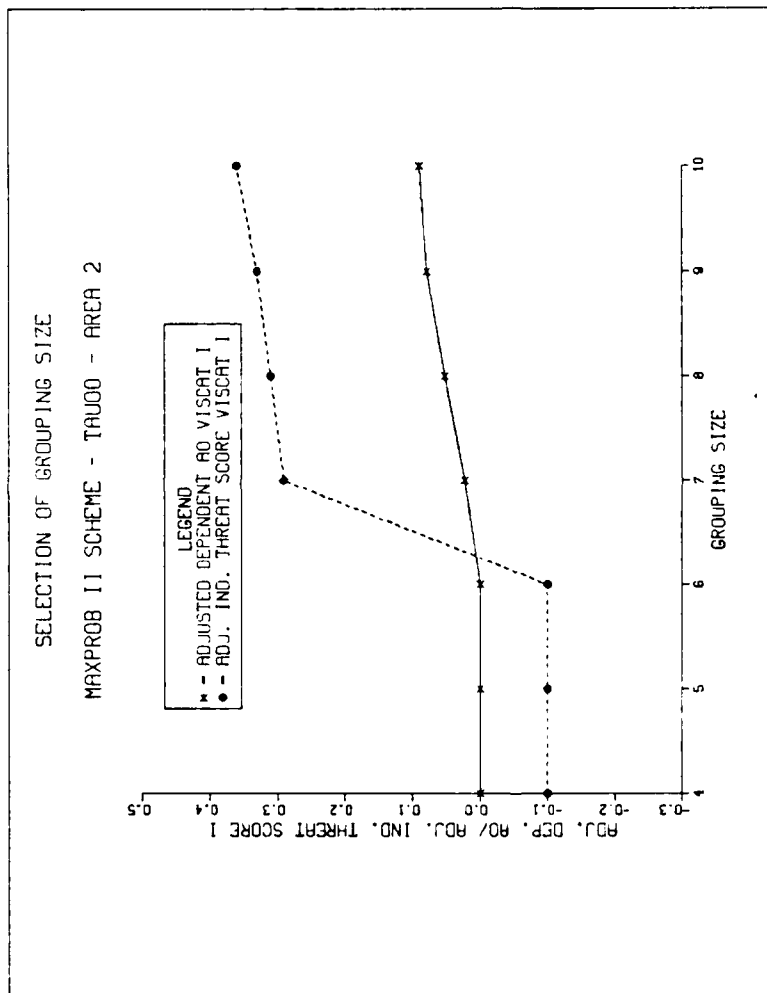
Figure 6. Relationship of equally populous grouping size to the adjusted A0 (dependent data) and the adjusted VISCAT I threat score (independent data) for area 2, TAU-00 (PR+BMD model, MAXPROB II strategy). For this case a grouping size of seven was selected strategy).

NUMBER OF PREDICTORS VS. SCORING TECHNIQUES

TAU00 - AREA 2 - MAXPROBI - GROUPING SIZE OF 7

PREDICTORS BMD1, ENTR, DVDP, SFC P, PBLD

INDEPENDENT DATA

AO=80.73% AAO= 3.16%

A1= 10.79%

TS1= 0.36   ATS1= 0.29

TS2= 0.0   ATS2= -0.12

TS12= 0.23 ATS12= 0.04

	1	2	3
FORECAST 3	31	83	715
FORECAST 2	0	0	0
FORECAST 1	56	20	50

OBSERVED

DEPENDENT DATA

AO=79.34% AAO= 2.23%

A1= 11.19%

TS1= 0.34   ATS1= 0.27

TS2= 0.0   ATS2= -0.13

TS12= 0.23 ATS12= 0.02

	1	2	3
FORECAST 3	72	167	1399
FORECAST 2	0	0	0
FORECAST 1	118	47	109

OBSERVED

LEGEND
□ - DEP. AO
◆ - DEP. THR. I
× - INDEP. AO
● - INDEP. THR. I

ADJUSTED AO & THREAT SCORE VISCAT I

NUMBER OF PREDICTORS

Figure 7a.   Skill diagram and contingency table results for area 2, TAU-00 (PR+BMD model) for the MAXPROB I strategy. The contingency table corresponds to those scores associated with the maximum independent VISCAT I threat score achieved at the first predictor level

135

NUMBER OF PREDICTORS VS. SCORING TECHNIQUES

TAU00 - AREA 2 - MAXPROB11 - GROUPING SIZE OF 7

PREDICTORS BMD1, ENTR, DVDP, SFC P, PBLD
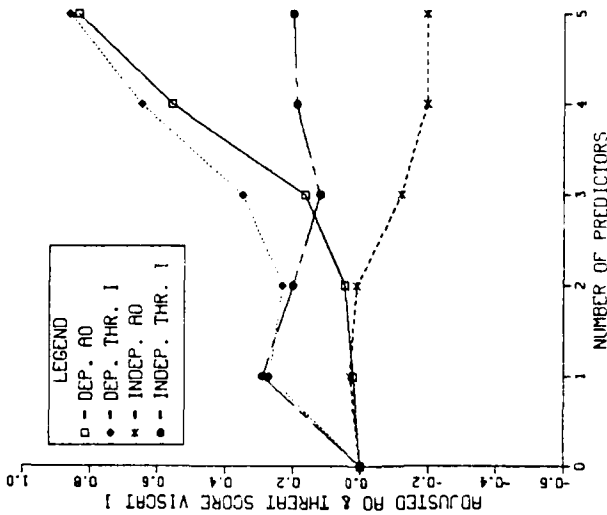
INDEPENDENT DATA

	1	2	3
3	31	83	715
2	0	0	0
1	56	20	50

FORECAST · OBSERVED

AO=80.73% AAO=3.16%

A1=10.79%

TS1=0.36   ATS1=0.29

TS2=0.0   ATS2=-0.12

TS12=0.23   ATS12=0.04

DEPENDENT DATA

	1	2	3
3	72	167	1399
2	0	0	0
1	118	47	109

FORECAST · OBSERVED

AO=79.34% AAO=2.23%

A1=11.19%

TS1=0.34   ATS1=0.27

TS2=0.0   ATS2=-0.13

TS12=0.23   ATS12=0.02

LEGEND
□ - DEP. AO
● - DEP. THR. I
× - INDEP. AO
● - INDEP. THR. I

Figure 7b.   Skill diagram and contingency table results for area 2, TAU-00 (PR+BMD model) for the MAXPROB II strategy.   The contingency table corresponds to those scores associated with the maximum independent VISCAT I threat score achieved at the first predictor level

NUMBER OF PREDICTORS VS. SCORING TECHNIQUES

TAU00 - AREA 2 - NAT REGR - GROUPING SIZE OF 7

PREDICTORS BMD1, ENTR, DVDP, SFC P, PBLD

INDEPENDENT DATA

$AO=74.87\%$ $AAO= -26.32\%$

$A1= 19.27\%$

$TS1= 0.24$, $ATS1= 0.17$
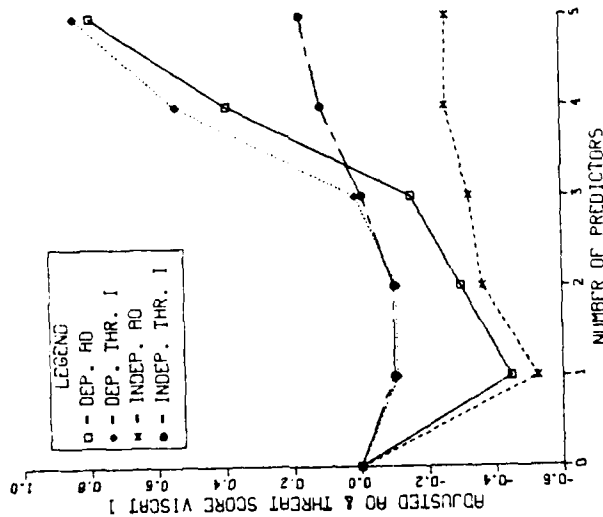
$TS2= 0.11$ $ATS2= 0.0$

$TS12= 0.18$ $ATS12= -0.03$

	1	2	3
3	36	67	663
2	22	23	82
1	29	13	20

FORECAST / OBSERVED

DEPENDENT DATA

$AO=95.61\%$ $AAO=79.21\%$

$A1=12.83\%$

$TS1=0.86$ $ATS1=0.84$

$TS2=0.67$ $ATS2=0.63$

$TS12=0.80$ $ATS12=0.75$

	1	2	3
3	0	40	1491
2	26	173	17
1	164	1	0

FORECAST / OBSERVED

LEGEND
□ - DEP. AO
□ - DEP. THR. I
• - INDEP. AO
x - INDEP. THR. I
• - INDEP. THR. I

ADJUSTED AO & THREAT SCORE VISCAT I

NUMBER OF PREDICTORS

Figure 7c. Skill diagram and contingency table results for area 2, TAU-00 (PR+BMD model) for the natural regression strategy. The contingency table corresponds to those scores associated with the maximum independent VISCAT I threat score achieved at the fifth predictor level

137

Predictor	FD(96)	FD	A0	A0(96)	A1	A1(05)
BMD1	0.1119		79.3%	37.5%	11.2%	33.1%
ENTR	0.1583	0.1121	79.9%	42.1%	11.2%	35.3%
DVDP	0.1938	0.1667	82.3%	54.1%	10.9%	29.0%
PS	0.2238	0.1940	90.6%	69.0%	6.4%	19.5%
PBLD	0.2502	0.2310	96.5%	74.9%	2.6%	15.9%

Figure 8. Functional dependence, A0/A1 statistics and 96%/05% confidence interval values for area 2, TAU-00 (PR+EMD model, MAXPROB II strategy)

138

DEPENDENT DATA

3	78	169	1417	AO $=80.07\%$ AAO $= 5.69\%$
				A1 $= 14.02\%$
2	31	33	56	TS1 $= 0.34$ ATS1 $= 0.27$
				TS2 $= 0.11$ ATS2 $= 0.00$
1	81	12	35	TS12 $= 0.23$ ATS12 $= 0.02$

FORECAST (vertical axis), OBSERVED 1 2 3 (horizontal axis)

INDEPENDENT DATA

3	34	86	719	AO $= 80.63\%$ AAO $= 2.63\%$
				A1 $= 14.66\%$
2	13	11	35	TS1 $= 0.38$ ATS1 $= 0.32$
				TS2 $= 0.07$ ATS2 $= -0.04$
1	40	6	11	TS12 $= 0.22$ ATS12 $= 0.02$

FORECAST (vertical axis), OBSERVED 1 2 3 (horizontal axis)

Figure 9. Contingency table results for the area 2,
TAU-00 equal variance threshold model

DEPENDENT DATA

FORECAST	1	2	3
3	80	169	1420
2	31	33	55
1	79	12	33

OBSERVED

$AO = 80.13\%$ $AAO = 5.94\%$

$A1 = 13.96\%$

$TS1 = 0.34$ $ATS1 = 0.26$

$TS2 = 0.11$ $ATS2 = 0.00$

$TS12 = 0.23$ $ATS12 = 0.02$

INDEPENDENT DATA

FORECAST	1	2	3
3	34	86	720
2	13	11	34
1	40	6	11

OBSERVED

$AO = 80.73\%$ $AAO = 3.16\%$

$A1 = 14.55\%$

$TS1 = 0.38$ $ATS1 = 0.32$

$TS2 = 0.07$ $ATS2 = -0.04$

$TS12 = 0.22$ $ATS12 = 0.02$

Figure 10. Contingency table results for the area 2,
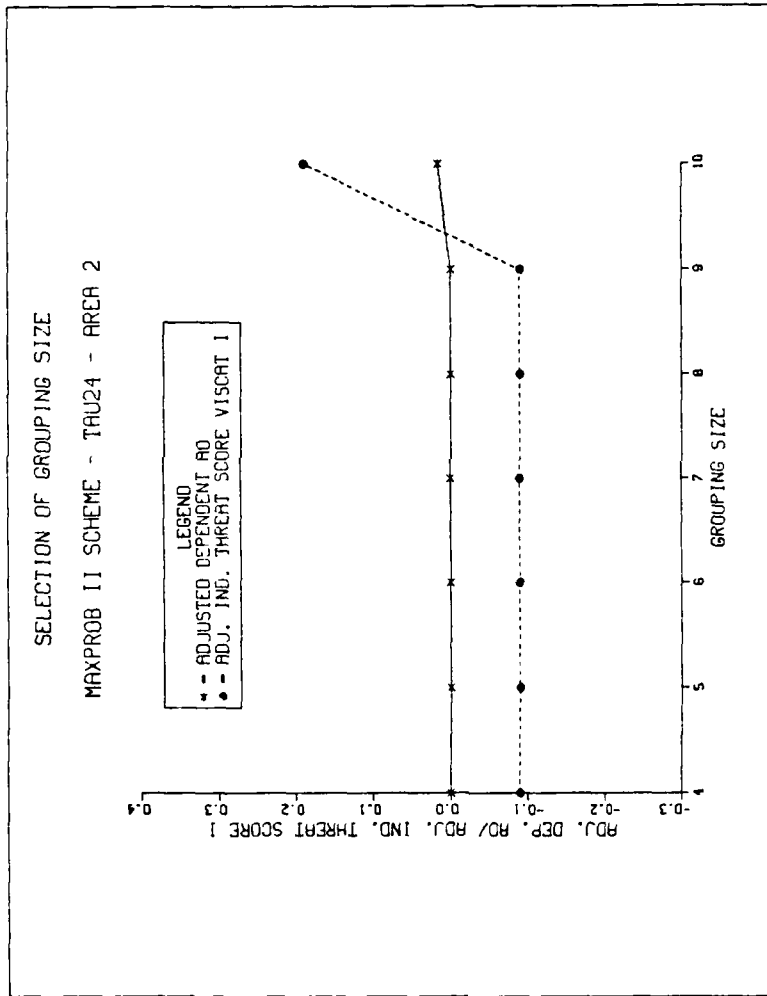   TAU-00 quadratic threshold model

Figure 11. Relationship of equally populous grouping size to the adjusted A0 (dependent data) and the adjusted VISCAT I threat score (independent data) for area 2, TAU-24 (PR model, MAXPROB II strategy). For this case a grouping size of ten was selected strategy).

NUMBER OF PREDICTORS VS. SCORING TECHNIQUES

TAU24 - AREA 2 - MAXPROB1 - GROUPING SIZE OF 10

PREDICTORS E850, ENTR, DVDP, DIV925
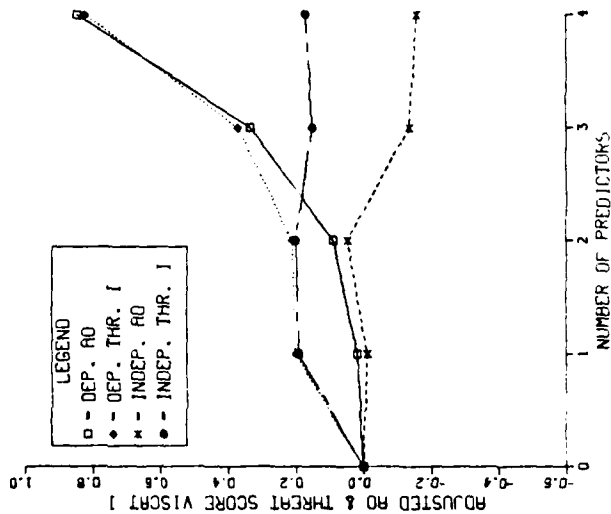
INDEPENDENT DATA

AO=81.68% AAO=4.73%

A1=11.15%

TS1=0.27 ATS1= 0.20

TS2=0.0 ATS2= -0.13

TS12=0.14 ATS12= -0.06

DEPENDENT DATA

AO=80.00% AAO= 8.81%

A1=11.70%

TS1=0.29 ATS1= 0.21

TS2=0.0 ATS2= -0.13

TS12=0.15 ATS12= -0.09

Figure 12a. Skill diagram and contingency table results for area 2, TAU-24 (PR model) for the MAXPROB I strategy. The contingency table corresponds to those scores associated with the maximum independent VISCAT I threat score achieved at the second predictor level

142

Figure 12b. Skill diagram and contingency table results for area 2, TAU-24 (PR model) for the MAXPROB II strategy. The contingency table corresponds to those scores associated with the maximum independent VISCAT I threat score achieved at the second predictor level

143

NUMBER OF PREDICTORS VS. SCORING TECHNIQUES

TAU24 - AREA 2 - NAT REGR - GROUPING SIZE OF 10
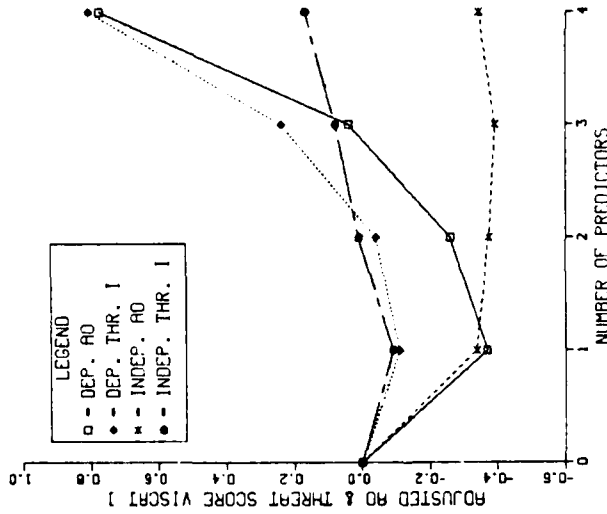
PREDICTORS E850, ENTR, DVDP, DIV925

INDEPENDENT DATA

	1	2	3	
FORECAST 3	31	64	601	AO=74.18% AAO=-34.32%
FORECAST 2	16	27	84	A1=19.45%
FORECAST 1	24	7	25	
	1	2	3	
		OBSERVED		

TS1=0.23 ATS1=0.17
TS2=0.14 ATS2=0.03
TS12=0.18 ATS12=-0.02

DEPENDENT DATA

	1	2	3	
FORECAST 3	0	28	1347	AO=95.17% AAO=77.98%
FORECAST 2	30	178	27	A1=4.83%
FORECAST 1	150	0	0	
	1	2	3	
		OBSERVED		

TS1=0.83 ATS1=0.81
TS2=0.68 ATS2=0.63
TS12=0.79 ATS12=0.73

LEGEND
□ - DEP. AO
♦ - DEP. THR. I
× - INDEP. AO
● - INDEP. THR. I

Figure 12c. Skill diagram and contingency table results for area 2, TAU-24 (PR model) for the natural regression strategy. The contingency table corresponds to those scores associated with the maximum independent VISCAT I threat score achieved at the fifth predictor level

144

Predictor	FD(96)	FD	A0	A0(96)	A1	A1(05)
E850	0.0944		78.4%	38.0%	11.7%	34.7%
ENTR	0.1334	0.0871	80.0%	46.0%	11.7%	33.6%
DVDP	0.1633	0.1318	85.3%	64.8%	9.1%	22.3%
DIV925	0.1885	0.1714	96.5%	75.5%	2.2%	15.5%

Figure 13. Functional dependence, A0/A1 statistics and 96%/05% confidence interval values for area 2, TAU-24 (PR model, MAXPROB II strategy)
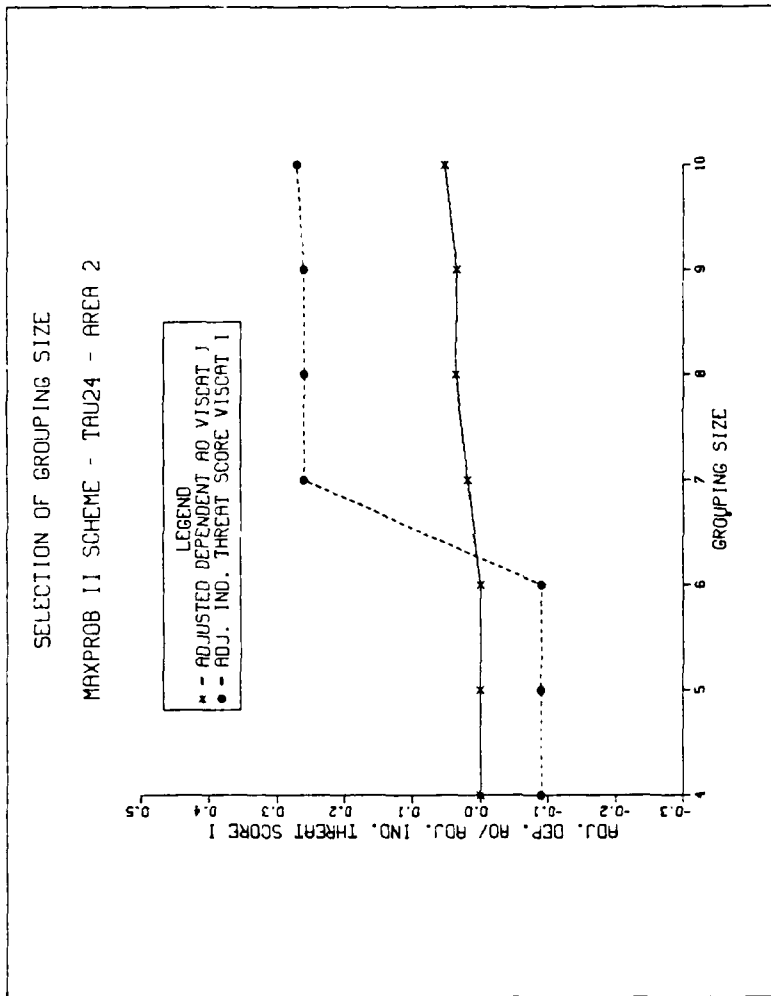
Figure 14. Relationship of equally populous grouping size to the adjusted A0 (dependent data) and the adjusted VISCAT I threat score (independent data) for area 2, TAU-24 (PR+BMD model, MAXPROB II strategy). For this case a grouping size of seven was selected strategy).

NUMBER OF PREDICTORS VS. SCORING TECHNIQUES

TAU24 - AREA 2 - MAXPROB1 - GROUPING SIZE OF 7
PREDICTORS BMD2, VRT925, ENTR, U1000, RH

INDEPENDENT DATA

$AO=80.32\%$ $AAO=-2.37\%$
$A1=11.15\%$
$TS1=0.32$ $ATS1=0.26$
$TS2=0.00$ $ATS2=-0.13$
$TS12=0.21$ $ATS12=0.02$

26	78	661
0	0	0
45	20	49

OBSERVED

FORECAST

DEPENDENT DATA

$AO=78.47\%$ $AAO=1.81\%$
$A1=11.70\%$
$TS1=0.35$ $ATS1=0.27$
$TS2=0.00$ $ATS2=-0.13$
$TS12=0.23$ $ATS12=0.01$

69	169	1270
0	0	0
111	37	104

OBSERVED

FORECAST

LEGEND
□ = DEP. AO
♦ = DEP. THR. I
× = INDEP. AO
● = INDEP. THR. I

ADJUSTED AO & THREAT SCORE VISCAT I

NUMBER OF PREDICTORS

Figure 15a. Skill diagram and contingency table results for area 2, TAU-24 (PR+BMD model) for the MAXPROB I strategy. The contingency table corresponds to those scores associated with the maximum independent VISCAT I threat score achieved at the first predictor level

147

NUMBER OF PREDICTORS VS. SCORING TECHNIQUES

TAU24 - AREA 2   MAXPROB11 - GROUPING SIZE OF 7
PREDICTORS BMD2, VRT925, ENTR, U1000, RH
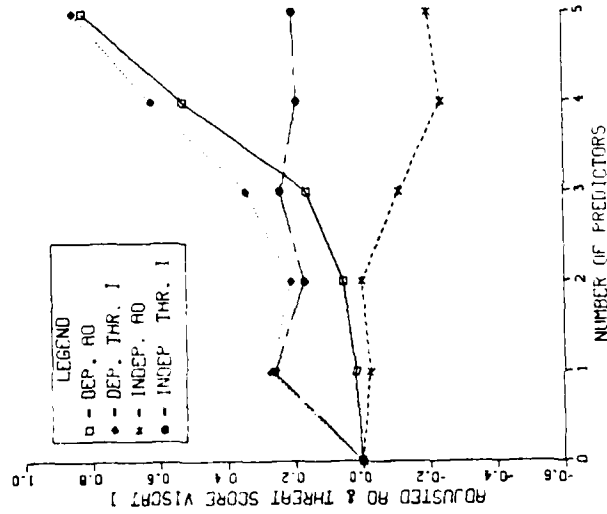
INDEPENDENT DATA

	1	2	3
3	26	78	661
2	0	0	0
1	45	20	49

FORECAST / OBSERVED

AO=80.32% AAO=-2.37%
A1= 11.15%
TS1= 0.32   ATS1= 0.26
TS2= 0.0   ATS2= -0.13
TS12= 0.21   ATS12= 0.02

DEPENDENT DATA

	1	2	3
3	69	169	1270
2	0	0	0
1	111	37	104

FORECAST / OBSERVED

AO=78.47% AAO=1.81%
A1= 11.70%
TS1= 0.35   ATS1= 0.27
TS2= 0.0   ATS2= -0.13
TS12= 0.23   ATS12= 0.01

LEGEND
□ = DEP. AO
● = DEP. THR. I
x = INDEP. AO
● = INDEP THR. I

ADJUSTED AO & THREAT SCORE(VISCAT)

NUMBER OF PREDICTORS

Figure 15b. Skill diagram and contingency table results for area 2, TAU-24
(PR+BMD model) for the MAXPROB II strategy. The contingency
table corresponds to those scores associated with the maximum
independent VISCAT I threat score achieved at the first
predictor level

148
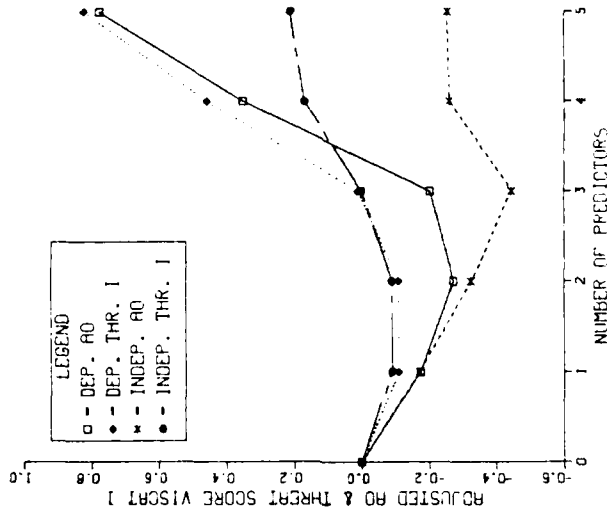
Figure 15c. Skill diagram and contingency table results for area 2, TAU-24 (PR+BMD model) for the natural regression strategy. The contingency table corresponds to those scores associated with the maximum independent VISCAT I threat score achieved at the fifth predictor level

Predictor	FD(96)	FD	A0	A0(96)	A1	A1(05)
BMD2	0.1146		78.5%	37.7%	11.7%	31.6%
VRT925	0.1621	0.0996	79.3%	42.6%	11.7%	35.3%
ENTR	0.1985	0.1642	81.6%	54.5%	11.5%	28.7%
U1000	0.2292	0.2185	89.6%	69.4%	6.9%	19.3%
RH	0.2563	0.2582	96.1%	75.3%	3.0%	15.8%

Figure 16. Functional dependence, A0/A1 statistics and 96%/05% confidence interval values for area 2, TAU-24 (PR+BMD model, MAXPROB II strategy)

DEPENDENT DATA

FORECAST			
3	80	172	1278
2	25	23	61
1	75	11	35
	1	2	3

OBSERVED

AO $=78.18\%$ AAO $=0.52\%$

A1 $=15.28\%$

TS1 $= 0.33$ ATS1 $= 0.26$

TS2 $= 0.08$ ATS2 $= -0.04$

TS12 $= 0.20$ ATS12 $= -0.02$

INDEPENDENT DATA

FORECAST			
3	31	74	668
2	7	14	27
1	33	10	15
	1	2	3

OBSERVED

AO $=81.34\%$ AAO $= 2.96\%$

A1 $= 13.42\%$

TS1 $= 0.34$ ATS1 $= 0.29$

TS2 $= 0.11$ ATS2 $= -0.01$

TS12 $= 0.22$ ATS12 $= 0.04$

Figure 17. Contingency table results for the area 2,
TAU-24 equal variance threshold model

151

DEPENDENT DATA

AO=**68.64%** AAO=**-43.01%**

A1= **27.50%**

TS1=**0.33**   ATS1= **0.26**

TS2= **0.14**   ATS2= **0.03**

TS12=**0.22**   ATS12= **0.0**

INDEPENDENT DATA

AO=**68.60%** AAO= **-63.31%**

A1=**27.53%**

TS1=**0.34**   ATS1= **0.29**

TS2=**0.11**   ATS2= **0.0**

TS12=**0.19**   ATS12= **0.0**

Figure 18.   Contingency table results for the area 2,
             TAU-24 quadratic threshold model

152
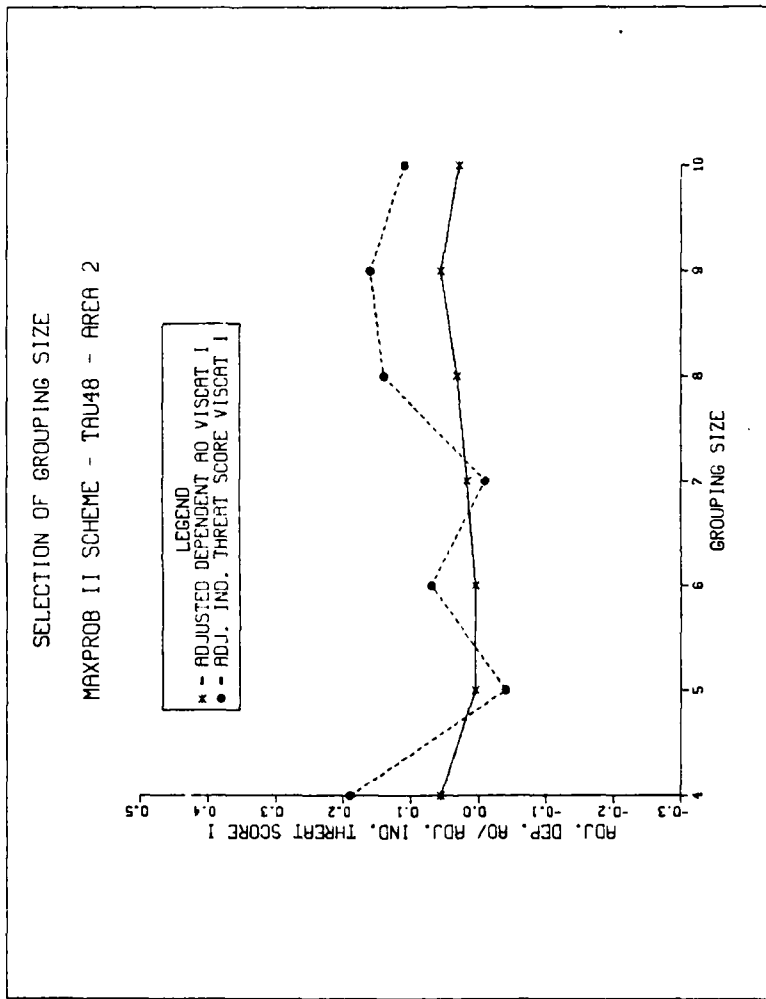
Figure 19. Relationship of equally populous grouping size to the adjusted A0 (dependent data) and the adjusted VISCAT I threat score (independent data) for area 2, TAU-48 (PR model, MAXPROB II strategy). For this case a grouping size of nine was selected strategy).

Predictor	FD(96)	FD	A0	A0(96)	A1	A1(05)
E850	0.0970		77.8%	38.0%	12.4%	33.3%
ENTR	0.1327	0.0930	79.0%	44.6%	12.4%	33.9%
DVDP	0.1643	0.1269	83.5%	61.1%	10.3%	24.8%
DRAG	0.1840	0.1696	89.2%	67.0%	7.3%	21.0%
DIV925	0.2167	0.1859	96.7%		2.5%	

Figure 20. Functional dependence, A0/A1 statistics and 96%/05% confidence interval values for area 2, TAU-48 (PR model, MAXPROB II strategy)

Figure 21a. Skill diagram and contingency table results for area 2, TAU-48 (PR model) for the MAXPROB I strategy. The contingency table corresponds to those scores associated with the maximum independent VISCAT I threat score achieved at the second predictor level

NUMBER OF PREDICTORS VS. SCORING TECHNIQUES

TAU48 - AREA 2 - MAXPROBII - GROUPING SIZE OF 9

PREDICTORS E850, ENTR, DVDP, DRAG, DIV925

INDEPENDENT DATA

	1	2	3
3	45	75	617
2	9	20	68
1	37	12	42

FORECAST / OBSERVED
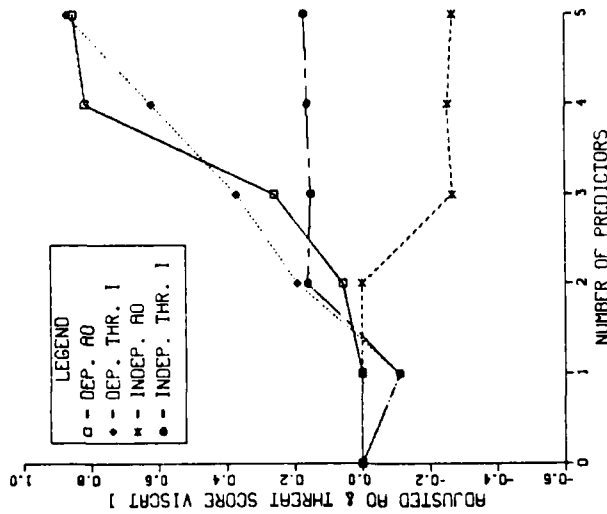
AO=72.86% AAO=-26.77%

A1=17.73%

TS1=0.26   ATS1=0.17

TS2=0.11   ATS2=-0.01

TS12=0.19   ATS12=-0.04

DEPENDENT DATA

	1	2	3
3	2	11	1398
2	1	213	28
1	179	6	14

FORECAST / OBSERVED

AO=96.65% AAO=84.95%

A1=2.48%

TS1=0.89   ATS1=0.87

TS2=0.82   ATS2=0.80

TS12=0.86   ATS12=0.82

LEGEND

□ - DEP. AO
♦ - DEP. THR. I
✳ - INDEP. AO
● - INDEP. THR. I

ADJUSTED AO & THREAT SCORE VISCAT I

NUMBER OF PREDICTORS

Figure 21b. Skill diagram and contingency table results for area 2, TAU-48 (PR model) for the MAXPROB II strategy. The contingency table corresponds to those scores associated with the maximum independent VISCAT I threat score achieved at the fifth predictor level

156

NUMBER OF PREDICTORS VS. SCORING TECHNIQUES

TAU48 - AREA 2 - NAT REGR - GROUPING SIZE OF 9
PREDICTORS E850, ENTR, DVDP, DRAG, DIV925

INDEPENDENT DATA

	1	2	3
3	48	79	608
2	23	21	103
1	20	7	16

FORECAST / OBSERVED

AO=70.16% AAO=-39.39%

AI= 22.92%

TS1= 0.18   ATS1= 0.09

TS2= 0.09   ATS2= -0.03

TS12= 0.13   ATS12= -0.11

DEPENDENT DATA

	1	2	3
3	8	103	1365
2	78	125	75
1	96	2	0

FORECAST / OBSERVED

AO=85.64% AAO= 35.44%

AI= 13.93%

TS1= 0.52   ATS1= 0.47

TS2= 0.33   ATS2= 0.23

TS12= 0.45   ATS12= 0.30

LEGEND
□ - DEP. AO
◆ - DEP. THR. I
✕ - INDEP. AO
● - INDEP. THR. I

ADJUSTED AO & THREAT SCORE VISCAT I

NUMBER OF PREDICTORS

Figure 21c.   Skill diagram and contingency table results for area 2, TAU-48
(PR model) for the natural regression strategy. The contingency
table corresponds to those scores associated with the maximum
independent VISCAT I threat score achieved at the fourth
predictor level

157

Figure 22. Relationship of equally populous grouping size to the adjusted A0 (dependent data) and the adjusted VISCAT I threat score (independent data) for area 2, TAU-48 (PR+BMD model, M₁ PROB II strategy). For this case a grouping size of nine was selected strategy).

NUMBER OF PREDICTORS VS. SCORING TECHNIQUES

TAU48 - AREA 2 - MAXPROBI - GROUPING SIZE OF 9
PREDICTORS BMD2, VRT925, ENTR, U500, DRAG
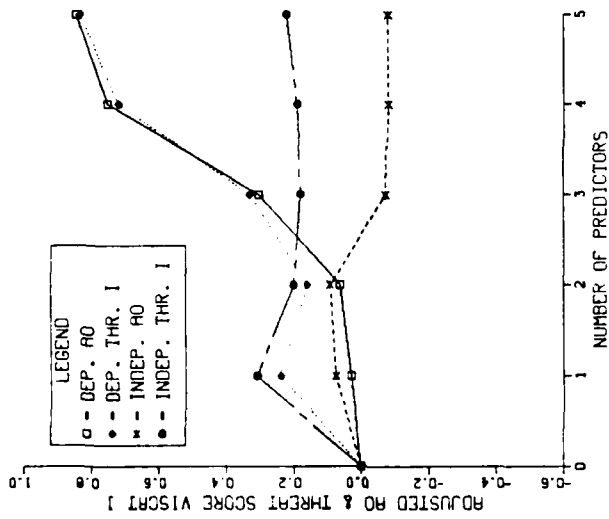
INDEPENDENT DATA

36	91	687
0	0	0
55	16	40

AO=80.22% AAO=7.58%

A1=11.57%

TS1=0.37 ATS1= 0.31

TS2=0.0 ATS2= -0.13

TS12=0.23 ATS12= 0.02

DEPENDENT DATA

89	198	1359
0	0	0
93	32	81

AO=78.40% AAO=2.91%

A1=12.42%

TS1=0.32 ATS1= 0.24

TS2=0.0 ATS2= -0.14

TS12=0.19 ATS12= -0.04

LEGEND
□ - DEP. AO
• - DEP. THR. I
× - INDEP. AO
● - INDEP. THR. I

Figure 23a.   Skill diagram and contingency table results for area 2, TAU-48 (PR+BMD model) for the MAXPROB I strategy. The contingency table corresponds to those scores associated with the maximum independent VISCAT I threat score achieved at the first predictor level

159

NUMBER OF PREDICTORS VS. SCORING TECHNIQUES

TAU48 - AREA 2 - MAXPROBII - GROUPING SIZE OF 9

PREDICTORS BMD2, VRT925, ENTR, U500, DRAG

INDEPENDENT DATA

AO=80.22% AAO= 7.58%

A1=11.57%

TS1= 0.37 ATS1= 0.31

TS2= 0.0 ATS2=-0.13
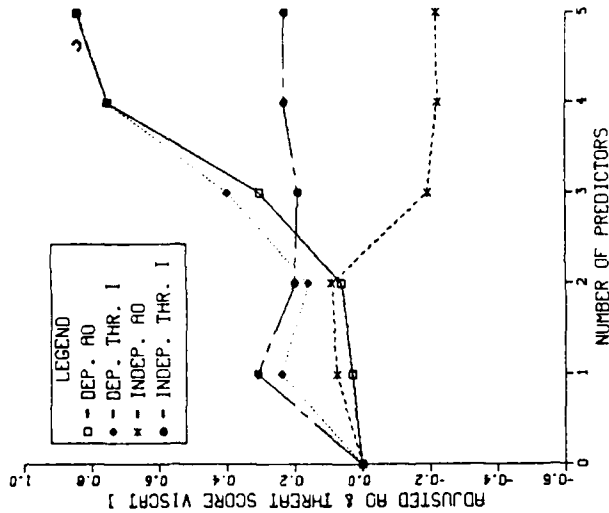
TS12=0.23 ATS12= 0.02

	1 OBSERVED	2	3
FORECAST 3	36	91	687
2	0	0	0
1	55	16	40

DEPENDENT DATA

AO=78.40% AAO= 2.91%

A1= 12.42%

TS1= 0.32 ATS1= 0.24

TS2= 0.0 ATS2=-0.14

TS12=0.19 ATS12=-0.04

	1 OBSERVED	2	3
FORECAST 3	89	198	1359
2	0	0	0
1	93	32	81

LEGEND
□ - DEP. AO
● - DEP. THR. I
× - INDEP. AO
● - INDEP. THR. I

ADJUSTED AO & THREAT SCORE (VISCAT I)

NUMBER OF PREDICTORS

Figure 23b. Skill diagram and contingency table results for area 2, TAU-48 (PR+BMD model) for the MAXPROB II strategy. The contingency table corresponds to those scores associated with the maximum independent VISCAT I threat score achieved at the first predictor level
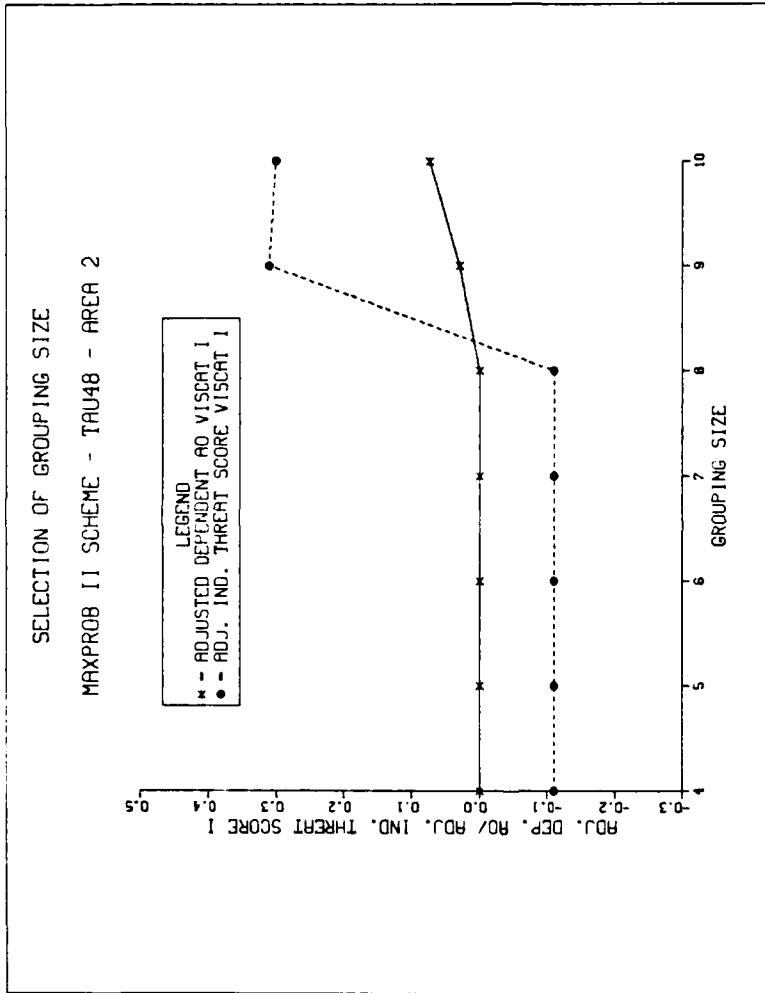
160

NUMBER OF PREDICTORS VS. SCORING TECHNIQUES

TAU48 - AREA 2 - NAT REGR - GROUPING SIZE OF 9
PREDICTORS BMD2, VRT925, ENTR, U500, DRAG
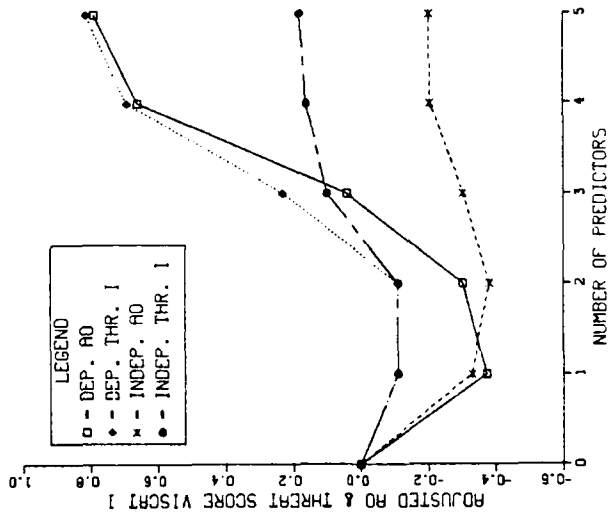
INDEPENDENT DATA

3	33	71	624
2	26	31	78
1	32	5	25
	1	2	3

FORECAST / OBSERVED

AO=74.27% AAO=-20.20%

A1=19.46%

TS1=0.26 ATS1=0.18

TS2=0.15 ATS2=0.04

TS12=0.21 ATS12=-0.01

DEPENDENT DATA

3	0	34	1418
2	32	196	22
1	150	0	0
	1	2	3

FORECAST / OBSERVED

AO=95.25% AAO=78.64%

A1=4.75%

TS1=0.82 ATS1=0.81

TS2=0.69 ATS2=0.65

TS12=0.80 ATS12=0.74

LEGEND
□ - DEP. AO
♦ - DEP. THR. I
× - INDEP. AO
● - INDEP. THR. I

ADJUSTED AO & THREAT SCORE VISCAT I

NUMBER OF PREDICTORS

Figure 23c. Skill diagram and contingency table results for area 2, TAU-48 (PR+BMD model) for the natural regression strategy. The contingency table corresponds to those scores associated with the maximum independent VISCAT I threat score achieved at the fifth predictor level

161

Predictor	FD(96)	FD	A0	A0(96)	A1	A1(05)
BMD2	0.0969		78.4%	38.0%	12.4%	33.2%
VRT925	0.1370	0.0888	79.1%	45.1%	12.4%	34.7%
ENTR	0.1678	0.1363	84.5%	60.8%	9.8%	24.9%
U500	0.1938	0.1729	94.4%	73.9%	3.7%	16.8%
DRAG	0.2168	0.1984	96.4%		2.1%	

Figure 24. Functional dependence, A0/A1 statistics and 96%/05% confidence interval values for area 2, TAU-48 (PR+BMD model, MAXPROB II strategy)

162

DEPENDENT DATA

3	89	197	1351	
2	28	21	57	
1	65	12	32	
	1	**2**	**3**	

FORECAST (vertical axis), OBSERVED (horizontal axis)

$AO = 77.59\%$ $AAO = -0.73\%$

$A1 = 15.87\%$

$TS1 = 0.29$ $ATS1 = 0.21$

$TS2 = 0.07$ $ATS2 = -0.07$

$TS12 = 0.17$ $ATS12 = -0.07$

INDEPENDENT DATA

3	40	88	685	
2	10	15	24	
1	41	4	18	
	1	**2**	**3**	

FORECAST (vertical axis), OBSERVED (horizontal axis)

$AO = 80.11\%$ $AAO = 7.07\%$

$A1 = 13.62\%$

$TS1 = 0.36$ $ATS1 = 0.29$

$TS2 = 0.11$ $ATS2 = -0.01$

$TS12 = 0.23$ $ATS12 = 0.02$

Figure 25.   Contingency table results for the area 2,
TAU-48 equal variance threshold model

163

DEPENDENT DATA

	1	2	3
3	101	197	1348
2	16	21	60
1	65	12	32

FORECAST (vertical axis) — OBSERVED (horizontal axis, 1 2 3)

$AO = 77.43\%$ $AAO = -1.46\%$

$A1 = 15.39\%$

$TS1 = 0.29$ $ATS1 = 0.21$

$TS2 = 0.07$ $ATS2 = -0.06$

$TS12 = 0.17$ $ATS12 = -0.07$

INDEPENDENT DATA

	1	2	3
3	44	91	684
2	6	12	25
1	41	4	18

FORECAST (vertical axis) — OBSERVED (horizontal axis, 1 2 3)

$AO = 79.68\%$ $AAO = 5.05\%$

$A1 = 13.62\%$

$TS1 = 0.36$ $ATS1 = 0.29$

$TS2 = 0.09$ $ATS2 = -0.03$

$TS12 = 0.22$ $ATS12 = 0.01$

Figure 26.   Contingency table results for the area 2,
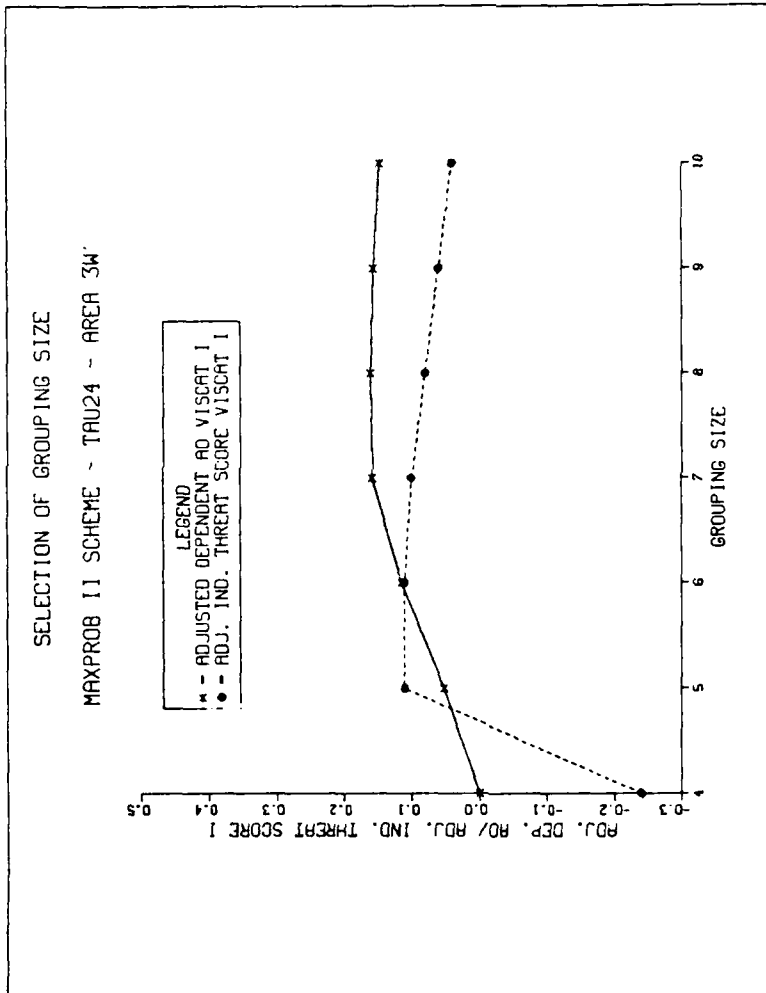TAU-48 quadratic threshold model

164

Figure 27. Relationship of equally populous grouping size to the adjusted AO (dependent data) and the adjusted VISCAT I threat score (independent data) for area 3W, TAU-24 (PR model, MAXPROB II strategy). For this case a grouping size of six was selected strategy).

NUMBER OF PREDICTORS VS. SCORING TECHNIQUES

TAU24 - AREA 3W - MAXPROB1 - GROUPING SIZE OF 6

PREDICTORS DTOP, SHWRS, ENTR, U1000, OUDP
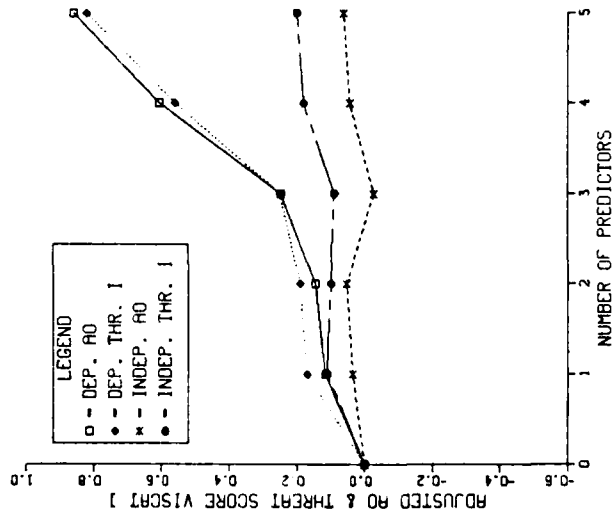
INDEPENDENT DATA

57	53	406	
13	22	37	
67	14	38	

FORECAST / OBSERVED

$AO = 70.01\%$ $AAO = 6.19\%$
$A1 = 16.55\%$
$TS1 = 0.35$ $ATS1 = 0.20$
$TS2 = 0.16$ $ATS2 = 0.04$
$TS12 = 0.30$ $ATS12 = -0.04$

DEPENDENT DATA

25	21	967	
11	151	3	
234	1	2	

FORECAST / OBSERVED

$AO = 95.55\%$ $AAO = 85.78\%$
$A1 = 2.54\%$
$TS1 = 0.86$ $ATS1 = 0.82$
$TS2 = 0.81$ $ATS2 = 0.78$
$TS12 = 0.86$ $ATS12 = 0.80$

LEGEND
□ - DEP. AO
♦ - DEP. THR. I
✕ - INDEP. AO
● - INDEP. THR. I

ADJUSTED AO & THREAT SCORE (VISCAT I)

NUMBER OF PREDICTORS

Figure 28a. Skill diagram and contingency table results for area 3W, TAU-24 (PR model) for the MAXPROB I strategy. The contingency table corresponds to those scores associated with the maximum independent VISCAT I threat score achieved at the fifth predictor level

166

NUMBER OF PREDICTORS VS. SCORING TECHNIQUES

TAU24 - AREA 3W - MAXPROBII - GROUPING SIZE OF 6
PREDICTORS DTOP, SHWRS, ENTR, U1000, DUDP
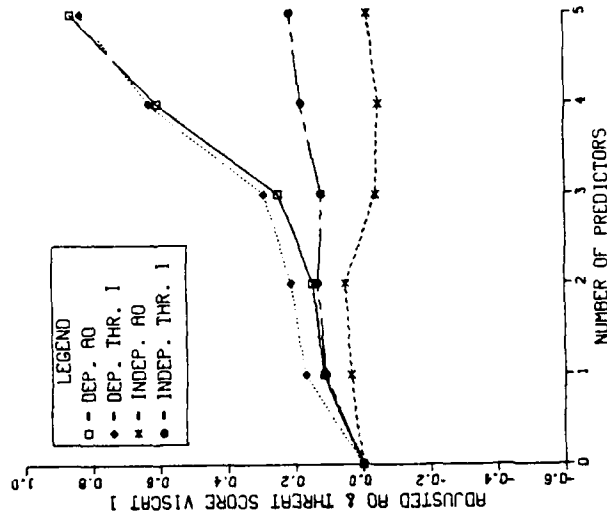
INDEPENDENT DATA

FORECAST			
3	48	47	378
2	12	22	46
1	77	20	57
	1	2	3

OBSERVED

AO=67.47% AAO=-1.77%

A1=17.68%

TS1=0.36 ATS1=0.21

TS2=0.15 ATS2=0.03

TS12=0.30 ATS12=-0.03

DEPENDENT DATA

FORECAST			
3	3	3	929
2	2	158	19
1	265	12	24
	1	2	3

OBSERVED

AO=95.55% AAO=85.78%

A1=1.23%

TS1=0.87 ATS1=0.83

TS2=0.81 ATS2=0.79

TS12=0.87 ATS12=0.81

LEGEND
□ - DEP. AO
◆ - DEP. THR. 1
✕ - INDEP. AO
● - INDEP. THR. 1

ADJUSTED AO & THREAT SCORE VISCAT 1

NUMBER OF PREDICTORS

Figure 28b. Skill diagram and contingency table results for area 3W, TAU-24 (PR model) for the MAXPROB II strategy. The contingency table corresponds to those scores associated with the maximum independent VISCAT I threat score achieved at the fifth predictor level

167

NUMBER OF PREDICTORS VS. SCORING TECHNIQUES

TAU24 - AREA 3W - NAT REGR - GROUPING SIZE OF 6
PREDICTORS OTDP, SHNRS, ENTR, U1000, DUDP
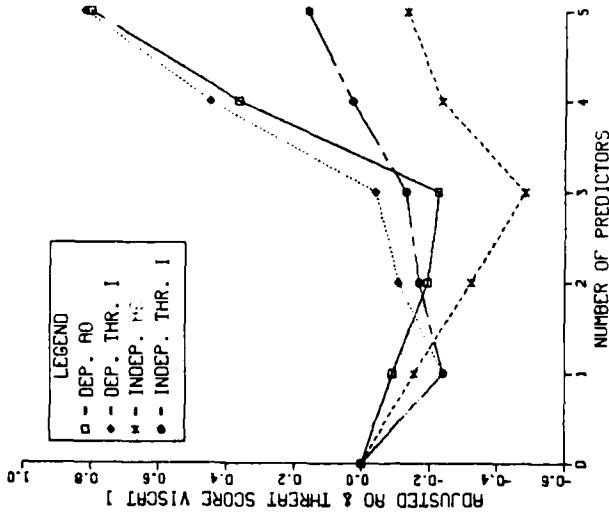
INDEPENDENT DATA

42	44	360
38	34	91
57	11	30

AO=63.79% AAO=-13.27%

A1=26.03%

TS1=0.32 ATS1=0.16

TS2=0.16 ATS2=0.03

TS12=0.26 ATS12=-0.08

DEPENDENT DATA

1	19	941
37	154	30
232	0	1

AO=93.78% AAO=80.14%

A1=6.08%

TS1=0.86 ATS1=0.82

TS2=0.64 ATS2=0.52

TS12=0.81 ATS12=0.73

Figure 28c. Skill diagram and contingency table results for area 3W, TAU-24 (PR model) for the natural regression strategy. The contingency table corresponds to those scores associated with the maximum independent VISCAT I threat score achieved at the fifth predictor level

168

Predictor	FD(96)	FD	A0	A0(96)	A1	A1(05)
DTDP	0.1350		72.3%	37.7%	12.2%	31.2%
SHWRS	0.1478	0.1236	73.2%	42.6%	12.2%	34.4%
ENTR	0.2002	0.1927	76.4%	53.1%	11.7%	29.7%
U1000	0.2871	0.2343	87.6%	68.0%	6.3%	20.6%
DUDP	0.2979	0.3011	95.5%	74.2%	2.5%	15.9%

Figure 29. Functional dependence, A0/A1 statistics and 96%/05% confidence interval values for area 3W, TAU-24 (PR model, MAXPROB II strategy)
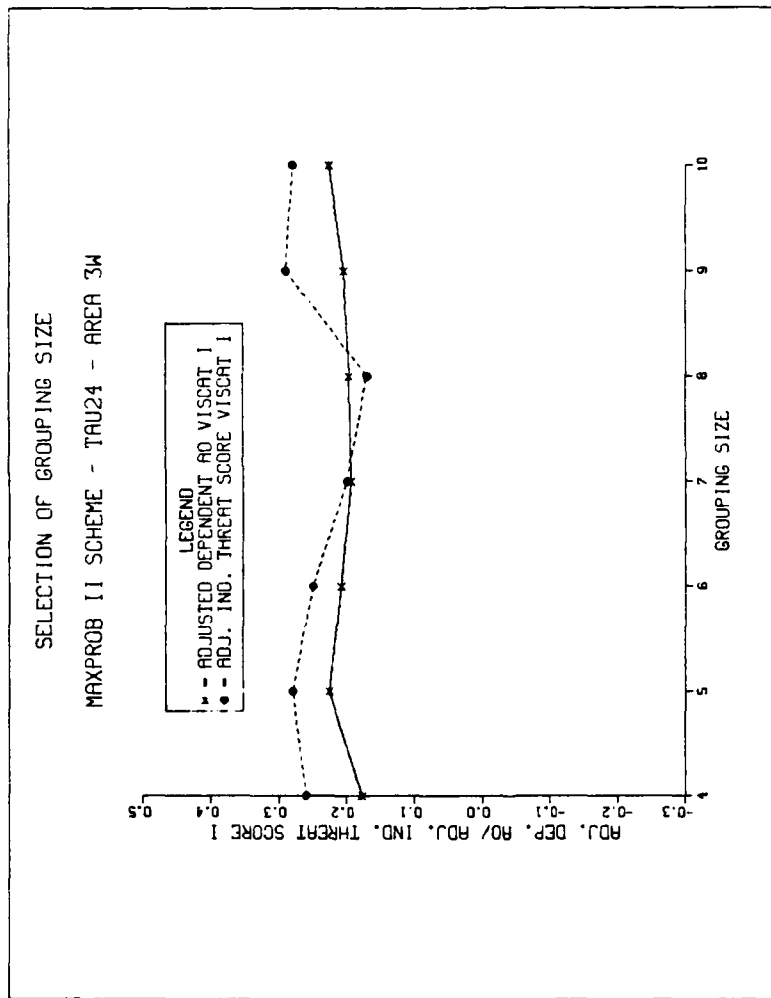
Figure 30. Relationship of equally populous grouping size to the adjusted AO (dependent data) and the adjusted VISCAT I threat score (independent data) for area 3W, TAU-24 (PR+BMD model, MAXPROB II strategy). For this case a grouping size of five was selected

NUMBER OF PREDICTORS VS. SCORING TECHNIQUES   INDEPENDENT DATA

TAU24 - AREA 3W - MAXPROBI - GROUPING SIZE OF 5

PREDICTORS BMD1, D500, DVDP, ENTR, U850

INDEPENDENT DATA
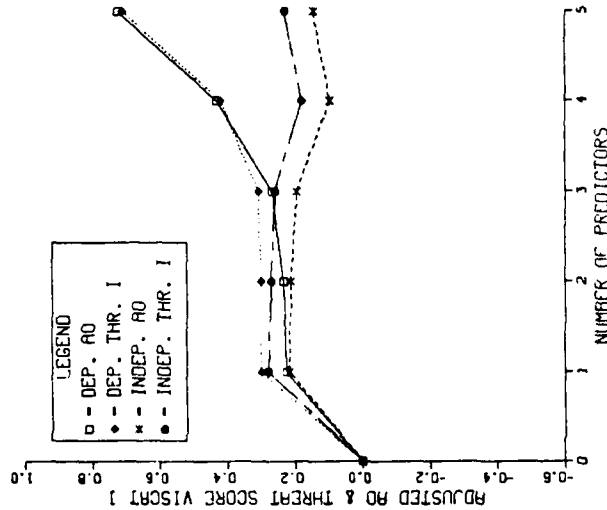
	1	2	3
3	56	66	449
2	0	0	0
1	81	23	32

FORECAST / OBSERVED

AO=74.96% AAO=21.68%

A1=12.59%

TS1=0.42   ATS1=0.28

TS2=0.0   ATS2=-0.14

TS12=0.31 ATS12=-0.01

DEPENDENT DATA

	1	2	3
3	102	125	904
2	0	0	0
1	168	48	68

FORECAST / OBSERVED

AO=75.76% AAO=22.57%

A1=12.23%

TS1=0.44   ATS1=0.30

TS2=0.0   ATS2=0.0

TS12=0.33 ATS12=0.02

LEGEND
□ - DEP. AO
♦ - DEP. THR. I
× - INDEP. AO
● - INDEP. THR. I

ADJUSTED AO & THREAT SCORE VISCAT I

NUMBER OF PREDICTORS

Figure 31a. Skill diagram and contingency table results for area 3W, TAU-24
(PR+BMD model) for the MAXPROB I strategy. The contingency
table corresponds to those scores associated with the maximum
independent VISCAT I threat score achieved at the first
predictor level

NUMBER OF PREDICTORS VS. SCORING TECHNIQUES INDEPENDENT DATA

TAU24 - AREA 3W - MAXPROB11 - GROUPING SIZE OF 5

PREDICTORS BMD1, O500, DVDP, ENTR, U850

AO=74.96% AAO=21.68%

A1=12.59%

TS1=0.42 ATS1=0.28

TS2=0.0 ATS2=-0.14

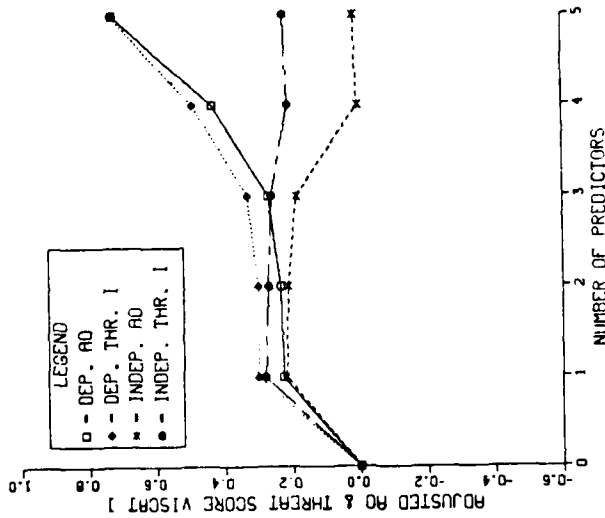TS12=0.31 ATS12=-0.01

AO=75.76% AAO=22.57%

A1=12.23%

TS1=0.44 ATS1=0.30

TS2=0.0 ATS2=-0.14

TS12=0.33 ATS12=0.02

DEPENDENT DATA

Figure 31b. Skill diagram and contingency table results for area 3W, TAU-24 (PR+BMD model) for the MAXPROB II strategy. The contingency table corresponds to those scores associated with the maximum independent VISCAT I threat score achieved at the first predictor level

172

NUMBER OF PREDICTORS VS. SCORING TECHNIQUES   INDEPENDENT DATA

TAU24 - AREA 3W - NAT REGR - GROUPING SIZE OF 5
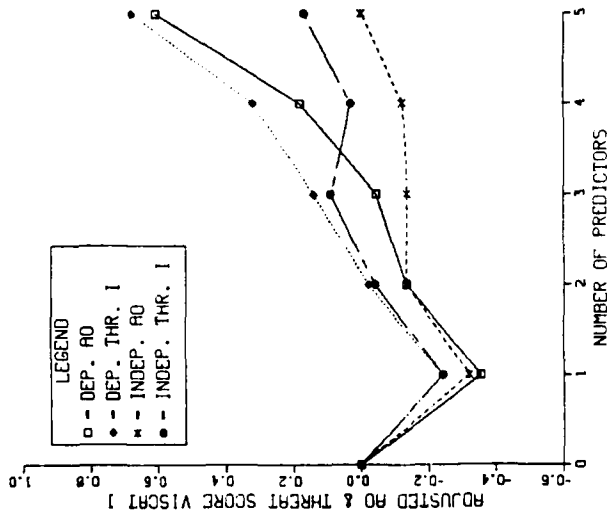
PREDICTORS BMD1, D500, DVDF, ENTR, U850

	1	2	3	
3	43	43	389	$AO=68.03\%$ $AAO=0.0\%$
2	34	32	62	$A1=21.64\%$
1	60	14	30	$TS1=0.33$ $ATS1=0.17$

FORECAST (vertical) OBSERVED

$TS1=0.33$ $ATS1=0.17$
$TS2=0.17$ $ATS2=0.05$
$TS12=0.29$ $ATS12=-0.04$

DEPENDENT DATA

	1	2	3	
3	2	40	908	$AO=87.77\%$ $AAO=60.95\%$
2	63	129	61	$A1=11.87\%$
1	205	4	3	$TS1=0.74$ $ATS1=0.68$

FORECAST (vertical) OBSERVED

$TS1=0.74$ $ATS1=0.68$
$TS2=0.43$ $ATS2=0.36$
$TS12=0.66$ $ATS12=0.50$

LEGEND
□ - DEP. AO
● - DEP. THR. I
× - INDEP. AO
● - INDEP. THR. I

ADJUSTED AO & THREAT SCORE VISCAT I

NUMBER OF PREDICTORS

Figure 31c. Skill diagram and contingency table results for area 3W, TAU-24 (PR+BMD model) for the natural regression strategy. The contingency table corresponds to those scores associated with the maximum independent VISCAT I threat score achieved at the fifth predictor level

173

Predictor	FD(96)	FD	A0	A0(96)	A1	A1(O5)
BMD1	0.1548		75.8%	37.2%	12.2%	31.1%
D500	0.2189	0.1832	76.0%	41.1%	12.2%	33.8%
DVDP	0.2681	0.2002	77.1%	48.6%	12.0%	31.9%
ENTR	0.3096	0.2624	82.2%	61.2%	10.0%	24.7%
U850	0.3461	0.3408	91.2%	70.4%	5.3%	18.4%

Figure 32. Functional dependence, A0/A1 statistics and 96%/05% confidence interval values for area 3W, TAU-24 (PR+BMD model, MAXPROB II strategy)

174

DEPENDENT DATA

FORECAST	3	105	120	878
	2	42	32	60
	1	123	21	34
		1	2	3

OBSERVED

AO = 73.00% AAO = 13.77%

A1 = 17.17%

TS1 = 0.38   ATS1 = 0.23

TS2 = 0.12   ATS2 = -0.01

TS12 = 0.29   ATS12 = -0.04

INDEPENDENT DATA

FORECAST	3	58	62	431
	2	25	17	35
	1	54	10	15
		1	2	3

OBSERVED

AO = 71.00% AAO = 9.29%

A1 = 18.67%

TS1 = 0.33   ATS1 = 0.17

TS2 = 0.11   ATS2 = -0.01

TS12 = 0.26   ATS12 = -0.09

Figure 33.   Contingency table results for the area 3W,
TAU-24 equal variance threshold model

175

DEPENDENT DATA

AO=73.22% AAO=14.45%

A1=17.60%

TS1= 0.37 ATS1=0.22

TS2= 0.11 ATS2= -0.01

TS12= 0.28 ATS12= -0.04

INDEPENDENT DATA

AO-71.43% AAO=10.62%

A1=18.95%

TS1= 0.32 ATS1= 0.16

TS2= 0.11 ATS2= -0.02

TS12= 0.25 ATS12= -0.10

Figure 34. Contingency table results for the area 3W, TAU-24 quadratic threshold model
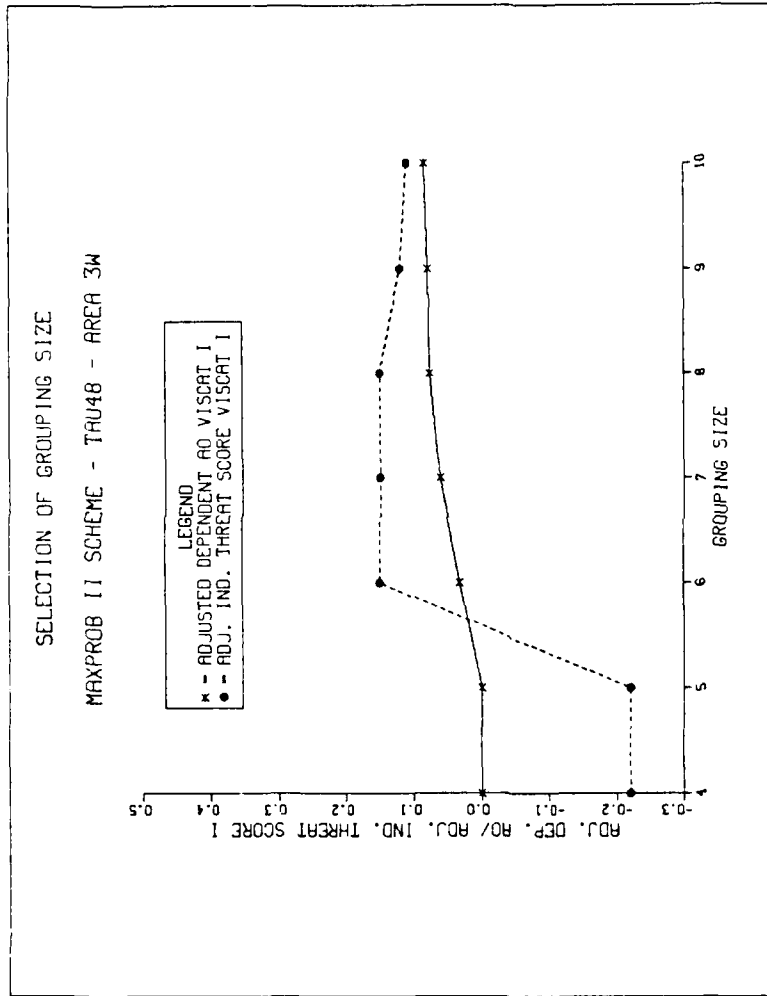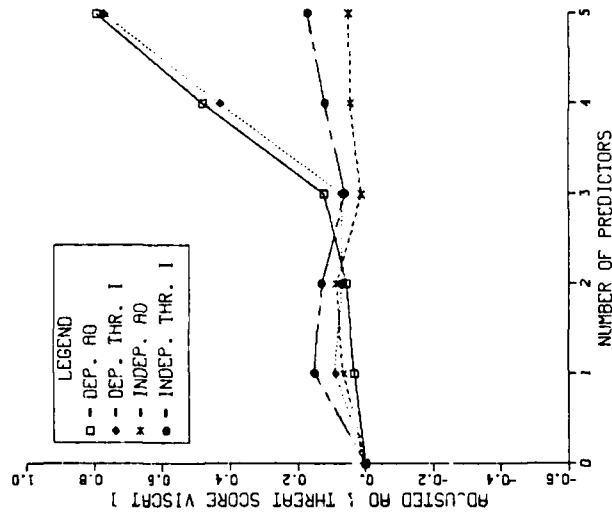
176

Figure 35. Relationship of equally populous grouping size to the adjusted A0 (dependent data) and the adjusted VISCATI threat score (independent data) for area 3W, TAU-48 (PR model, MAXPROB II strategy). For this case a grouping size of six was selected strategy).

NUMBER OF PREDICTORS VS. SCORING TECHNIQUES

TAU48 - AREA 3W - MAXPROB1 - GROUPING SIZE OF 6

PREDICTORS DTOP, SHWRS, ENTR, U850, DIV925

INDEPENDENT DATA

AO=68.91% AAO=4.94%

A1= 17.77%

TS1= 0.32   ATS1= 0.17

TS2= 0.11   ATS2=-0.05

TS12=0.24   ATS12=-0.13

67	75	438
7	16	30
58	20	32

FORECAST 3 2 1   OBSERVED 1 2 3

DEPENDENT DATA

AO=93.34% AAO=79.20%

A1= 3.83%

TS1= 0.82   ATS1= 0.77

TS2= 0.71   ATS2= 0.67

TS12=0.80   ATS12= 0.70

37	42	1004
10	141	2
243	3	5

FORECAST 3 2 1   OBSERVED 1 2 3

LEGEND
□ - DEP. AO
♦ - DEP. THR. I
× - INDEP. AO
● - INDEP. THR. I

NUMBER OF PREDICTORS

ADJUSTED AO ; THREAT SCORE VISCAT I

Figure 36a.   Skill diagram and contingency table results for area 3W, TAU-48
(PR model) for the MAXPROB I strategy. The contingency table
corresponds to those scores associated with the maximum
independent VISCAT I threat score achieved at the fifth
predictor level

178

NUMBER OF PREDICTORS VS. SCORING TECHNIQUES

TAU48 - AREA 3W - MAXPROB11 - GROUPING SIZE OF 6
PREDICTORS DTDP, SHWRS, ENTR, U850, D1V925
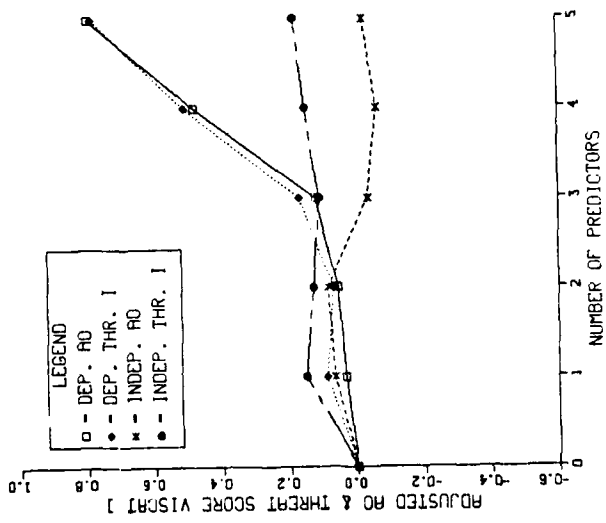
INDEPENDENT DATA

	52	55	397
	8	25	46
	72	31	57

FORECAST / OBSERVED

AO=66.49% AAO=-2.47%

A1=18.84%

TS1=0.33 ATS1=0.18

TS2=0.15 ATS2=0.0

TS12=0.28 ATS12=-0.07

DEPENDENT DATA

	3	5	940
	1	162	32
	286	19	39

FORECAST / OBSERVED

AO=93.34% AAO=79.20%

A1=3.83%

TS1=0.82 ATS1=0.78

TS2=0.74 ATS2=0.70

TS12=0.82 ATS12=0.74

Figure 36b. Skill diagram and contingency table results for area 3W, TAU-48 (PR model) for the MAXPROB II strategy. The contingency table corresponds to those scores associated with the maximum independent VISCAT I threat score achieved at the fifth predictor level

179

NUMBER OF PREDICTORS VS. SCORING TECHNIQUES

TAU48 - AREA 3W - NAT REGR - GROUPING SIZE OF 6

PREDICTORS DTOP, SHWRS, ENTR, U850, DIV925
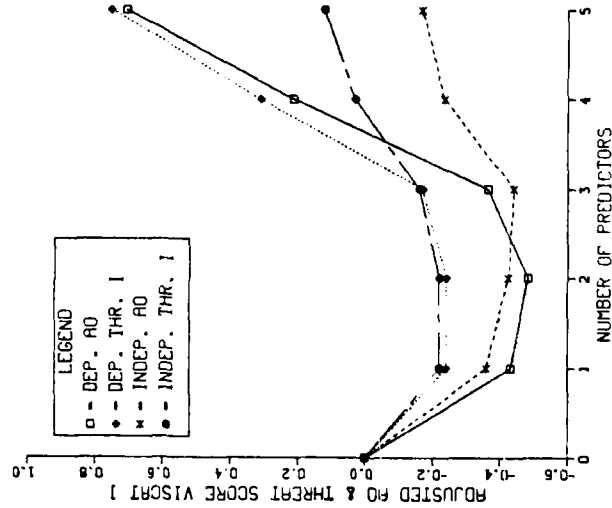
INDEPENDENT DATA

AO=61.78% AAO=-16.87%

A1=28.13%

TS1=0.27 ATS1=0.12

TS2=0.14 ATS2=-0.02

TS12=0.22 ATS12=-0.15

DEPENDENT DATA

AO=90.59% AAO=70.59%

A1=9.35%

TS1=0.80 ATS1=0.75

TS2=0.52 ATS2=0.45

TS12=0.73 ATS12=0.60

Figure 36c. Skill diagram and contingency table results for area 3W, TAU-48 (PR model) for the natural regression strategy. The contingency table corresponds to those scores associated with the maximum independent VISCAT I threat score achieved at the fifth predictor level

180

Predictor	FD(96)	FD	A0	A0(96)	A1	A1(05)
DTDP	0.1321		69.0%	38.1%	12.5%	31.5%
SHWRS	0.1951	0.1187	69.8%	42.4%	12.5%	35.2%
ENTR	0.2356	0.1928	71.9%	52.9%	12.6%	29.3%
U850	0.2701	0.2606	83.4%	66.8%	8.8%	20.9%
DIV925	0.3007	0.3047	93.3%	74.1%	3.8%	16.5%

Figure 37. Functional dependence, A0/A1 statistics and 96%/05% confidence interval values for area 3W, TAU-48 (PR model, MAXPROB II strategy)
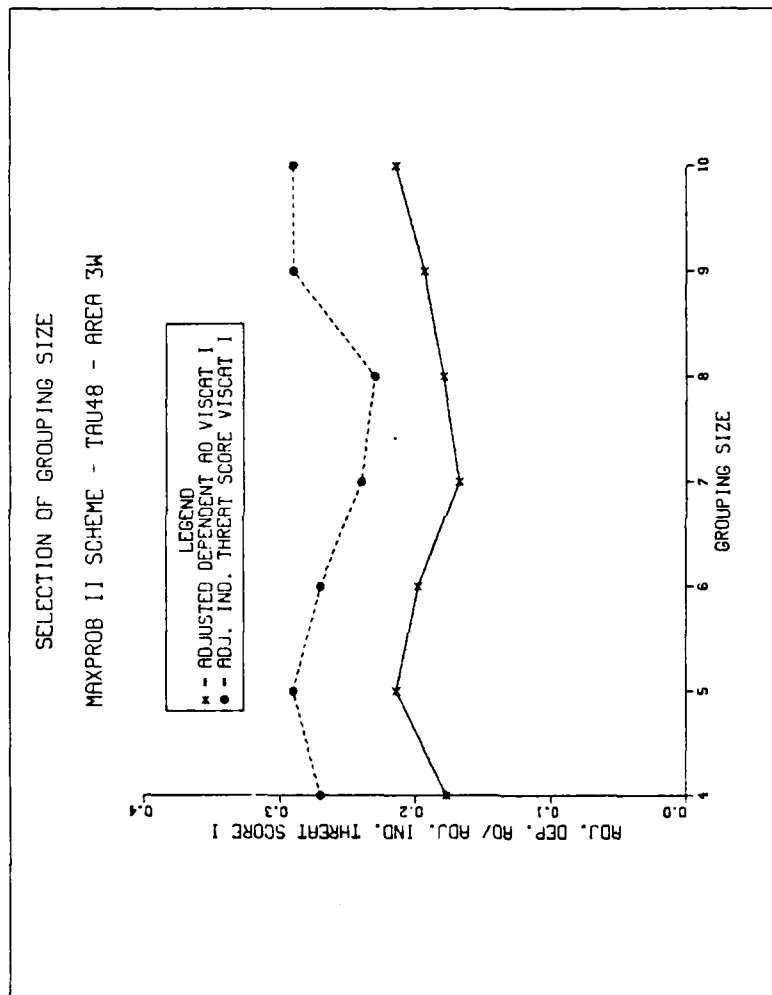
181

Figure 38. Relationship of equally populous grouping size to the adjusted A0 (dependent data) and the adjusted VISCAT I threat score (independent data) for area 3W, TAU-48 (PR+BMD model, MAXPROB II strategy). For this case a grouping size of five was selected

Figure 39a. Skill diagram and contingency table results for area 3W, TAU-48 (PR+BMD model) for the MAXPROB I strategy. The contingency table corresponds to those scores associated with the *maximum* independent VISCAT I threat score achieved at the first predictor level

NUMBER OF PREDICTORS VS. SCORING TECHNIQUES

TAU48 - AREA 3W - MAXPROBII - GROUPING SIZE OF 5

PREDICTORS BMD2, U1000, ENTR, DVOP, EAIR

LEGEND
□ - DEP. AO
◆ - DEP. THR. I
✕ - INDEP. AO
● - INDEP. THR. I

ADJUSTED AO & THREAT SCORE VISCAT I

NUMBER OF PREDICTORS
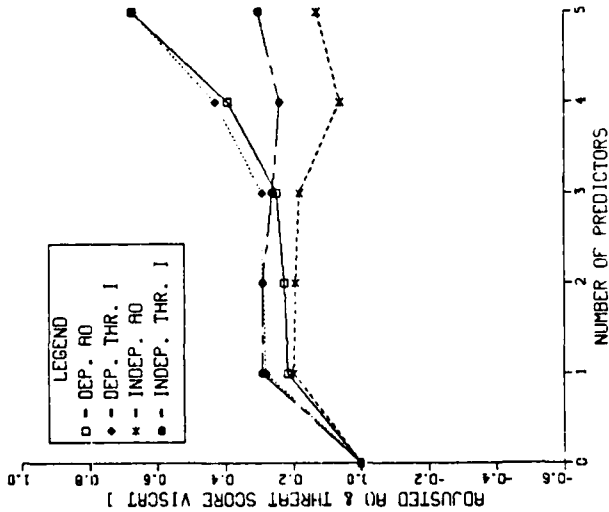
INDEPENDENT DATA

	1	2	3
3	27	63	423
2	13	16	25
1	92	32	52

FORECAST / OBSERVED

AO=71.47% AAO=12.76%

A1=17.90%

TS1=0.43 ATS1=0.30

TS2=0.11 ATS2=-0.05

TS12=0.34 ATS12=0.02

DEPENDENT DATA

	1	2	3
3	12	27	924
2	2	131	31
1	276	28	56

FORECAST / OBSERVED

AO=89.51% AAO=67.23%

A1=5.92%

TS1=0.74 ATS1=0.67

TS2=0.60 ATS2=0.54

TS12=0.72 ATS12=0.59

Figure 39b. Skill diagram and contingency table results for area 3W, TAU-48 (PR+BMD model) for the MAXPROB II strategy. The contingency table corresponds to those scores associated with the maximum independent VISCAT I threat score achieved at the fifth predictor level

Figure 39c. Skill diagram and contingency table results for area 3W, TAU-48 (PR+BMD model) for the natural regression strategy. The contingency table corresponds to those scores associated with the maximum independent VISCAT I threat score achieved at the fifth predictor level

185

Predictor	FD(96)	FD	A0	A0(96)	A1	A1(05)
BMD2	0.1541		74.8%	37.5%	12.5%	31.3%
U1000	0.2179	0.1917	75.2%	40.7%	12.6%	35.0%
ENTR	0.2670	0.2151	75.9%	48.4%	12.1%	32.3%
DVDP	0.3082	0.2778	80.5%	61.3%	10.8%	24.5%
EAIR	0.3446	0.3395	89.5%	70.3%	5.9%	18.5%

Figure 40. Functional dependence, A0/A1 statistics and 96%/05% confidence interval values for area 3W, TAU-48 (PR+BMD model, MAXPROB II strategy)

186

DEPENDENT DATA

	1	2	3	
3	125	125	920	
2	50	28	51	
1	115	33	40	
	1	2	3	

FORECAST (vertical axis) / OBSERVED (horizontal axis)

AO =71.49% AAO =10.92%

A1=17.42%

TS1= 0.32   ATS1= 0.15

TS2= 0.10   ATS2= -0.03

TS12=0.25   ATS12= -0.10

INDEPENDENT DATA

	1	2	3	
3	57	73	461	
2	21	17	20	
1	54	21	19	
	1	2	3	

FORECAST (vertical axis) / OBSERVED (horizontal axis)

AO=71.60% AAO=13.17%

A1=18.17%

TS1= 0.31   ATS1=0.17

TS2=0.11   ATS2= -0.04

TS12= 0.25   ATS12= -0.11

Figure 41. Contingency table results for the area 3W,
TAU-48 equal variance threshold model

187

DEPENDENT DATA

AO = 71.22% AAO = 10.08%

A1 = 17.82%

TS1 = 0.31   ATS1 = 0.14

TS2 = 0.10   ATS2 = -0.03

TS12 = 0.25   ATS12 = -0.11

INDEPENDENT DATA

AO - 71.47% AAO = 12.76%

A1 - 18.71%

TS1 - 0.32   ATS1 = 0.17

TS2 = 0.11   ATS2 - -0.04

TS12 - 0.25   ATS12 - -0.11

Figure 42.   Contingency table results for the area 3N,
             TAU-48 quadratic threshold model

188
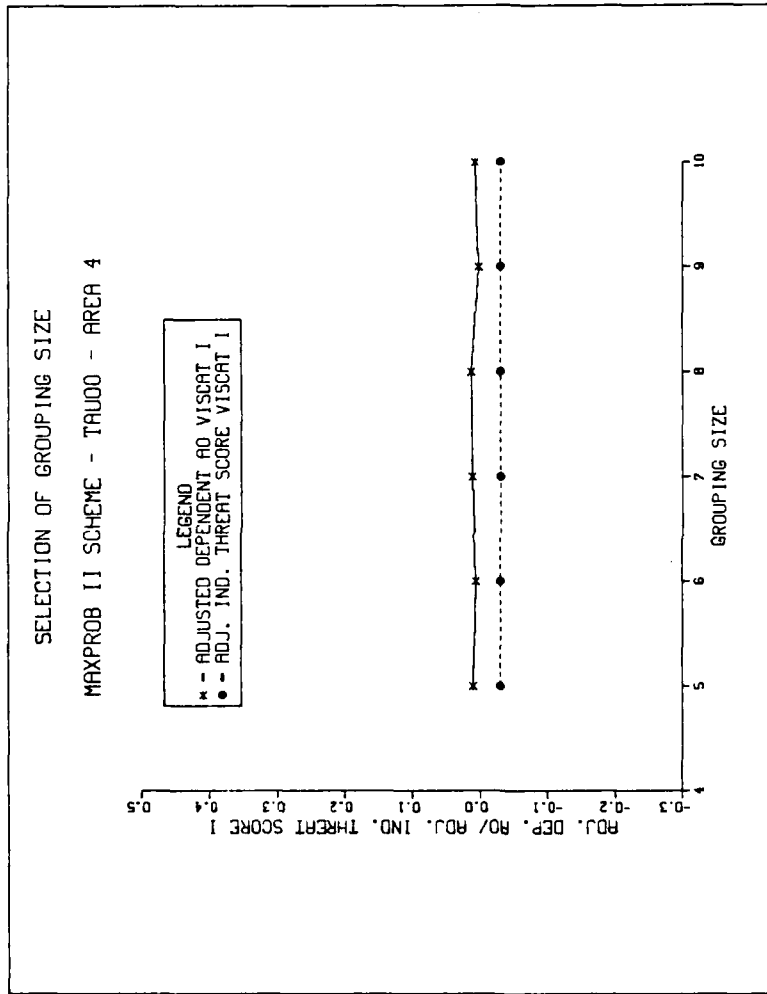
Figure 43. Relationship of equally populous grouping size to the adjusted AO (dependent data) and the adjusted VISCAT I threat score (independent data) for area 4, TAU-OO (PR model, MAXPROB II strategy). For this case a grouping size of eight was selected strategy).

189

NUMBER OF PREDICTORS VS. SCORING TECHNIQUES   INDEPENDENT DATA

TAU00 - AREA 4 - MAXPROB1 - GROUPING SIZE OF 8
PREDICTORS V500, DVDP, SIRTH, E500, ENTR
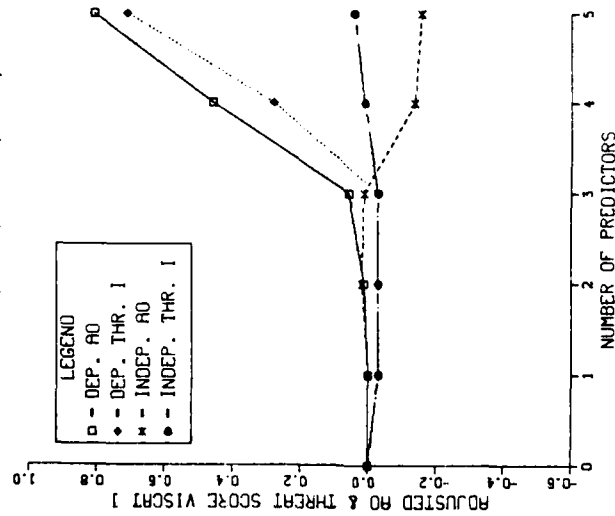
INDEPENDENT DATA

	1	2	3
3	29	149	1264
2	11	43	77
1	4	5	8

FORECAST / OBSERVED

$AO=82.45\%$ $AAO=-15.77\%$
$A1= 15.22\%$
$TS1= 0.07$ $ATS1= 0.04$
$TS2= 0.15$ $ATS2= 0.03$
$TS12= 0.14$ $ATS12= -0.01$

DEPENDENT DATA

	1	2	3
3	14	63	2689
2	9	337	6
1	62	0	1

FORECAST / OBSERVED

$AO=97.08\%$ $AAO=80.82\%$
$A1= 2.45\%$
$TS1=0.72$ $ATS1= 0.71$
$TS2=0.81$ $ATS2=0.79$
$TS12=0.81$ $ATS12=0.78$

LEGEND
□ - DEP. AO
♦ - DEP. THR. I
× - INDEP. AO
● - INDEP. THR. I

ADJUSTED AO & THREAT SCORE VISCAT I

NUMBER OF PREDICTORS

Figure 44a. Skill diagram and contingency table results for area 4, TAU-00
(PR model) for the MAXPROB I strategy. The contingency
table corresponds to those scores associated with the
maximum independent VISCAT I threat score achieved at the
fifth predictor level

190

Figure 44b. Skill diagram and contingency table results for are 4, TAU-00 (PR model) for the MAXPROB II strategy. The contingency table corresponds to those scores associated with the maximum independent VISCAT I threat score achieved at the fifth predictor level

END

FILMED

DTIC

MICROCOPY RESOLUTION TEST CHART
NATIONAL BUREAU OF STANDARDS 1963 A

NUMBER OF PREDICTORS VS. SCORING TECHNIQUES

TAU00 - AREA 4 - NAT REGR - GROUPING SIZE OF 8

PREDICTORS V500, DVDP, STRTH, E500, ENTR

INDEPENDENT DATA

AO=80.50% AAO=-28.63%

A1=17.30%

TS1=0.07 ATS1= 0.04
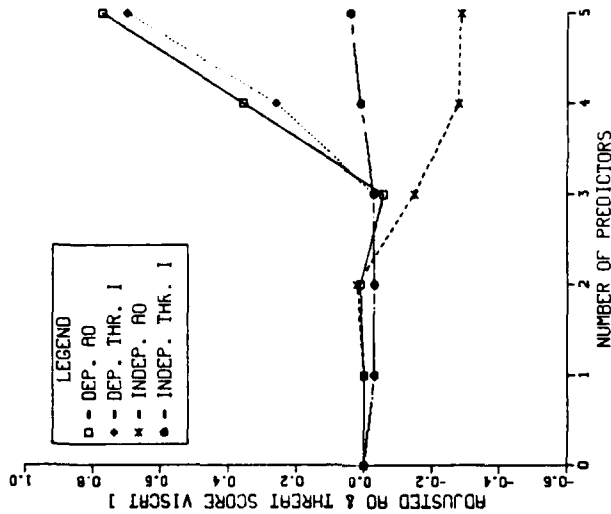
TS2=0.17 ATS2=0.05

TS12=0.16 ATS12=0.02

3	27	135	1219
2	13	57	122
1	4	5	8
	1	2	3

FORECAST — OBSERVED

DEPENDENT DATA

AO=96.54% AAO=77.32%

A1=3.46%

TS1= 0.71 ATS1=0.70

TS2=0.75 ATS2=0.72

TS12=0.78 ATS12=0.74

3	0	63	2674
2	25	337	22
1	60	0	0
	1	2	3

FORECAST — OBSERVED

LEGEND
□ - DEP. AO
◆ - DEP. THR. I
✕ - INDEP. AO
● - INDEP. THR. I

ADJUSTED AO & THREAT SCORE VISCAT I

NUMBER OF PREDICTORS

Figure 44c. Skill diagram and contingency table results for area 4, TAU-00 (PR model) for the natural regression strategy. The contingency table corresponds to those scores associated with the maximum independent VISCAT I threat score achieved at the fifth predictor level

192

Predictor	FD(96)	FD	A0	A0(96)	A1	A1(05)
V500	0.0976		84.8%	36.8%	12.6%	34.5%
DVDP	0.1380	0.2819	84.0%	40.6%	12.4%	34.8%
STRTTH	0.1690	0.1374	85.6%	50.9%	11.9%	31.6%
E500	0.1954	0.1839	91.8%	67.0%	6.9%	21.1%
ENTR	0.2183	0.2125	97.1%		2.5%	

Figure 45. Functional dependence, A0/A1 statistics and 96%/05% confidence interval values for area 4, TAU-00 (PR model, MAXPROB II srategy)
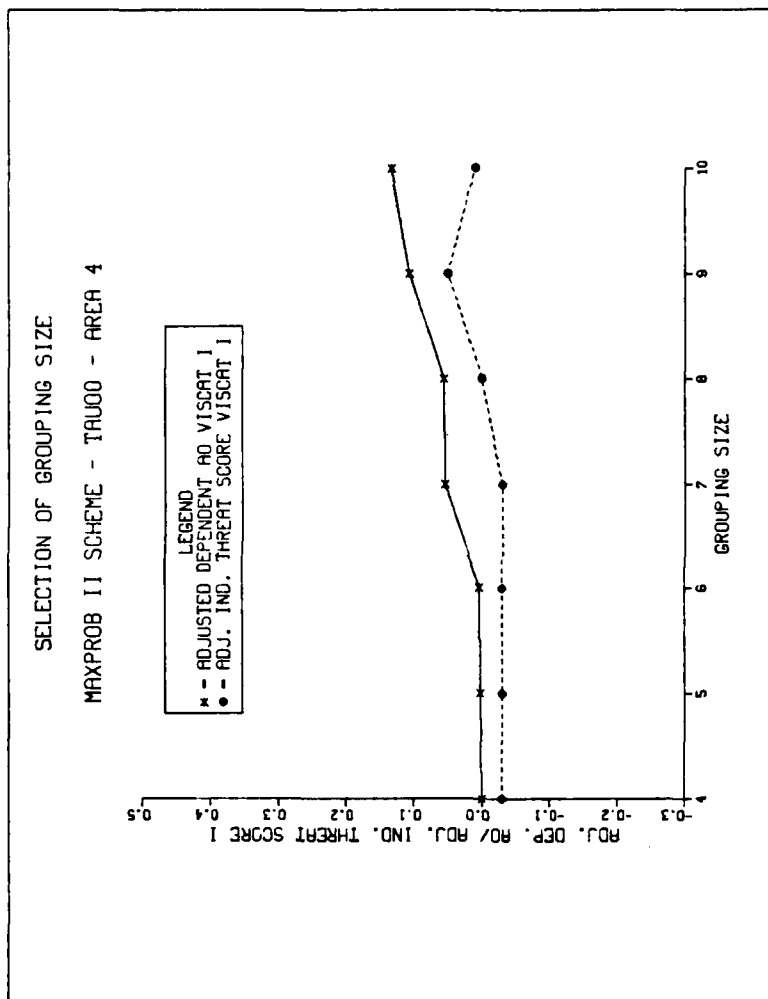
Figure 46. Relationship of equally populous grouping size to the adjusted A0 (dependent data) and the adjusted VISCAT I threat score (independent data) for area 4, TAU-00 (PR+BMD model, MAXPROB II strategy). For this case a grouping size of nine was selected

NUMBER OF PREDICTORS VS. SCORING TECHNIQUES

TAU00 - AREA 4 - MAXPROB1 - GROUPING SIZE OF 9

PREDICTORS BMD2, DUDP, ENTR, DEOP, U1000

INDEPENDENT DATA

AO=81.95% AAO=-19.09%

A1=15.16%

TS1=0.10 ATS1=0.07

TS2=0.17 ATS2=0.05

TS12=0.16 ATS12=0.01
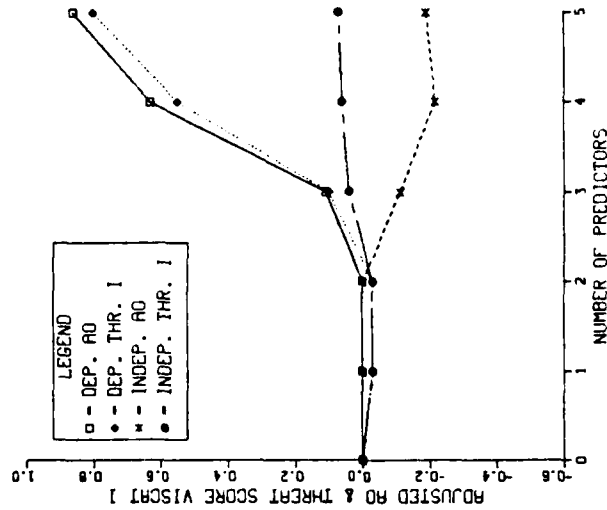
INDEPENDENT DATA

FORECAST	3	27	141	1247
	2	10	49	83
	1	7	7	19
		1	2	3
		OBSERVED		

AO=97.86% AAO=85.98%

A1=1.85%

TS1=0.80 ATS1=0.80

TS2=0.86 ATS2=0.84

TS12=0.86 ATS12=0.84

DEPENDENT DATA

FORECAST	3	8	47	2691
	2	9	353	4
	1	69	0	1
		1	2	3
		OBSERVED		

LEGEND
□ - DEP. AO
◆ - DEP. THR. I
⋈ - INDEP. AO
● - INDEP. THR. I

NUMBER OF PREDICTORS

ADJUSTED AO & THREAT SCORE VISCAT I

Figure 47a. Skill diagram and contingency table results for area 4, TAU-00 (PR+BMD model) for the MAXPROB I strategy. The contingency table corresponds to those scores associated with the maximum independent VISCAT I threat score achieved at the fifth predictor level

195

NUMBER OF PREDICTORS VS. SCORING TECHNIQUES

TAU00 - AREA 4 - MAXPROBII - GROUPING SIZE OF 9

PREDICTORS BMD2, DUDP, ENTR, DEDP, U1000
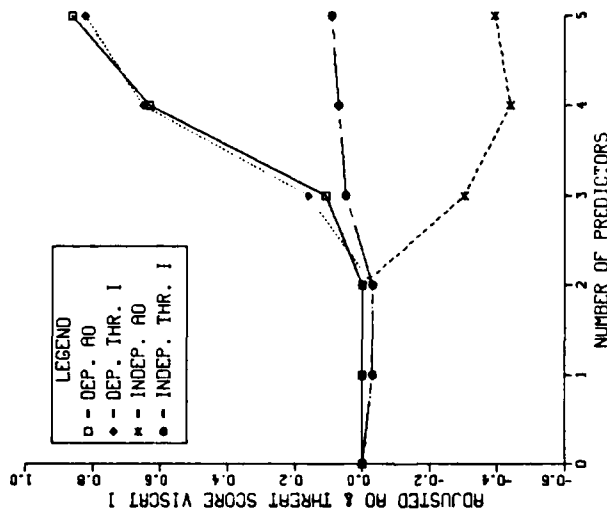
INDEPENDENT DATA

	1	2	3	
3	25	133	1191	
2	9	53	126	
1	10	11	32	

FORECAST / OBSERVED

AO=78.87% AAO=-39.42%

A1=17.55%

TS1=0.11 ATS1=0.09

TS2=0.16 ATS2=0.04

TS12=0.16 ATS12=0.01

DEPENDENT DATA

	1	2	3	
3	0	10	2647	
2	3	384	40	
1	82	6	9	

FORECAST / OBSERVED

AO=97.86% AAO=85.98%

A1=1.85%

TS1=0.82 ATS1=0.82

TS2=0.87 ATS2=0.85

TS12=0.87 ATS12=0.85

Figure 47b. Skill diagram and contingency table results for area 4, TAU-00 (PR+BMD model) for the MAXPROB II strategy. The contingency table corresponds to those scores associated with the maximum independent VISCAT I threat score achieved at the fifth predictor level

196

NUMBER OF PREDICTORS VS. SCORING TECHNIQUES INDEPENDENT DATA

TAU00 - AREA 4 - NAT REGR - GROUPING SIZE OF 9

PREDICTORS BMD2, DUDP, ENTR, DEDP, U1000

	24	135	1223
	13	55	109
	7	7	17

FORECAST (3, 2, 1) — OBSERVED (1, 2, 3)
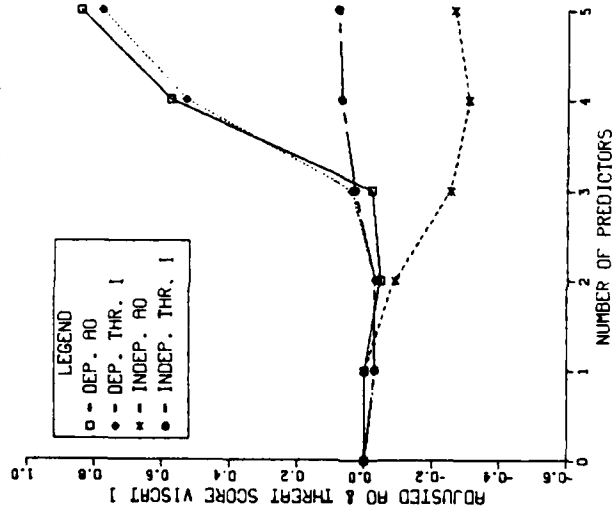
AO=80.82% AAO=-26.56%

A1=16.60%

TS1=0.10 ATS1=0.08

TS2=0.17 ATS2=0.06

TS12=0.17 ATS12=0.02

DEPENDENT DATA

	0	46	2683
	18	354	13
	67	0	0

FORECAST (3, 2, 1) — OBSERVED (1, 2, 3)

AO=97.58% AAO=84.12%

A1= 2.42 %

TS1=0.79 ATS1=0.78

TS2=0.82 ATS2=0.80

TS12=0.90 ATS12=0.88

LEGEND
□ - DEP. AO
● - DEP. THR. I
× - INDEP. AO
● - INDEP. THR. I

NUMBER OF PREDICTORS

ADJUSTED AO & THREAT SCORE VISCAT I

Figure 47c. Skill diagram and contingency table results for area 4, TAU-00
(PR+BMD model) for the natural regression strategy. The contingency
table corresponds to those scores associated with the maximum
independent VISCAT I threat score achieved at the fifth
predictor level

197

Predictor	FD(96)	FD	A0	A0(96)	A1	A1(05)
BMD2	0.0904		84.8%	37.1%	12.6%	35.3%
DUDP	0.1324	0.0908	84.9%	42.1%	12.6%	36.2%
ENTR	0.1628	0.1295	86.4%	56.6%	11.5%	27.5%
DEDP	0.1890	0.1685	94.4%	72.4%	4.8%	17.5%
U1000	0.2120	0.1945	97.6%		2.1%	

Figure 48. Functional dependence, A0/A1 statistics and 96%/05% confidence interval values for area 4, TAU-00 (PR+BMD model, MAXPROB II strategy)
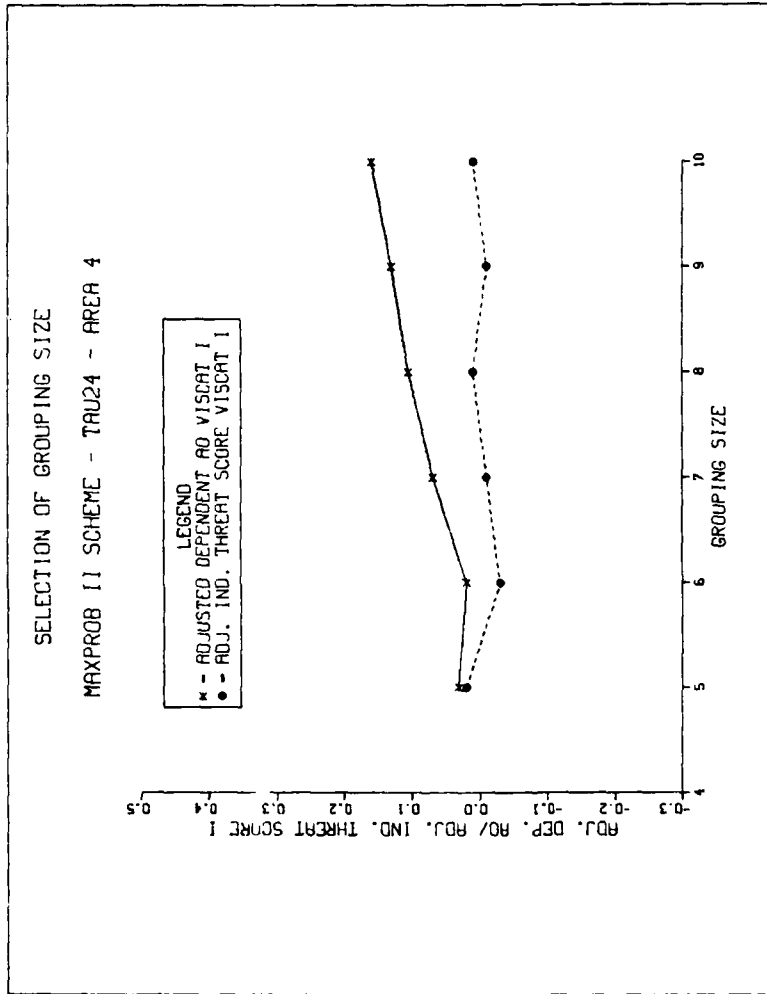
Figure 49. Relationship of equally populous grouping size to the adjusted AO (dependent data) and the adjusted VISCAT I threat score (independent data) for area 4, TAU-24 (PR model, MAXPROB II strategy). For this case a grouping size of five was selected strategy).

NUMBER OF PREDICTORS VS. SCORING TECHNIQUES

TAU24 - AREA 4 - MAXPROB1 - GROUPING SIZE OF 5

PREDICTORS VRT925, DTDP, ENTR, V850, DVRTDP
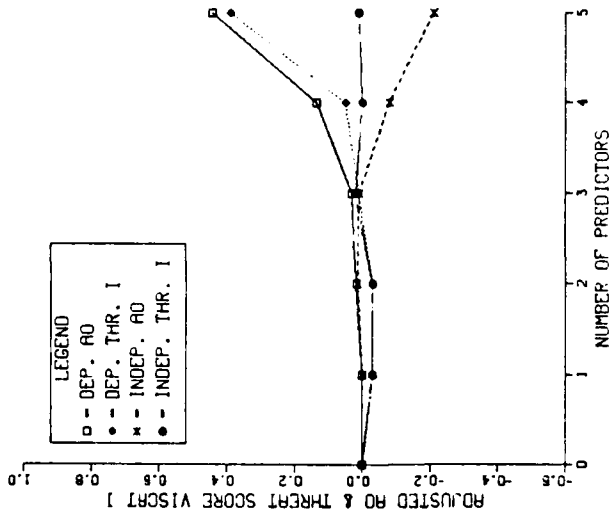
INDEPENDENT DATA

FORECAST	3	34	158	1243
	2	2	13	13
	1	2	4	0
		1	2	3
			OBSERVED	

AO=85.64% AAO=0.94%

A1=12.05%

TS1=0.05 ATS1=0.02

TS2=0.07 ATS2=-0.06

TS12=0.06 ATS12=-0.09

DEPENDENT DATA

FORECAST	3	70	328	2462
	2	8	38	25
	1	3	2	2
		1	2	3
			OBSERVED	

AO=85.19% AAO=3.12%

A1=12.36%

TS1=0.04 ATS1=0.01

TS2=0.09 ATS2=-0.03

TS12=0.09 ATS12=-0.08

LEGEND
□ — DEP. AO
● — DEP. THR. I
× — INDEP. AO
● — INDEP. THR. I

ADJUSTED AO & THREAT SCORE VISCAT I

NUMBER OF PREDICTORS

Figure 50a. Skill diagram and contingency table results for area 4, TAU-24 (PR model) for the MAXPROB I strategy. The contingency table corresponds to those scores associated with the maximum independent VISCAT I threat score achieved at the third predictor level

NUMBER OF PREDICTORS VS. SCORING TECHNIQUES

TAU24 - AREA 4 - MAXPROBII - GROUPING SIZE OF 5
PREDICTORS VRT925, DTDP, ENTR, V850, DVRTDP
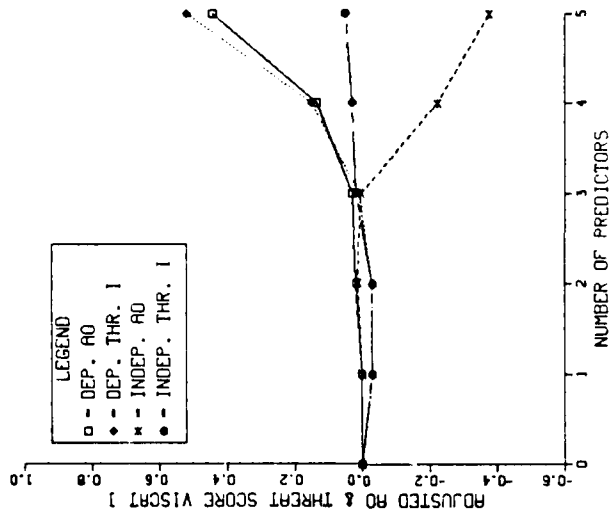
INDEPENDENT DATA

FORECAST	OBSERVED		
3	29	112	1121
2	4	50	117
1	5	13	18
	1	2	3

AO=80.05% AAO=-37.56%
A1=16.75%
TS1=0.07 ATS1=0.05
TS2=0.17 ATS2=0.06
TS12=0.16 ATS12=0.02

DEPENDENT DATA

FORECAST	OBSERVED		
3	15	97	2370
2	7	259	101
1	59	12	18
	1	2	3

AO=91.49% AAO=44.32%
A1=7.38%
TS1=0.53 ATS1=0.52
TS2=0.54 ATS2=0.48
TS12=0.56 ATS12=0.48

LEGEND
□ - DEP. AO
♦ - DEP. THR. I
× - INDEP. AO
● - INDEP. THR. I

ADJUSTED AO & THREAT SCORE VISCAT I

NUMBER OF PREDICTORS

Figure 50b. Skill diagram and contingency table results for area 4, TAU-24 (PR model) for the MAXPROB II strategy. The contingency table corresponds to those scores associated with the maximum independent VISCAT I threat score achieved at the fifth predictor level

NUMBER OF PREDICTORS VS. SCORING TECHNIQUES

Figure 50c. Skill diagram and contingency table results for area 4, TAU-24 (PR model) for the natural regression strategy. The contingency table corresponds to those scores associated with the maximum independent VISCAT I threat score achieved at the fifth predictor level

Predictor	FD(96)	FD	A0	A0(96)	A1	A1(05)
VRT925	0.1424		84.7%	36.3%	12.5%	31.7%
DTDP	0.2162	0.3007	85.0%	38.5%	12.5%	35.8%
ENTR	0.2465	0.2223	85.2%	43.9%	12.4%	35.5%
V850	0.2847	0.2778	86.8%	53.8%	11.2%	29.5%
DVRTDP	0.3507	0.3493	91.5%	7.4%	65.6%	21.9%

Figure 51. Functional dependence, A0/A1 statistics and 96%/05% confidence interval values for area 4, TAU-24 (PR model, MAXPROB II strategy)
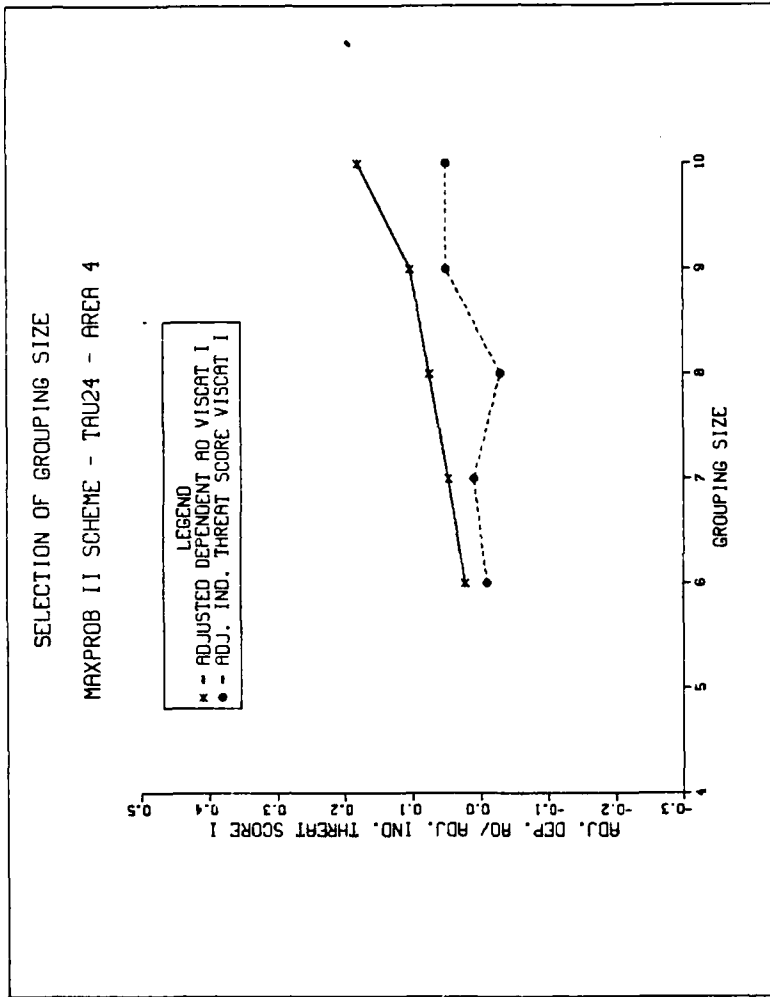
Figure 52. Relationship of equally populous grouping size to the adjusted AO (dependent data) and the adjusted VISCAT I threat score (independent data) for area 4, TAU-24 (PR+BMD model, MAXPROB II strategy). For this case a grouping size of nine was selected

NUMBER OF PREDICTORS VS. SCORING TECHNIQUES

TAU24 - AREA 4 - MAXPROB1 - GROUPING SIZE OF 9
PREDICTORS BMD2, T1000, ENTR, DUDP, DIV925
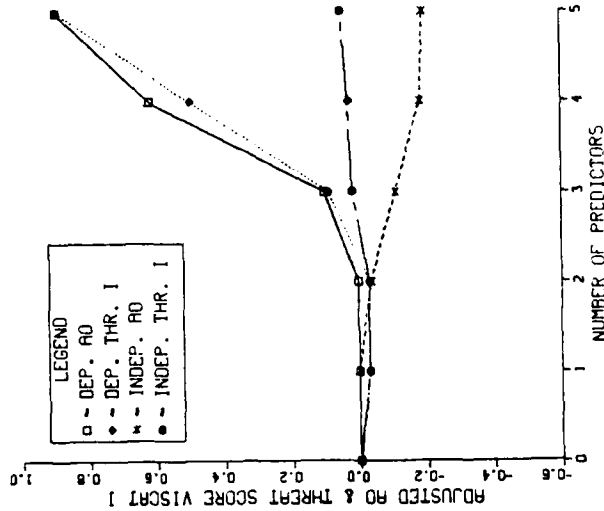
INDEPENDENT DATA

23	133	1174
11	37	71
4	5	11

AO=82.71% AAO=-19.25%

A1=14.98%

TS1=0.07 ATS1=0.05

TS2=0.14 ATS2=0.03

TS12=0.14 ATS12=-0.01

DEPENDENT DATA

4	41	2487
5	327	2
72	0	0

AO=98.23% AAO=88.42%

A1=1.63%

TS1=0.89 ATS1=0.89

TS2=0.87 ATS2=0.85

TS12=0.88 ATS12=0.86

Figure 53a. Skill diagram and contingency table results for area 4, TAU-24 (PR+BMD model) for the MAXPROB I strategy. The contingency table corresponds to those scores associated with the maximum independent VISCAT I threat score achieved at the fifth predictor level

205

NUMBER OF PREDICTORS VS. SCORING TECHNIQUES   INDEPENDENT DATA

TAU24 - AREA 4 - MAXPROBII - GROUPING SIZE OF 9
PREDICTORS BMD2, T1000, ENTR, DUDP, DIV925

INDEPENDENT DATA
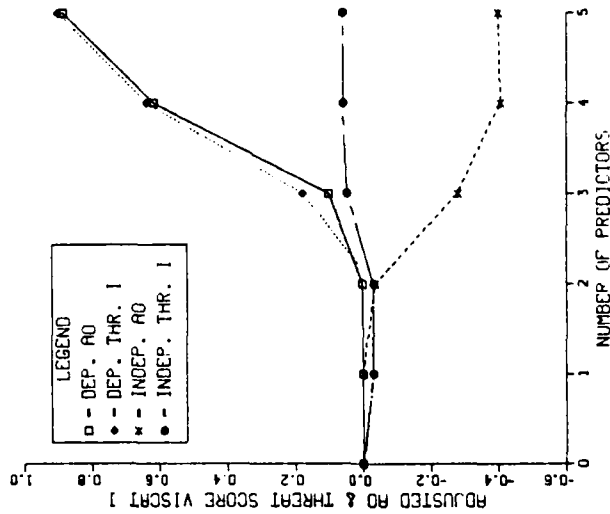
	1	2	3
3	21	121	1122
2	11	43	113
1	6	11	21

FORECAST / OBSERVED

$AO = 79.71\%$ $AAO = -39.91\%$
$A1 = 17.43\%$
$TS1 = 0.09$ $ATS1 = 0.06$
$TS2 = 0.14$ $ATS2 = 0.03$
$TS12 = 0.14$ $ATS12 = -0.01$

DEPENDENT DATA

	1	2	3
3	0	2	2444
2	1	362	41
1	80	4	4

FORECAST / OBSERVED

$AO = 98.23\%$ $AAO = 88.42\%$
$A1 = 1.63\%$
$TS1 = 0.90$ $ATS1 = 0.90$
$TS2 = 0.88$ $ATS2 = 0.87$
$TS12 = 0.89$ $ATS12 = 0.87$

LEGEND
□ - DEP. AO
♦ - DEP. THR. I
✕ - INDEP. AO
● - INDEP. THR. I

ADJUSTED AO & THREAT SCORE VISCAT I

NUMBER OF PREDICTORS

Figure 53b.   Skill diagram and contingency table results for area 4, TAU-24 (PR+BMD model) for the MAXPROB II strategy. The contingency table corresponds to those scores associated with the maximum independent VISCAT I threat score achieved at the fifth predictor level

NUMBER OF PREDICTORS VS. SCORING TECHNIQUES   INDEPENDENT DATA

TAU24 - AREA 4 - NAT REGR - GROUPING SIZE OF 9

PREDICTORS BMD2, T1000, ENTR, DUDP, DIV925

INDEPENDENT DATA

AO=81.14% AAO=-30.05%

A1=16.81%

TS1=0.06   ATS1=0.03

TS2=0.15   ATS2=0.04
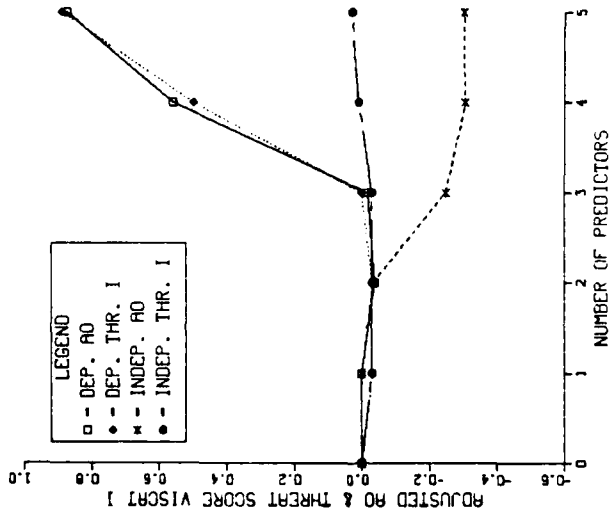
TS12=0.15   ATS12=0.00

	1	2	3
FORECAST 3	20	125	1141
2	15	45	102
1	3	5	10

OBSERVED

DEPENDENT DATA

AO=98.09% AAO=87.53%

A1=1.91%

TS1=0.89   ATS1=0.89

TS2=0.85   ATS2=0.83

TS12=0.88   ATS12=0.85

	1	2	3
FORECAST 3	0	41	2483
2	9	327	6
1	72	0	0

OBSERVED

LEGEND
□ - DEP. AO
◆ - DEP. THR. I
✕ - INDEP. AO
● - INDEP. THR. I

ADJUSTED AO & THREAT SCORE VISCAT I

NUMBER OF PREDICTORS

Figure 53c.   Skill diagram and contingency table results for area 4, TAU-24
(PR+BMD model) for the natural regression strategy. The
contingency table corresponds to those scores associated
with the maximum independent VISCAT I threat score achieved
at the fifth predictor level

Predictor	FD(96)	FD	A0	A0(96)	A1	A1(05)
BMD2	0.0899		84.7%	34.7%	12.5%	34.3%
T1000	0.1271	0.0833	84.8%	42.5%	12.6%	36.4%
ENTR	0.1557	0.1277	86.3%	56.8%	11.6%	27.5%
DUDP	0.1798	0.1564	94.2%	72.6%	4.9%	17.4%
DIV925	0.2010	0.2025	98.2%		1.6%	

Figure 54. Functional dependence, A0/A1 statistics and 96%/05% confidence interval values for area 4, TAU-24 (PR+BMD model, MAXPROB II strategy)

208

DEPENDENT DATA

	3	65	299	2386
FORECAST	2	5	37	71
	1	11	32	32
		1	2	3

OBSERVED

AO =82.85% AAO = -12.25%

A1 =13.85%

TS1 = 0.08   ATS1 = 0.05

TS2 = 0.08   ATS2 = -0.05

TS12 = 0.08   ATS12 = -0.09

INDEPENDENT DATA

	3	31	145	1207
FORECAST	2	2	16	34
	1	5	14	15
		1	2	3

OBSERVED

AO = 83.59% AAO = -13.15%

A1 = 13.27%

TS1 = 0.07   ATS1 = 0.05

TS2 = 0.08   ATS2 = -0.05

TS12 = 0.08   ATS12 = -0.08

Figure 55.   Contingency table results for the area 4,
             TAU-24 equal variance threshold model

209
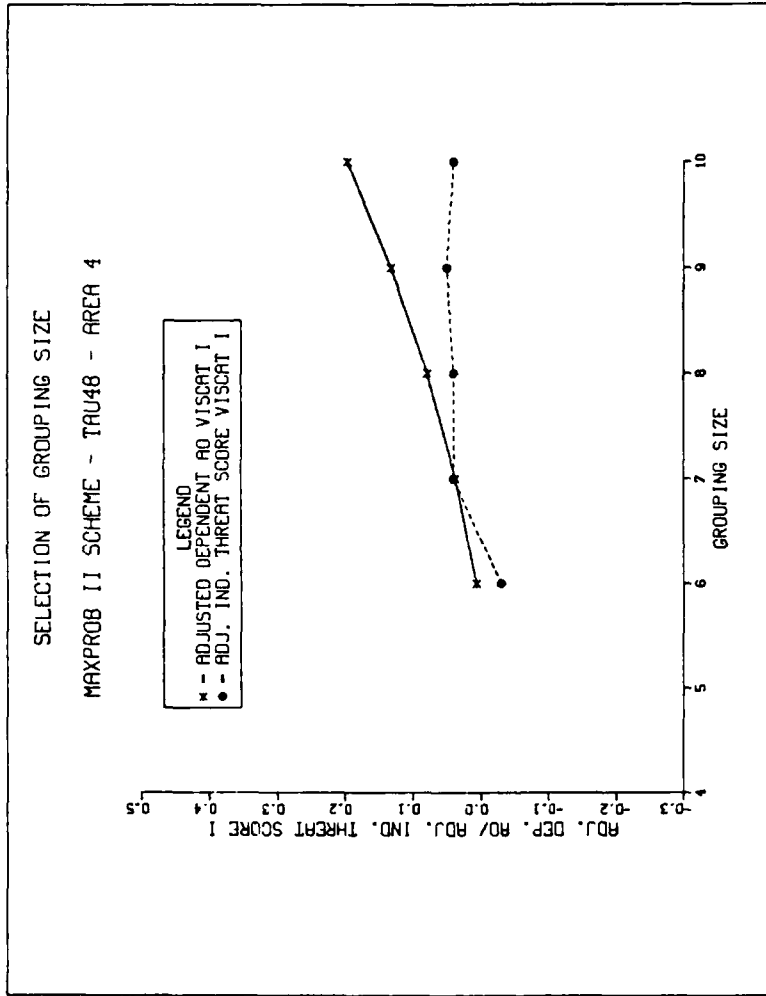
Figure 56. Relationship of equally populous grouping size to the adjusted AO (dependent data) and the adjusted VISCAT I threat score (independent data) for area 4, TAU-48 (PR model, MAXPROB II strategy). For this case a grouping size of seven was selected strategy).

NUMBER OF PREDICTORS VS. SCORING TECHNIQUES

TAU48 - AREA 4 - MAXPROB1 - GROUPING SIZE OF 7
PREDICTORS VRT925, DVRTOP, ENTR, DUDP, RH
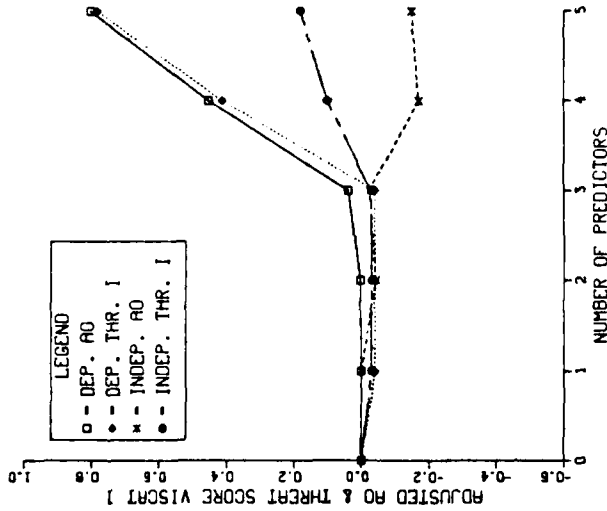
INDEPENDENT DATA

3	27	146	1193	AO=81.86% AAO=-14.94%
				A1=15.46%
2	5	44	79	TS1=0.20 ATS1=0.18
				TS2=0.16 ATS2=0.03
1	13	6	14	TS12=0.17 ATS12=0.02
	1	2	3	
		OBSERVED		

FORECAST

DEPENDENT DATA

3	18	76	2537	AO=96.63% AAO=80.00%
				A1=2.78%
2	4	329	4	TS1=0.79 ATS1=0.78
				TS2=0.79 ATS2=0.76
1	87	1	0	TS12=0.80 ATS12=0.76
	1	2	3	
		OBSERVED		

FORECAST

LEGEND
□ - DEP. AO
● - DEP. THR. I
× - INDEP. AO
● - INDEP. THR. I

ADJUSTED AO & THREAT SCORE VISCAT I

NUMBER OF PREDICTORS

Figure 57a.   Skill diagram and contingency table results for area 4, TAU-48
(PR model) for the MAXPROB I strategy. The contingency table
corresponds to those scores associated with the maximum
independent VISCAT I threat score achieved at the fifth
predictor level

211

Figure 57b. Skill diagram and contingency table results for area 4, TAU-48 (PR model) for the MAXPROB II strategy. The contingency table corresponds to those scores associated with the maximum independent VISCAT I threat score achieved at the fifth predictor level

212

NUMBER OF PREDICTORS VS. SCORING TECHNIQUES

TAU48 - AREA 4 - NAT REGR - GROUPING SIZE OF 7

PREDICTORS VRT925, DVRTDP, ENTR, DUDP, RH
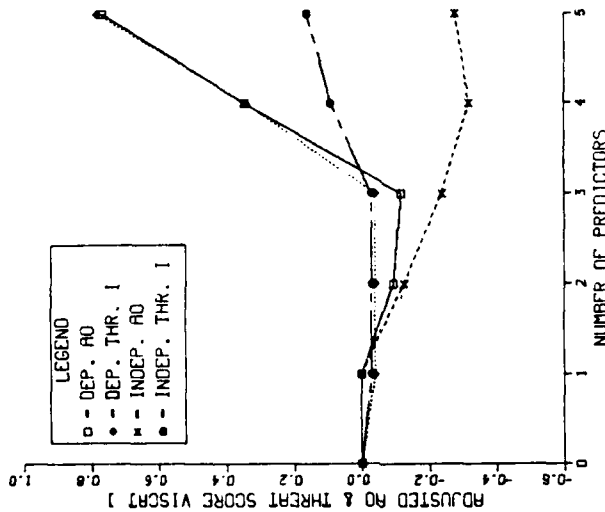
INDEPENDENT DATA

	1	2	3
3	25	138	1154
2	8	53	118
1	12	5	14

FORECAST

OBSERVED

AO=79.83% AAO=-27.80%

A1=17.62%

TS1=0.19   ATS1=0.16

TS2=0.16   ATS2=0.04

TS12=0.17 ATS12=0.02

DEPENDENT DATA

	1	2	3
3	1	73	2516
2	21	332	25
1	87	1	0

FORECAST

OBSERVED

AO=96.04% AAO=76.50%

A1=3.93%

TS1=0.79   ATS1=0.78

TS2=0.73   ATS2=0.69

TS12=0.78 ATS12=0.73

LEGEND

□ - DEP. AO
● - DEP. THR. I
× - INDEP. AO
● - INDEP. THR. I

ADJUSTED AO & THREAT SCORE VISCAT 1

NUMBER OF PREDICTORS

Figure 57c. Skill diagram and contingency table results for area 4, TAU-48
(PR model) for the natural regression strategy. The contingency
table corresponds to those scores associated with the maximum
independent VISCAT I threat score achieved at the fifth
predictor level

213

Predictor	FD(96)	FD	A0	A0(96)	A1	A1(05)
VRT925	0.1069		83.1%	36.7%	13.3%	32.7%
DVRTDP	0.1512	0.1212	83.2%	40.6%	13.4%	37.0%
ENTR	0.1857	0.1473	83.8%	50.6%	12.8%	31.5%
DUDP	0.2143	0.2061	90.8%	66.3%	7.4%	21.4%
RH	0.2390	0.2543	96.6%		2.8%	

Figure 58. Functional dependence, A0/A1 statistics and 96%/05% confidence interval values for area 4, TAU-48 (PR model, MAXPROB II strategy)
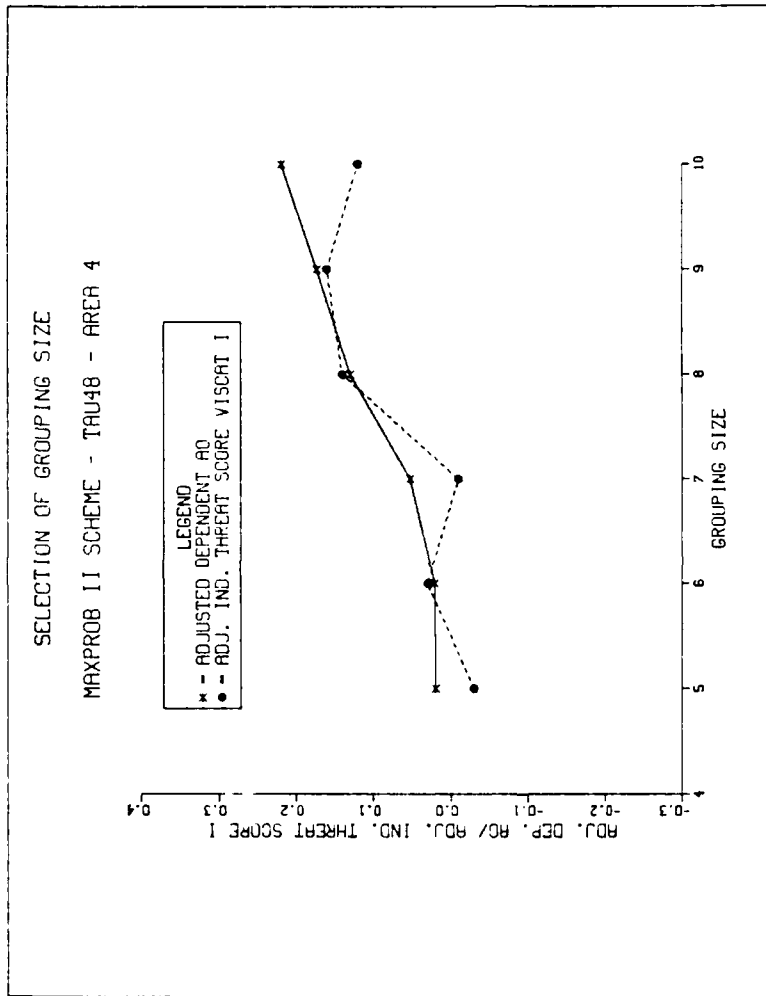
Figure 59. Relationship of equally populous grouping size to the adjusted AO (dependent data) and the adjusted VISCAT I threat score (independent data) for area 4, TAU-48 (PR+BMD model, MAXPROB II strategy). For this case a grouping size of nine was selected

NUMBER OF PREDICTORS VS. SCORING TECHNIQUES   INDEPENDENT DATA

THU48 - AREA 4 - MAXPROB1 - GROUPING SIZE OF 9
PREDICTORS BMD1, DDVDP, DDJDP, ENTR, PRECIP
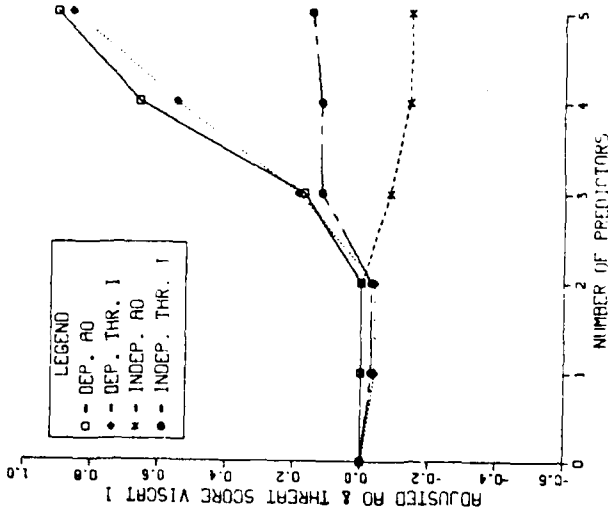
21	141	1192
12	47	79
12	8	15

FORECAST / OBSERVED

AO=81.93% AAO=-14.52%

A1=15.25%

TS1=0.18   ATS1=0.15

TS2=0.16   ATS2=0.04

TS12=0.15 ATS12=0.00

DEPENDENT DATA

10	34	2539
3	371	1
96	1	1

FORECAST / OBSERVED

AO=98.36% AAO=90.29%

A1=1.28%

TS1=0.86   ATS1=0.86

TS2=0.90   ATS2=0.89

TS12=0.90 ATS12=0.88

Figure 60a.   Skill diagram and contingency table results for area 4, TAU-48
(PR+BMD model) for the MAXPROB I strategy. The contingency
table corresponds to those scores associated with the
maximum independent VISCAT I threat score achieved at the
fifth predictor level

216

NUMBER OF PREDICTORS VS. SCORING TECHNIQUES

TAU48 - AREA 4 - MAXPROBII - GROUPING SIZE OF 9
PREDICTORS BMD1, DDVDP, DUDP, ENTR, PRECIP

INDEPENDENT DATA

			AO=79.70%	AAO=-28.63%
20	128	1145	A1=16.58%	
8	55	112	TS1=0.20	ATS1=0.17
17	13	29	TS2=0.17	ATS2=0.05
			TS12=0.17	ATS12=0.02

DEPENDENT DATA

			AO=94.27%	AAO=66.02%
9	46	2439	A1=4.55%	
3	345	75	TS1=0.64	ATS1=0.63
97	15	27	TS2=0.71	ATS2=0.67
			TS12=0.72	ATS12=0.66

Figure 60b. Skill diagram and contingency table results for area 4, TAU-48 (PR+BMD model) for the MAXPROB II strategy. The contingency table corresponds to those scores associated with the maximum independent VISCAT I threat score achieved at the third predictor level

217

NUMBER OF PREDICTORS VS. SCORING TECHNIQUES

TAU48 - AREA 4 - NAT RCGR - GROUPING SIZE OF 9
PREDICTORS BMD1, DDVOP, DUDP, ENTR, PRECIP

INDEPENDENT DATA

FORECAST
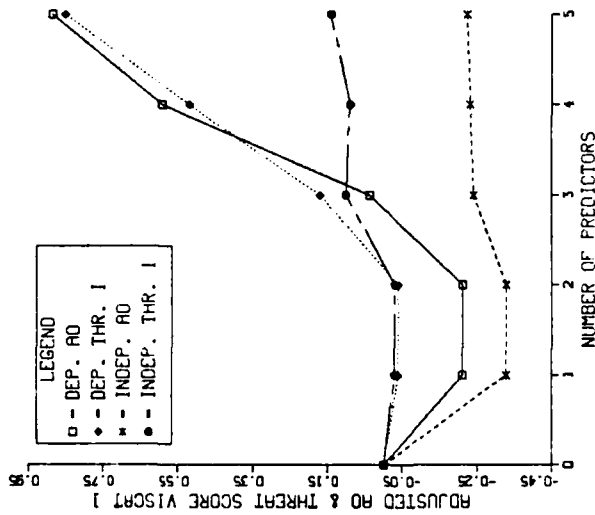
	1	2	3
3	19	134	1167
2	15	54	104
1	11	8	15

OBSERVED

AO=80.68% AAO=-22.41%

AI=16.58%

TS1=0.16 ATS1=0.14

TS2=0.17 ATS2=0.05

TS12=0.16 ATS12=0.01

DEPENDENT DATA

FORECAST

	1	2	3
3	0	31	2528
2	15	374	13
1	94	1	0

OBSERVED

AO=98.04% AAO=88.35%

AI=1.96%

TS1=0.85 ATS1=0.85

TS2=0.86 ATS2=0.84

TS12=0.89 ATS12=0.86

LEGEND
□ - DEP. AO
♦ - DEP. THR. I
✕ - INDEP. AO
● - INDEP. THR. I

NUMBER OF PREDICTORS

ADJUSTED AO & THREAT SCORE VISCAT I

Figure 60c. Skill diagram and contingency table results for area 4, TAU-48
(PR+BMD model) for the natural regression strategy. The
contingency table corresponds to those scores associated with
the maximum independent VISCAT I threat score achieved
at the fifth predictor level

218

Predictor	FD(96)	FD	A0	A0(96)	A1	A1(05)
BMD1	0.0913		83.1%	37.1%	13.3%	35.0%
DDVDP	0.1290	0.0872	83.2 %	42.2%	13.3%	36.7%
DUDP	0.1580	0.1390	86.1%	56.5%	11.6%	27.8%
ENTR	0.1825	0.1625	94.3%	72.3%	4.5%	17.8%
PRECIP	0.2044		98.4%		1.9%	

Figure 61. Functional dependence, A0/A1 statistics and 96%/05% confidence interval values for area 4, TAU-48 (PR+BMD model, MAXPROB II strategy)

219

DEPENDENT DATA

	1	2	3	
3	92	353	2468	
2	14	53	73	
1	3	0	0	

FORECAST (vertical axis), OBSERVED (horizontal axis)

AO = 82.59% AAO = -3.30%

A1 = 12.73%

TS1 = 0.03   ATS1 = -0.01

TS2 = 0.11   ATS2 = -0.03

TS12 = 0.10   ATS12 = -0.09

INDEPENDENT DATA

	1	2	3	
3	39	175	1245	
2	5	21	40	
1	1	0	1	

FORECAST (vertical axis), OBSERVED (horizontal axis)

AO = 82.97% AAO = -7.88%

A1 = 14.41%

TS1 = 0.02   ATS1 = -0.01

TS2 = 0.09   ATS2 = -0.05

TS12 = 0.08   ATS12 = -0.09

Figure 62.   Contingency table results for the area 4,
             TAU-48 equal variance threshold model

220

DEPENDENT DATA

	1	2	3
FORECAST 3	96	368	2511
FORECAST 2	8	37	30
FORECAST 1	5	1	0

OBSERVED

AO = 83.54%   AAO = 2.33%
A1 = 13.32%

TS1 = 0.05   ATS1 = 0.01
TS2 = 0.08   ATS2 = -0.06
TS12 = 0.08   ATS12 = -0.11

INDEPENDENT DATA

	1	2	3
FORECAST 3	42	181	1266
FORECAST 2	1	13	18
FORECAST 1	2	2	2

OBSERVED

AO = 83.89%   AAO = -2.07%
A1 = 13.23%

TS1 = 0.04   ATS1 = 0.01
TS2 = 0.06   ATS2 = -0.08
TS12 = 0.06   ATS12 = -0.12

Figure 63. Contingency table results for the area 4,
TAU-48 quadratic threshold model

221

NUMBER OF PREDICTORS VS. SCORING TECHNIQUES

TAU24,1984 - AREA 2 - MAXPROB II- GROUPING SIZE OF 7
PREDICTORS BMD2, VRT925, ENTR, U1000, RH
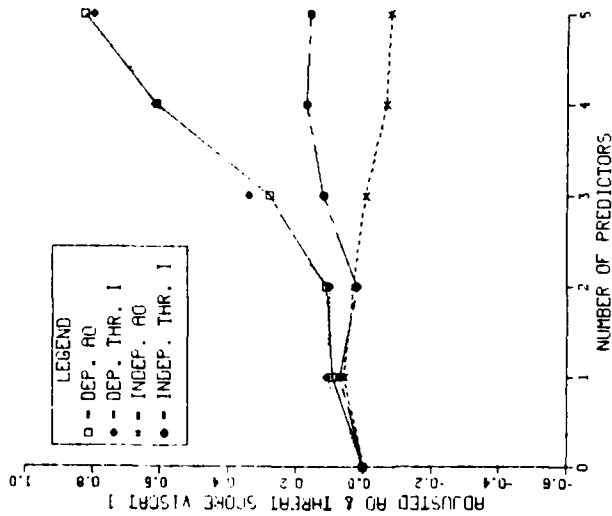
INDEPENDENT DATA

3	61	66	393
FORECAST 2	13	14	47
1	85	19	69
	1	2	3

OBSERVED

AO = 64.15% AAO = -6.59%

A1 = 17.81%

TS1 = 0.34   ATS1 = 0.17

TS2 = 0.09   ATS2 = -0.05

TS12 = 0.26 ATS12 = 0.13

DEPENDENT DATA

3	22	34	909
FORECAST 2	0	141	39
1	287	30	74
	1	2	3

OBSERVED

AO = 87.04% AAO = 61.28%

A1 = 7.03%

TS1 = 0.69   ATS1 = 0.62

TS2 = 0.58   ATS2 = 0.51

TS12 = 0.76 ATS12 = 0.69

LEGEND
□ - DEP. AO
● - DEP. THR. I
□ - INDEP. AO
● - INDEP. THR. I

ADJUSTED AO & THREAT SCORE VISCAT I

NUMBER OF PREDICTORS

Figure 64. Skill diagram and contingency table results for area 2, TAU-24, 1984 data (PR+BMD model) for the MAXPROB II strategy. The contingency table corresponds to those scores associated with the maximum independent VISCAT I threat score achieved at the fourth predictor level

222

COMPARISON OF THRESHOLD SCHEMES

Figure 65. Graph of threat score versus threat frequency (unadjusted scores for a standardized two by two contingency table) for the minimum probable error threshold model and the maximum-likelihood-of-detection threshold model. This graph reflects VISCAT I+II versus VISCAT III and VISCAT I versus VISCAT II separations

COMPARISON OF THRESHOLD SCHEMES
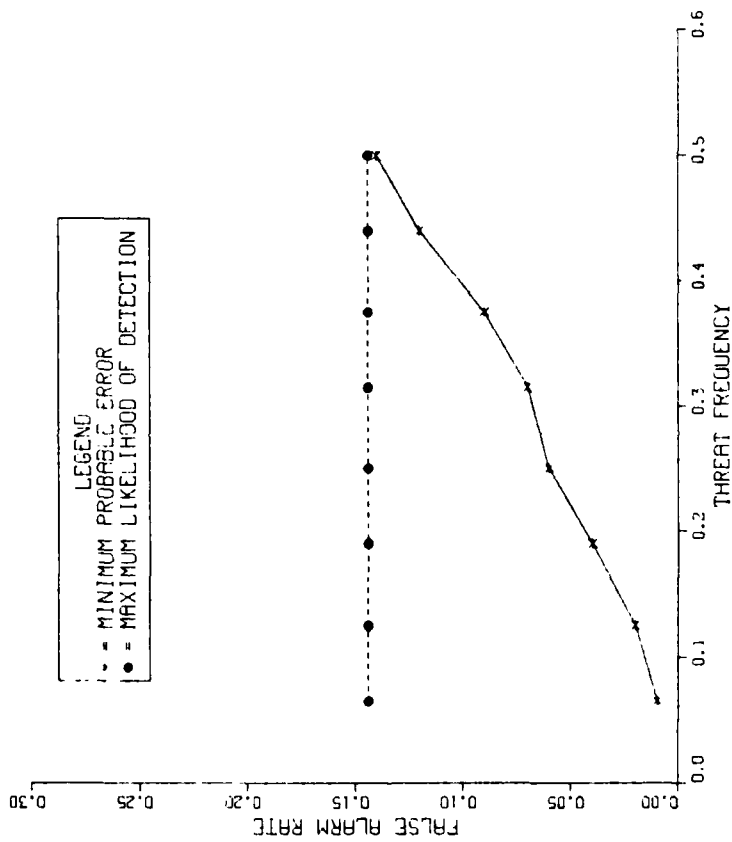
Figure 66. Graph of false alarm rate versus threat frequency (unadjusted scores for a standardized two by two contingency table) for the minimum probable error threshold model and the maximum-likelihood-of-detection threshold model. This graph reflects VISCAT I+II versus VISCAT III and VISCAT I versus VISCAT II separations
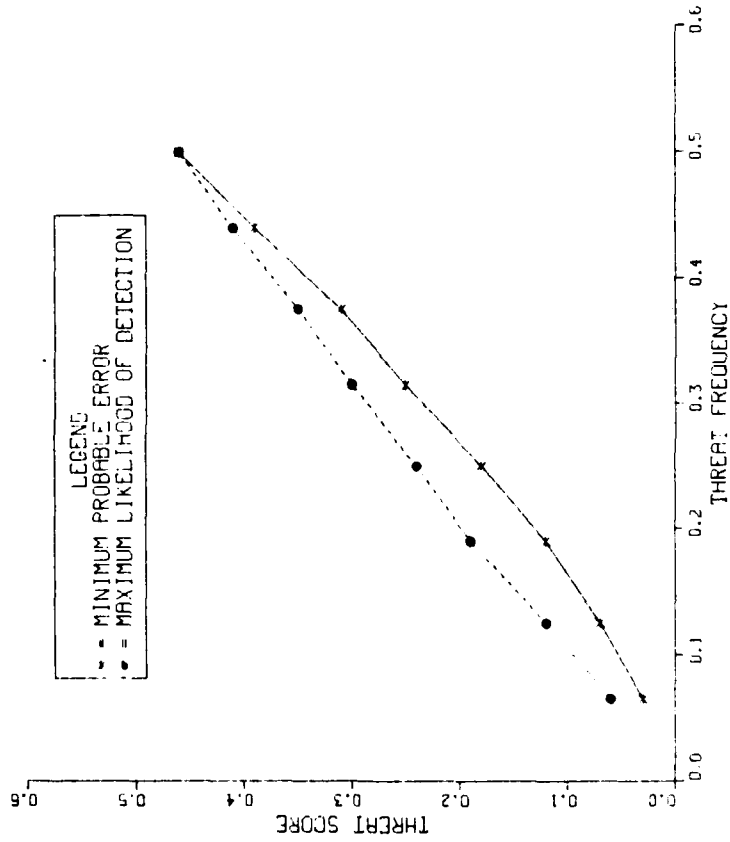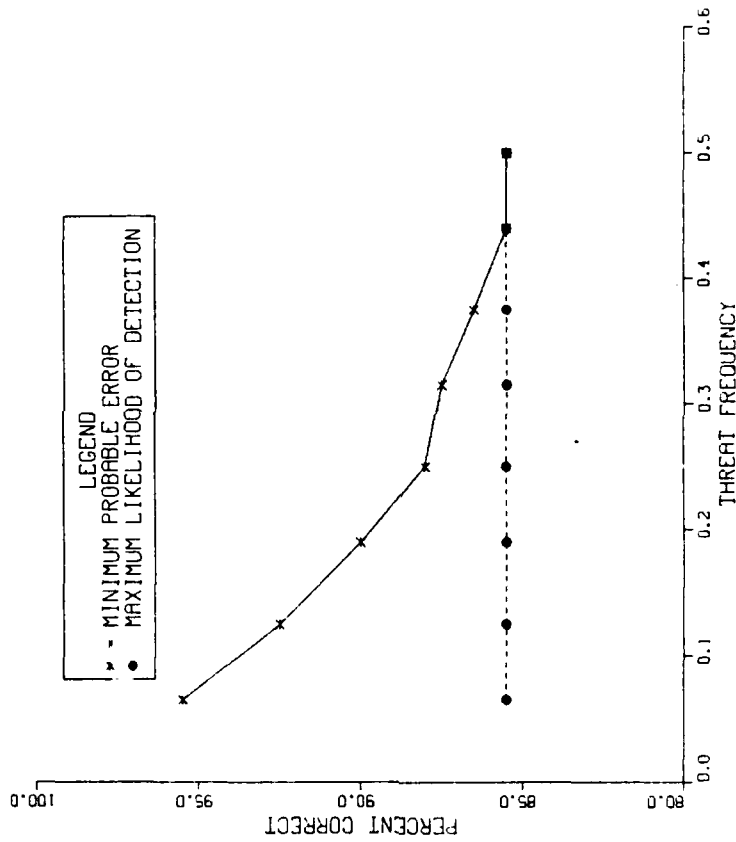
Figure 67. Graph of percent correct versus threat frequency (unadjusted scores for a standardized two by two contingency table) for the minimum probable error threshold model and the maximum-likelihood-of-detection threshold model. This graph reflects VISCAT I+II versus VISCAT III and VISCAT I versus VISCAT II separations

225

DEPENDENT DATA

	1	2	3	
3	35	133	1662	AO = 58.13% AAO = 0.01%
				A1 = 12.53%
2	0	0	0	TS1 = 0.04 ATS1 = 0.01
				TS2 = 0.0 ATS2 = -0.14
1	46	235	827	TS12 = 0.05 ATS12 = -0.04

FORECAST (vertical axis label)

1   2   3
OBSERVED

INDEPENDENT DATA

	1	2	3	
3	16	58	857	AO = 59.84% AAO = 0.01%
				A1 = 11.91%
2	0	0	0	TS1 = 0.04 ATS1 = 0.01
				TS2 = 0.0 ATS2 = -0.14
1	22	117	399	TS12 = 0.04 ATS12 = 0.0

FORECAST (vertical axis label)

1   2   3
OBSERVED

Figure 68. Contingency table results for the minimum
probable error threshold model (EVAR) for
area 4, TAU-24. The contingency tables reflect
VISCAT I+II versus VISCAT III and VISCAT I
versus VISCAT II separations

226

DEPENDENT DATA

	1	2	3
3	35	133	1662
2	22	134	659
1	24	101	168

FORECAST / OBSERVED

AO = 61.95% AAO = 0.01%

A1 = 40.78%

TS1 = 0.07   ATS1 = 0.04

TS2 = 0.13   ATS2 = 0.0

TS12 = 0.05   ATS12 = 0.01

INDEPENDENT DATA

	1	2	3
3	16	58	857
2	11	75	319
1	11	42	80

FORECAST / OBSERVED

AO = 64.19% AAO = 0.01%

A1 = 29.27%

TS1 = 0.07   ATS1 = 0.04

TS2 = 0.15   ATS2 = 0.03

TS12 = 0.14   ATS12 = 0.04

Figure 69.   Contingency table results for the maximum-likelihood-of-detection threshold model for area 4, TAU-24. The contingency tables reflect VISCAT I+II versus VISCAT III and VISCAT I versus VISCAT II separations

227

LIST OF REFERENCES

Aldinger, W.T., 1979: Experiments on Estimating Open Ocean Visibilities Using Model Output Statistics. M.S. Thesis (R.J. Renard, advisor), Dept. of Meteorology, Naval Postgraduate School, Monterey, CA, 81 pp.

Best, D.L., and Pryor, S.P., 1983: Air Weather Service Model Output Statistics System Project Report. AFGWC/PR-83/001, United States Air Force Air Weather Service (MAC), Air Force Global Weather Central, Offutt AFB, NE, 85pp.

Department of the Navy, 1979: CV NATOPS MANUAL, Office of the Chief of Naval Operations, Washington, D.C., 156 pp.

Glahn, H.R., 1983: MOS Support for Military Locations From the Techniques Development Laboratory. TDL Office Note 83-9, National Weather Service, NOAA, U.S. Department of Commerce, 10 pp.

_____, and Lowry, D.A., 1972: The Use of Model Output Statistics (MOS) in Objective Weather Forecasting. J. Appl. Meteor., 11, pp. 1203-1211.

Godfrey, R.S. and P.R. Lowe, 1979: An Application of Model Output Statistics to Forecasting the Occurrence of the Levante Wind. Preprints, Sixth Conference on Probability and Statistics in Atmospheric Sciences, Banaff, Alta., Amer. Meteor. Soc., Boston, MA, pp. 83-86.

Karl, M.L., 1984: Experiments in Forecasting Atmospheric Marine Horizontal Visibility using Model Output Statistics with Conditional Probabilities of Discretized Parameters. M.S. Thesis (R.J. Renard, advisor), Dept. of Meteorology, Naval Postgraduate School, Monterey, CA, 165 pp.

Klein, W.H., 1981: Design of a MOS System for the Navy. Final Report. NEPRF Contract No. N00228-80-C-LV22, Intercon Weather Consultants, Inc., Camp Springs, MD.

Koziara, M.C., R.J. Renard and W.J. Thompson, 1983: Estimating Marine Fog Probability Using a Model Output Statistics Scheme. Monthly Weather Review. 111, pp. 2333-2340.

228

Lewit, H.L., 1980: SOCAL MOS Ceiling/Visibility Forecast
    Algorithms. Task 3 Final Report: Forecast Algorithm
    Development, and Task IV, Section I: Test of Forecast
    Algorithms Employing Dependent Data. NEPRD Contract No.
    N00228-78-C-3289, Ocean Data Systems, Inc., Monterey,
    CA.

Lowe, P., 1984a: The Use of Decision Theory for Determining
    Thresholds for Categorical Forecasts, unpublished manu-
    script, Navy Environmental Prediction Research Facility,
    Monterey, CA.

_____, 1984b: The Use of Multi-Variate Statistics for
    Defining Homogeneous Atmospheric Regions Over the North
    Atlantic Ocean, unpublished manuscript, Navy Environmental
    Prediction Research Facility, Monterey, CA.

_____, 1984c: The Use of Adjusted Scores and Significance
    Tests in the Verification of Categorical Forecasts,
    unpublished manuscript, Navy Environmental Prediction
    Research Facility, Monterey, CA.

Miller, I., and Freund, J.E., 1977: Probability and Statis-
    tics for Engineers, 2nd. Ed., Prentice-Hall, Inc., Engle-
    wood Cliffs, NJ, 528 pp.

Naval Environmental Prediction Research Facility, Monterey,
    CA, 1982: MOS Forecasts for U.S. Navy and Marine Corps
    CONUS Locations--User's Manual, NAVENPREDRSHFAC Document
    No. 7W0513-Um-07, Commander, Naval Oceanography Command,
    Bay St. Louis, MS, 18 pp.

Nelson, T.S., 1972: Numerical-Statistical Prediction of
    Visibility at Sea. M.S. Thesis (R.J. Renard, advisor),
    Dept. of Meteorology, Naval Postgraduate School,
    Monterey, CA, 33 pp.

Preisendorfer, R.W., 1983a: Proposed Studies of Some Basic
    Marine Atmospheric Visibility Prediction Schemes Using
    Model Output Statistics, unpublished manuscript, Depart-
    ment of Meteorology, Naval Postgraduate School, Monterey,
    CA, 28 pp.

_____, 1983b: Maximum-Probability and Natural-Regression
    Prediction Strategies, unpublished manuscript, Department
    of Meteorology, Naval Postgraduate School, Monterey, CA,
    10 pp.

_____, 1983c: Tests for Functional Dependence of Predic-
    tors, unpublished manuscript, Department of Meteorology,
    Naval Postgraduate School, Monterey, CA, 5 pp.

229

_____, 1984: Update of MAXPROB MOS Prediction Method, unpublished manuscript, Department of Meteorology, Naval Postgraduate School, Monterey, CA, 3 pp.

Renard, R.J. and W.T. Thompson, 1984: Estimating Visibility Over the North Pacific Ocean Using Model Output Statistics. National Weather Digest, Vol. 9, No. 2, pp. 18-25.

Schramm, W.G., 1966: Analysis and Prediction of Visibility at Sea. M.S. Thesis (R.J. Renard, advisor), Dept. of Meteorology, Naval Postgraduate School, Monterey, CA, 224 pp.

Selsor, H.D., 1980: Further Experiments Using a Model Output Statistics Method in Estimating Open Ocean Visibility. M.S. Thesis (R.J. Renard, advisor), Dept. of Meteorology, Naval Postgraduate School, Monterey, CA, 121 pp.

University of California, 1983: BMDP Statistical Software, 1983 Edition, Department of Biomathematics, University of California at Los Angeles, University of California Press, 726 pp.

Yavorsky, P.G., 1980: Experiments Concerning Categoriecal Forecasts of Open-Ocean Visibility Using Model Output Statistics. M.S. Thesis (R.J. Renard, advisor), Dept. of Meteorology, Naval Postgraduate School, Monterey, CA, 87 pp.

INITIAL DISTRIBUTION LIST

		No. Copies
1.	Defense Technical Information Center Cameron Station Alexandria, VA 22314	2
2.	Library, Code 0142 Naval Postgraduate School Monterey, CA 93943	2
3.	Meteorology Reference Center, Code 63 Department of Meteorology Naval Postgraduate School Monterey, CA 93943	1
4.	Professor Robert J. Renard, Code 63Rd Chairman, Department of Meteorology Naval Postgraduate School Monterey, CA 93943	6
5.	Chairman (Code 68Mr) Department of Oceanography Naval Postgraduate School Monterey, CA 93943	1
6.	Dr. Rudolph W. Preisendorfer NOAA/PMEL/R/E/PM Bin 015700 Bldg. 3 7600 Sand Point Way, N.E. Seattle, WA 98115-0070	1
7.	Mr. Paul Lowe Naval Environmental Prediction Research Facility Monterey, CA 93940	1
8.	Dr. Robert Godfrey Naval Environmental Prediction Research Facility Monterey, CA 93940	1
9.	Lt. Mark Diunizio 10855 Charbono Point San Diego, CA 92131	1
10.	Director Naval Oceanography Division Naval Observatory 34th and Massachusetts Avenue NW Washington, DC 20390	1

11. Commander   1
    Naval Oceanography Command
    NSTL Station
    Bay St. Louis, MS   39522

12. Commanding Officer   1
    Naval Oceanographic Office
    NSTL Station
    Bay St. Louis, MS   39522

13. Commanding Officer   1
    Fleet Numerical Oceanography Center
    Monterey, CA   93940

14. Commanding Officer   1
    Naval Ocean Research and Development
      Activity
    NSTL Station
    Bay St. Louis, MS   39522

15. Commanding Officer   1
    Naval Environmental Prediction
      Research Facility
    Monterey, CA   93940

16. Chairman, Oceanography Department   1
    U.S. Naval Academy
    Annapolis, MD   21402

17. Chief of Naval Research   1
    800 N. Quincy Street
    Arlington, VA   22217

18. Office of Naval Research (Code 480)   1
    Naval Ocean Research and Development
      Activity
    NSTL Station
    Bay St. Louis, MS   39522

19. Commander (Air-370)   1
    Naval Air Systems Command
    Washington, D.C.   20360

20. Chief, Ocean Services Division   1
    National Oceanic and Atmospheric
      Administration
    8060 Thirteenth Street
    Silver Spring, MD   20910

21. Dr. Alan Weinstein   1
    Leader, Code 422
    Ocean Sciences Division
    Office of Naval Research
    Arlington, VA   22217

22. LCdr. Michael L. Karl   1
    USS Peleliu (LHA-5)
    FPO San Francisco, CA   96624

24. LCdr. Mike Wooster   1
    SMC #1136
    Naval Postgraduate School
    Monterey, CA   93943

25. LCdr. Kris Elias   1
    SMC #1542
    Naval Postgraduate School
    Monterey, CA   93943

26. Mr. Gil Ross, Met 09   1
    Meteorological Office
    Bracknell, Berkshire
    England

27. Chief, Technical Procedures Branch   1
    Meteorological Services Division
    National Oceanic and Atmospheric
      Administration
    National Weather Service
    Silver Spring, MD   20910

28. Chief, Technical Services Division   1
    United States Air Force
    Air Weather Service (MAC)
    Air Force Global Weather Central
    Offutt AFB, NB   68113

END

FILMED

5-85

DTIC